

Tatiana S. Vassilieff

Department of Chemistry, McGill University
Montréal, Québec, Canada

**Dumbbell Shaped Dendrimers:
Synthesis, Characterization and
Applications in Assembling Silver
Nanoparticles.**

M. Sc. Thesis submitted to the Faculty of Graduate Studies and Research
at McGill University.

December 2007

© Tatiana S. Vassilieff , 2007

Acknowledgements

I would like to deeply thank my supervisor, Dr. Ashok K. Kakkar for his mentorship and guidance throughout these two years of research. His permanent optimism and patience often helped me stay motivated and to surpass the difficulties I was facing.

This M. Sc. thesis could not have been achieved without the support of my parents and my sister, physically far away but always present when I needed it.

I was very lucky to working among genuinely kind and motivated people and I would like to thank my present colleagues, Rami Hourani, Xiaojun Liu, Amy Sutton and especially Florence Quist to constantly be by my side. I would also like to thank colleagues of the past: Mickael Four, Jessica McDonald, Samuel Mitton, Morgane Pasco and Nelly von Aderkas.

I gratefully acknowledge the assistance provided by the following contributors:

- Mr. Nadim Saadeh for mass spectral analysis,
- Ms. Antisar Hlil for MALDI-TOF analysis,
- Mr. Fred Morin for his help with the NMR measurements,
- Mr. Robert Gagnon for his help with the X-Ray Powder Diffraction spectra,
- Ms. Jennize Mui for her help with the Transmission Electron Microscopy pictures.

Finally I would also like to thank the following people that are dear to me, for their friendship and support: Anne-Laure Bouvier, Veronique Genestier, Lilian Guichard-Callin and Rebecca Murray.

Abstract

Synthesis and detailed characterization of dendrimers that evolve symmetrically from a linear bifunctional core (2-butyne-1,4-diol) with 3,5-dihydroxybenzyl alcohol based dendron wedges, are reported. The divergent, layer-by-layer build-up of the dumbbell shaped dendrimers, is based on simple acid-base hydrolytic chemistry of bis(dimethylamino)dimethylsilane with OH terminated molecules. Evaluation of some of the structure-property relationships in these dendrimers was carried out to obtain a better understanding of their potential applications. The self-assembly of these dendrimers in THF and water is significantly influenced by their generation number, the backbone structure and the solvent. Generations 1-3 dendrimers form aggregates at a higher critical aggregation concentration (*cac*) compared to generation 4 in THF. This behavior is related to the open structure in the lower generations with a linear core becoming important in their self-assembly, while in generation 4, more globular architecture with more prominent hydrogen bonding sites, facilitates self-assembly at lower concentrations. In water and in generations 1 and 2 dendrimers, the inability of more polar solvent to interact with their backbones, leads to aggregates that are formed by minimizing the repulsive forces. In generations 3 and 4, the major interaction of the solvent with the dendrimer is at the periphery which has a higher concentration of polar OH groups, and it does not interfere significantly with their ability to self-associate. Using these dendrimers as templates, a simple methodology in which silver nanoparticles are synthesized in one pot reaction, has been developed. The dendrimer structure provides reactive peripheral hydroxyl groups as well as a stabilizing acetylenic core/benzene backbone structure. The shape of the silver metal nanoparticles is strongly influenced by the dendrimers, and it evolves from spheres to cubes as the generation number increases.

Résumé

Ce master présente la synthèse et la caractérisation détaillée de dendrimères symétriques constitués d'un noyau bifonctionnel linéaire (2-butyne-1,4-diol) et de dendrons formés à partir de l'alcool 3,5-dihydroxybenzylique. La construction divergente, couche-par-couche de ces dendrimères en forme d'haltères est basée sur une simple hydrolyse acido-basique entre l'aminosilane $\text{Me}_2\text{Si}(\text{NMe}_2)_2$ et les molécules possédant des groupements hydroxyles terminaux.

Certaines propriétés physiques de ces dendrimères ont été explorées afin de mieux comprendre leurs applications potentielles. Notamment, nous avons démontré que l'auto- assemblage de ces dendrimères en agrégats dépend du nombre de génération, de leur structure et du solvant. En effet, les dendrimères de générations 1 à 3 forment des agrégats à une *concentration critique d'agrégation* plus élevée que celle des dendrimères de génération 4 dans le THF. Ce phénomène est dû à la structure plutôt ouverte des dendrimères de basse génération qui possèdent un noyau linéaire devenant prédominant dans le phénomène d'auto-assemblage. Par contre, les dendrimères de génération 4 adoptent une architecture plus globulaire qui favorisent les liaisons hydrogène et facilitent leur auto assemblage à basses concentrations. Dans l'eau, les dendrimères générations 1 et 2 forment des agrégats en minimisant leurs forces répulsives, ce solvant plus polaire ne pouvant que très peu interagir avec les noyaux aromatiques constituant les dendrons. Dans le cas des dendrimères de générations 3 et 4, le solvant interagit principalement avec les groupes hydroxyles terminaux présents à plus haute concentration, et ceci n'influence pas de manière significative leur capacité à s'auto associer.

Utilisant les propriétés de ces dendrimères, nous avons développé une méthodologie en une seule étape simple et efficace de fabrication de nanoparticules d'argent. La structure des dendrimères est telle qu'elle permet de fournir des groupes hydroxyles périphériques mais aussi un noyau et un squelette stabilisateur. La forme des nanoparticules d'argent, fortement influencée par les dendrimères, évolue de la sphère au cube avec le nombre de générations des dendrimères.

Table of Contents

Preface	
Acknowledgements	2
Abstract	3
Résumé	4
Table of Contents	5
List of Figures	8
List of Schemes	11
List of Abbreviations and Acronyms	13

CHAPTER 1: Dendrimers: Monodispersed Macromolecules with Unique Properties

1. Hyperbranched Polymers and Dendrimers	16
1.1 Dendrimers	18
1.1.2 Synthesis	18
1.1.3 Properties	23
1.1.4 Applications	25
1.1.5 Dumbbell Shaped Dendrimers	28
1.1.6 Characterization	37
1.2 Goals	40
1.3 References	42

CHAPTER 2: Metal Nanoparticles: Building Nanodevices by Atom Assembly

2.1 Introduction	48
2.2 Synthesis	48
2.3 Characterization	54
2.4 Applications	55

2.4.1 Catalysis	55
2.4.2 Carbon Nanotubes	55
2.4.3 Films/ Coatings	56
2.4.4 Quantum Dots	56
2.4.5 Biomedical Applications	57
2.5 Importance of Size and Shape of Metal Nanoparticles	57
2.6 Silver Nanoparticles	60
2.7 References	65

CHAPTER 3: Synthesis and Self-Assembly of Dumbbell Shaped Dendrimers

3.1 Introduction	72
3.2 Results and Discussion	73
3.2.1 Synthesis of Dumbbell Shaped Dendrimers	73
3.2.2 Self-Assembly of Dumbbell Shaped Dendrimers	75
3.3 Conclusions	81
3.4 Experimental Section	82
3.5 References	88

CHAPTER 4: Application of Dumbbell Shaped Dendrimers in the Synthesis of Silver Nanoparticles

4.1 Introduction	91
4.2 Results and Discussion	92
4.3 Conclusions	98
4.4 Experimental Section	99
4.5 References	101

CHAPTER 5: Conclusions and Future Outlook

5.1 Conclusions	104
5.1.1 Dumbbell Shaped Dendrimers	104
5.1.2 Applications in Synthesizing Silver Nanoparticles	105
5.2 Future Outlook	106

List of Figures

	Page
Figure 1: Schematic drawing showing the hybridization detection at the dendrimer/ quartz-crystal microbalance (QCM) biosensor.	26
Figure 2: Schematic presentation of the principle of encapsulation and shape-selective liberation.	27
Figure 3: Transition metal catalyst fragment can be attached at the periphery (a) or at the core (b).	28
Figure 4: Bolas with an electroneutral and a positively charged head group used to neutralize surface charges of polyelectrolytes or a solvent for hydrophobic molecules.	31
Figure 5: Attachment of Fréchet-type wedges to poly(ethylene oxide).	33
Figure 6: Molecular structures of ABA-extended amphiphilic dendrons 1 and 2.	34
Figure 7: Ionization using the MALDI technique.	39
Figure 8: Schematic representation of the Dendrimer/Pd ²⁺ chemically reduced to yield dendrimer-encapsulated Pd ⁰ nanoparticles.	51
Figure 9: Schematic representation of the stabilization of maghemite nanoparticles by carboxyl-terminated poly(amidoamine) dendrimer (generation 4.5).	51
Figure 10: Molecular structure of a second generation (G2) amine-terminated PAMAM dendrimer where the metal ions chelated to the primary amine groups (A) and G2 hydroxyl-terminated PAMAM dendrimer, with the metal ions chelating to the interior tertiary amine groups (B).	52

- Figure 11:** Simulated absorption spectra of copper nanocrystals differing by their shapes 3 nm cuboctahedron (**A**), 3 nm decahedron (**B**), 23 nm flat nanodisks (**C**), and 1.5 nm (red), 3 nm (green), 5 nm (blue), and 6 nm (black), ellipsoidal particles with an aspect ratio of 2 (**D**). 58
- Figure 12:** Different shapes of clusters: cuboctahedra (**A**), decahedra (**B**), icosahedra (**C**). 59
- Figure 13:** Scheme of the growth mechanism from clusters to a given shape of nanocrystals **I**) truncated decahedral nanocrystals, **II**) cubic nanocrystals, **III**) nanodisks. 60
- Figure 14:** TEM images of silver nanodisks at various hydrazine contents. 63
- Figure 15:** (**A**) UV-Vis absorption spectra of dendrimer generation 1 at concentrations of 1 to 10 mg/mL in THF, and (**B**) plot of absorbance vs concentration of dendrimers 1 in THF at 340 nm. 76
- Figure 16:** Transmission electron micrographs and particle size distributions of dendrimer generations 1 (**A**), 2 (**B**), 3 (**C**) and 4 (**D**) in THF at 4 mg/mL. 77
- Figure 17:** Transmission electron micrographs and particle size distributions of dendrimer generations 1 (**A**), 2 (**B**), 3 (**C**) and 4 (**D**) in THF at 8 mg/mL. 79
- Figure 18:** Transmission electron micrographs and particle size distributions of dendrimer generations 1 (**A**), 2 (**B**), 3 (**C**) and 4 (**D**) in H₂O at 4 mg/mL. 80
- Figure 19:** TEM image of silver metal particles synthesized using generation 1 (**A**), 2 (**B**) and 3 (**C**) dendrimer templates. 93
- Figure 20:** UV-Vis spectra of silver metal particles synthesized using generation 1 (**A**), 2 (**B**) and 3 (**C**) dendrimers as templates. 94

Figure 21: XRPD pattern of silver metal particles synthesized using generation 1(A), 2(B) and 3(C) dendrimers as templates. 95

Figure 22: Size distribution graphs for generation 1 (A), 2 (B) and 3 (C) templated silver particles. 96

List of Schemes

	Page
Scheme 1: Schematic representation of a hyperbranched polymer constructed by the homopolymerisation of AB ₂ type monomers.	16
Scheme 2: Description of the dendritic structure.	18
Scheme 3: Divergent approach for the construction of PAMAM dendrimers.	20
Scheme 4: Construction of a poly(arylether) fourth generation dendron following Fréchet's convergent route.	22
Scheme 5: Attaching the Fréchet type dendron to a trifunctional core.	22
Scheme 6: Schematic representation of the organization of amphiphilic dendrimers in a monolayer on the water surface.	25
Scheme 7: Description of dumbbell shaped dendrimers	29
Scheme 8: Schematic drawings of a bolaamphiphile	30
Scheme 9: Representation of a monolayer lipid membrane of a vesicle with charged headgroups.	30
Scheme 10. Chemical structure of dumbbell-shaped molecules 1-3	35
Scheme 11. Representation of the reversible transformation of helical fibers into a spherical capsule.	36
Scheme 12. Chemical structure of dumbbell-shaped macromolecule D ₄ -BABAB-D ₄ .	37
Scheme 13: Chemical structure of sodium citrate	49

Scheme 14: Chemical Structure of A) PVP, B) PSS and C) PEO.	50
Scheme 15: Schematic representation of the three methods used to generate bimetallic nanoparticles within a dendritic host.	53
Scheme 16: Schematic process for carbon nanotube synthesis by Chemical Vapor Deposition (CVD) on a catalytic nanoparticle derived from PAMAM dendrimer template.	56
Scheme 17: Preparation of dumbbell shaped dendrimers, following the acid base hydrolytic divergent methodology.	74
Scheme 18: Structures of generation 1-3 dendrimers.	92
Scheme 19: dendrimers templation process of silver nanoparticles.	97

List of Abbreviations and Acronyms

AFM	Atomic Force Microscopy
amu	Atomic mass unit
a.u.	Arbitrary units
BD	2-butyne-1,4-diol
<i>cac</i>	<i>Critical aggregation concentration</i>
CI-MS	Chemical Ionization-Mass Spectrometry
CNT	Carbon nanotube
CVD	Chemical Vapor Deposition
DDA	Discrete dipolar approximation
DEN	Dendrimer-Encapsulated Nanocomposite
DHBA	3,5-dihydroxybenzyl alcohol
DLS	Dynamic Light Scattering
EI-MS	Electron Impact-Mass Spectroscopy
FAB-MS	Fast Atom Bombardment-Mass Spectroscopy
FT-IR	Fourier Transformer-Infrared
G _n	Generation number
[G-1]-(OH) ₄	Dendrimer generation 1
[G-2]-(OH) ₈	Dendrimer generation 2
[G-3]-(OH) ₁₆	Dendrimer generation 3
[G-4]-(OH) ₃₂	Dendrimer generation 4
[G-5]-(OH) ₆₄	Dendrimer generation 5
[G-6]-(OH) ₁₂₈	Dendrimer generation 6
H-bonding	Hydrogen bonding
MHz	Megahertz
LbL	Layer-by-layer
M	Metal
MALDI-TOF	Matrix Assisted Laser Desorption Ionization-Time of Flight
<i>m/z</i>	Mass-to-charge ratio
NMR	Nuclear Magnetic Resonance
NPs	Nanoparticles

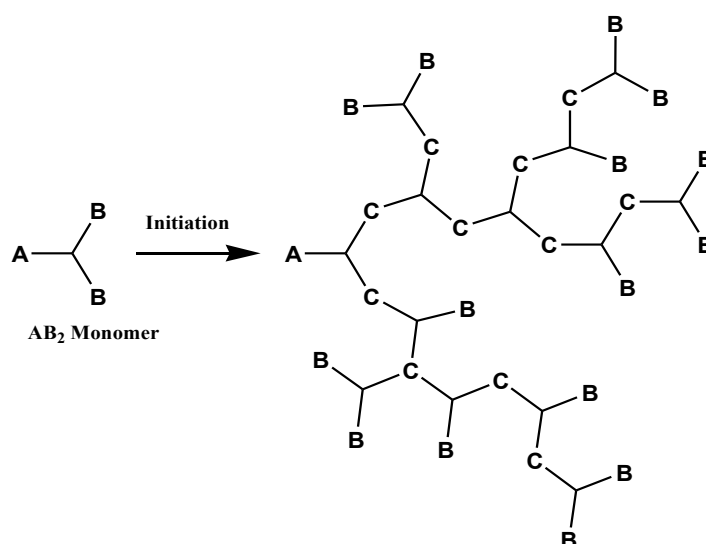
<i>p</i> -	Para
PAMAM	Poly(amido amine)
ppm	Part per million
SPB	Surface plasmon band
SWNT	Single-walled nanotube
TEM	Transmission electron microscopy
THF	Tetrahydrofuran
UV-Vis	Ultra violet-visible
XRPD	X-Ray Powder Diffraction
π^*	Antibonding pi orbital
π	Bonding pi orbital
δ	Chemical shift
°	Degree
°C	Degree Celsius
ν	Frequency (stretching)
δ	Frequency (bending)
[η]	Intrinsic viscosity

CHAPTER 1

Dendrimers: Monodisperse Macromolecules with Unique Properties

1. Hyperbranched Polymers and Dendrimers

Over the past 20 years, the number of compositions and architectures of macromolecules has grown very rapidly. The ability to easily tune the size, chemistry, topology and the properties of polymers through chemical synthesis, has led to their use in a variety of technological applications¹⁻⁸, such as Nylon, Polyethylene, Teflon, silicone, just to name a few. Today, linear polymers find applications in nearly every industry and area of life. But the need of more complex architectures for specific applications has led to the synthesis of hyperbranched polymers, which are a relatively new class of macromolecules⁹. They are typically imperfectly branched and polydisperse systems in terms of molecular weight characteristics and their branching factors, and are prepared in one-step procedures, mostly by polycondensation of AB_x monomers⁹⁻¹³. If $x \geq 2$ and the functionality A reacts only with functionality B of another molecule, the polymerization of AB_x monomers results in highly branched polymers⁹. Apart from polycondensation, addition polymerization of monomers that contain initiating and propagating functionalities in the same molecule¹⁴, ring-opening polymerization¹⁵, and self-condensing vinyl polymerization¹⁶ can be used for the synthesis of hyperbranched polymers. These procedures lead to uncontrolled statistical growth, and an irregular architecture with incomplete branching points dispersed in the structure, as shown in **Scheme 1**.



Scheme 1: Schematic representation of a hyperbranched polymer constructed by the homopolymerisation of AB_2 type monomers¹⁷.

Due to their branched structure, hyperbranched polymers are usually amorphous materials. Thus, the glass transition temperature, T_g , is one of the most

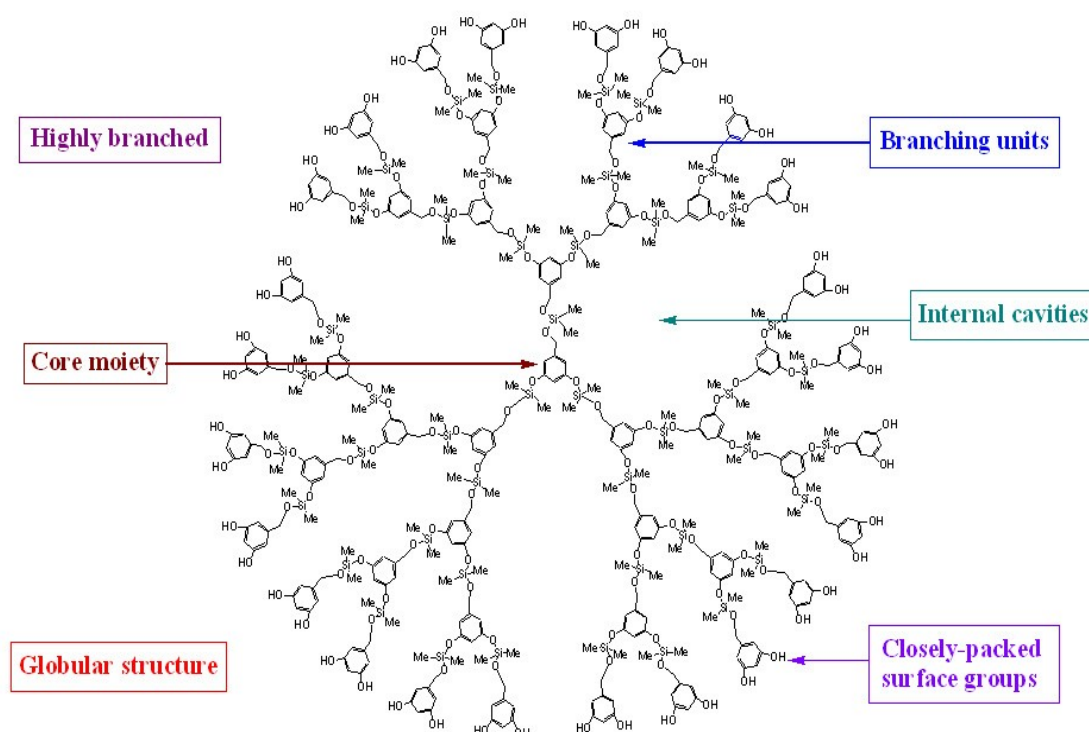
important thermal properties with respect to their potential applications in the field of rheology modifiers. Upon heating, amorphous components convert at T_g from a glassy state to a liquid state. T_g of hyperbranched polymers is not only affected by the chain-end composition but also by the molar mass and the macromolecular composition¹⁸. It increases with generation number to a limit, above which it remains nearly constant¹⁸. This increase in T_g with generation number reflects a decrease in chain mobility due to branching. In addition to their thermal properties, hyperbranched polymers present interesting mechanical and rheological properties. Their non-entangled state leads to unique mechanical properties, resulting in brittle dendritic polymers¹⁹. This is due to their globular structure, which does not permit the process of chain extension and orientation. However, intermolecular interactions like hydrogen bonding and possibly intermolecular crystallization of linear segments, provide connections between hyperbranched polymers²⁰.

The viscosity behaviour of these macromolecules is quite different from their linear counterparts. For linear polymers, above a critical molar mass, a drastic increase in melt viscosity is observed. But hyperbranched polymers show a continuous slope of 1.1 up to 100,000 a.m.u. with no critical mass limit. Indeed, at low molar mass, linear polymers consist of random coil chains, and as the molar mass increases, start to entangle at a critical molecular size, leading to a sharp increase in melt viscosity. Unlike linear polymers, the lack of chain entanglement of hyperbranched polymers leads to considerably smaller melt viscosities^{14,19,21,22}.

A variety of hyperbranched polymers are commercially available in large quantities and at a low cost. Most of the applications of hyperbranched polymers are based on the absence of chain entanglements, almost globular shape, and the nature and large number of functional groups within a molecule. Modification of the number and type of functional groups on hyperbranched polymers is essential to control their solubility, compatibility, reactivity, adhesion to various surfaces, self-assembly, chemical recognition, and electrochemical and luminescent properties. In other words, the large number of functional groups allows for tailoring of their thermal, rheological, and solution properties, and provides a powerful tool to design hyperbranched polymers for a wide variety of applications^{17,19,23-25}. These advantages of hyperbranched architecture can be further advanced by the inclusion of monodisperse nature.

1.1 Dendrimers

The word dendrimer is derived from the Greek words *dendri-* (tree branch-like) and *meros* (part of). Dendrimers, highly branched and monodisperse macromolecules, are the recently recognized members of the polymer field, with the first dendrimer report published in 1980s by the groups of Vögtle²⁶, Denkewalter, Tomalia²⁷ and Newkome²⁸. A dendrimer is a three-dimensional monodisperse polymeric molecule, consisting of three distinct areas, as shown in **Scheme 2**: the polyfunctional central core or focal point which represents the center of symmetry; various well-defined radial-symmetrical layers of repeating units (also called generations) and the peripheral or terminal surface groups.



Scheme 2: Description of the dendritic structure²⁹⁻³⁰

The two most widely known dendrimers are the ones developed by Tomalia (PAMAM dendrimers)²⁷ and Fréchet poly(aryl ether)³¹.

1.1.2 Synthesis

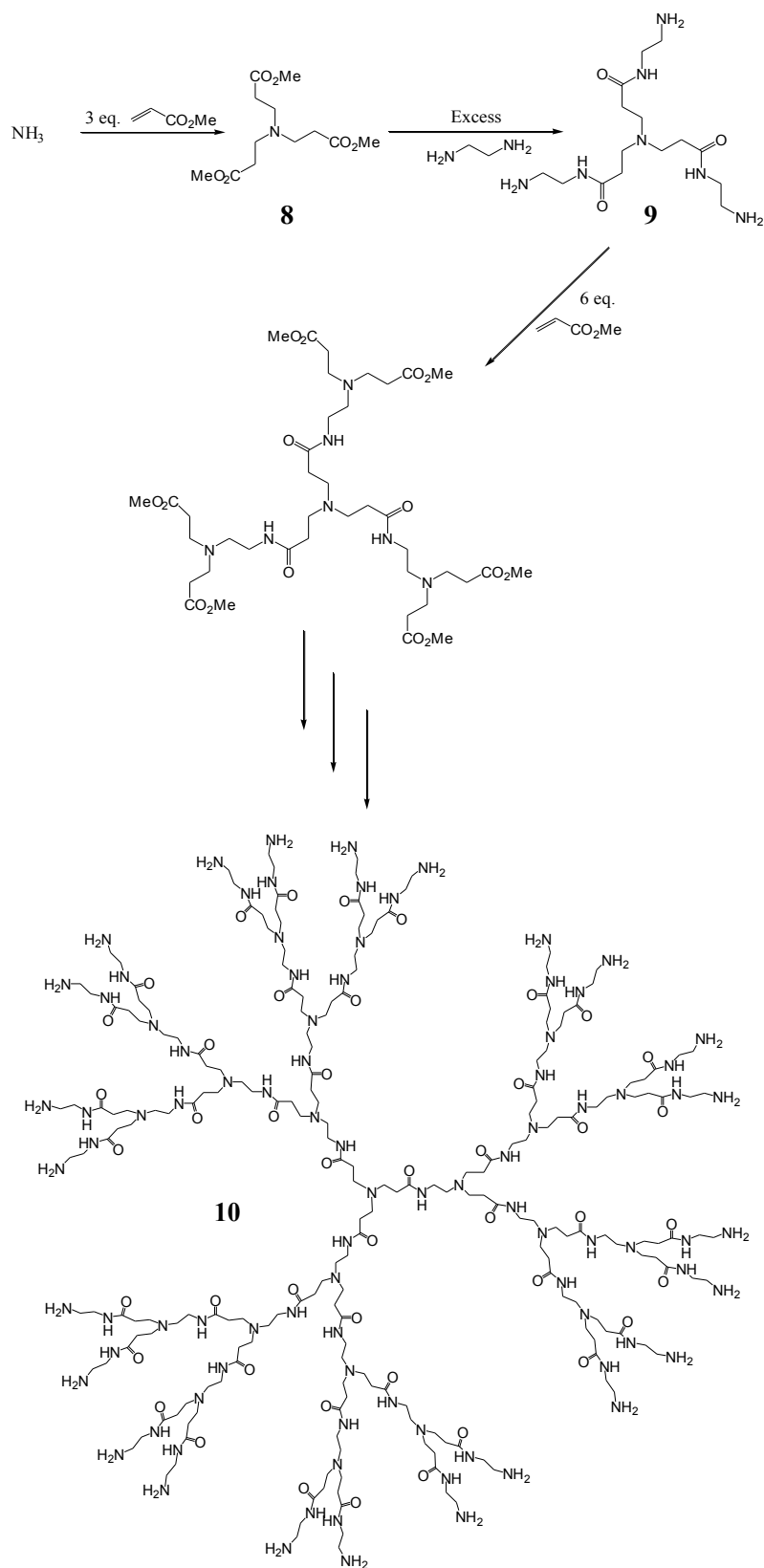
These highly well-defined macromolecules are obtained by an iterative sequence of reaction steps^{27,28,32,33}. Indeed one can choose between two different strategies to

synthesize dendrimers: the divergent (inside out) and the convergent (outside in) routes depending on the need and design for a particular application.

A) Divergent route

Divergent dendritic construction results from sequential monomer addition beginning from a core and proceeding outward towards the macromolecular surface³⁴. The divergent methodology is also called the “inside-out” approach. In 1978, Vögtle and coworkers²⁶ elaborated the first iterative reaction sequence, using a “divergent”-type methodology and leading to a simple dendritic structure.

Tomalia²⁷ used the conventional divergent approach to prepare the well known poly(amido amine) (PAMAM) dendrimers, produced on a kilogram scale and distributed commercially now. Synthesis of the PAMAM dendrimers (**Scheme 3**) begins from a trifunctional core, ammonia. This core molecule is converted into a three-armed, β -amino acid ester as intermediate (**8**) by using a Michael-type addition of methyl methacrylate. Large excess of ethylenediamine is required for amidation of the ester to form the first generation PAMAM dendrimer **9**. Repetition of this two-step reaction sequence leads to the growth of the dendrimer. Seventh generation PAMAM dendrimer has been reported to be prepared following this synthetic procedure.³⁴ Because they can be produced on a commercial scale, poly(propylene imine) dendrimers of Meijer et al.^{32,35,36} and PAMAM dendrimers have demonstrated that the divergent route can be a powerful route for synthesizing dendritic macromolecules. Surface modifications of these two dendrimers led to a variety of dendrimers synthesized using a divergent route.³⁴

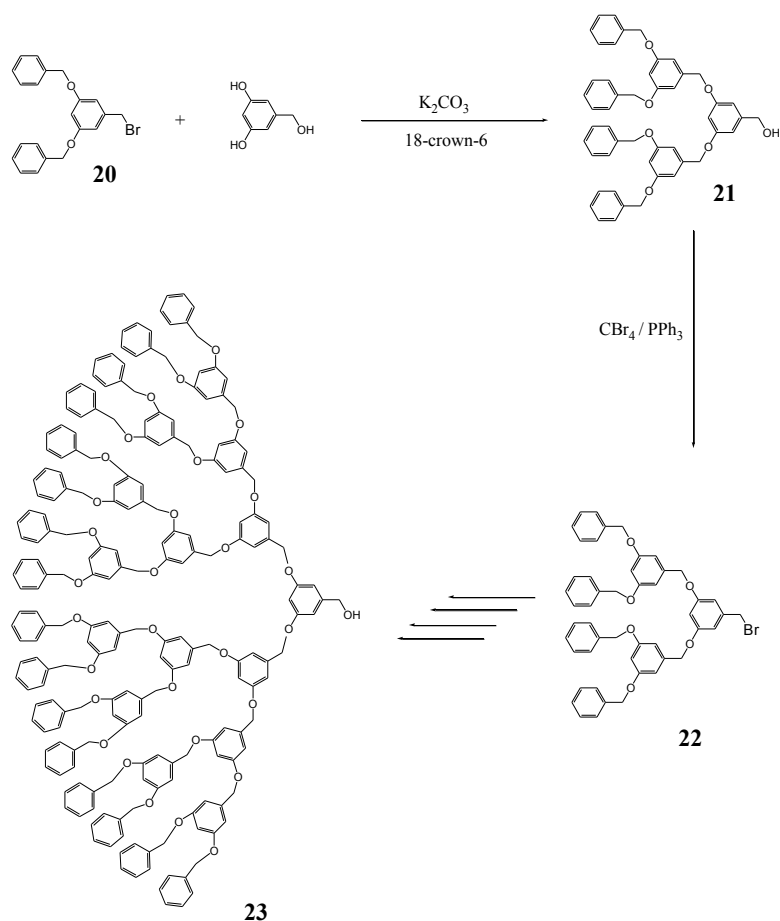


Scheme 3: Divergent approach for the construction of PAMAM dendrimers.²⁷

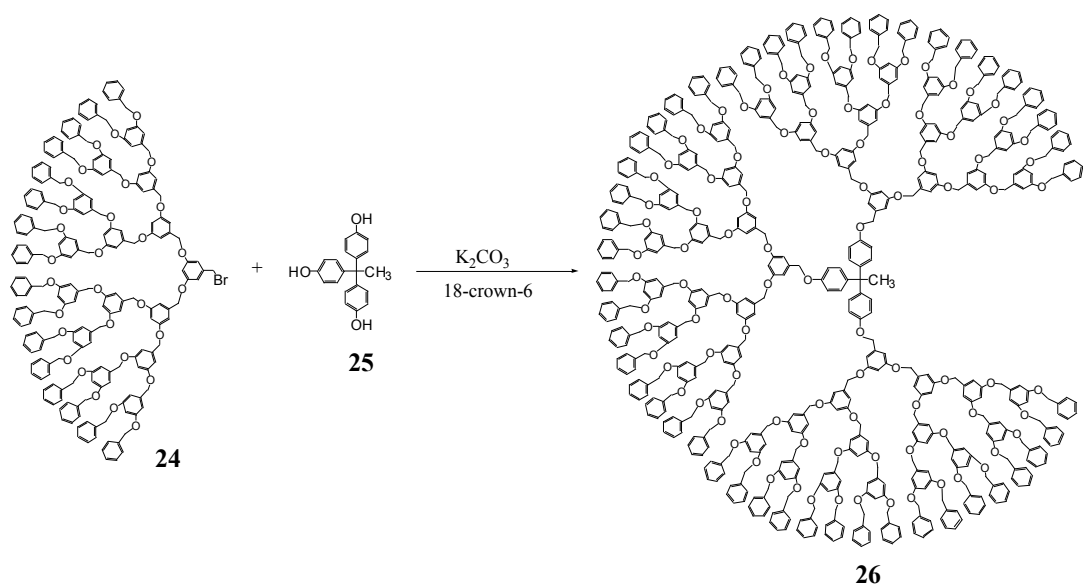
The divergent methodology presents some disadvantages although it is a powerful synthetic tool. Divergently built dendrimers might contain structural defects due to steric congestion as the macromolecule grows in size. An excess of reagent is often needed to force reaction completion and its removal can become a problem. The divergent methodology is a quite rigid method. This layer-by-layer protocol makes it very difficult to build up dendrimers with structurally different dendrons. Also, reaching high generation numbers can be long and tedious.

B) Convergent route

On the other hand, dendrimers can be prepared by using the convergent methodology, also called the “outside-in” approach³⁴. With this synthesis, the branched polymeric arms (dendrons) are synthesized first, and attached in a final step to a polyfunctional core molecule. Preparation of the first generation begins by connecting two peripheral units to one complementary monomer containing a masked branch site. The protected functional group also called focal group, is then unmasked, and reacts with half an equivalent of the masked monomer to yield second-generation dendron. Repetition of this reaction sequence yields dendrons with the desired generation number. Structurally different dendrons, synthesized separately with different monomers can be attached to the same polyfunctional core during the final step of dendrimer formation. First introduced by Neenan & Miller^{37,38} separately, the convergent methodology has been widely used to build dendrimers with a variety of structures. The convergent strategy designed by Hawker and Fréchet³¹ in the construction of poly(aryl ether) dendrimers (**Scheme 4**) has inspired many other research groups in the field of dendrimer chemistry. Dendrons are built starting from a first generation benzylic bromide **20**. Second generation benzylic alcohol **21** is prepared by coupling the first generation benzylic bromide with half an equivalent of 3,5-dihydroxybenzyl alcohol in the presence of 18-crown-6 and potassium carbonate. In order to restore the reactive bromomethyl functionality at focal point of the growing wedge, the benzylic alcohol group of the second generation dendron is converted into benzylic bromide functionality (**22**). This two-step reaction sequence is repeated to obtain fourth generation dendron (**23**). The latter is then converted into its benzylic bromide analogue **24**, and attached to a trifunctional core molecule, 1,1,1-tris(4'-hydroxyphenyl)ethane **25**, to afford dendrimer **26** (**Scheme 5**).



Scheme 4: Construction of a poly(arylether) fourth generation dendron following Fréchet's convergent route.³¹



Scheme 5: Attaching the Fréchet type dendron to a trifunctional core.³¹

Compared to the divergent route, the convergent methodology requires a fewer number of steps. The convergent strategy allows the synthesis of asymmetric dendrimers, or dendrimers having mixed structural elements. This approach to create heterogeneous dendrimers incorporates several “active sites” in one dendrimer to create multifunctional macromolecular structures. However, the convergent approach often limits the maximum size of the resulting dendrimers. Large dendritic wedges may induce steric congestion that may prevent their connection to small core molecules.

1.1.3 Properties

As described earlier, dendrimers are highly well defined macromolecules and may be viewed as unique and nanoscale devices. Each architectural component manifests a specific function, while at the same time defining properties for these nanostructures as they grow generation by generation. For example the core may be thought as the molecular information center from which, size, shape, directionality, and multiplicity are expressed *via* the covalent connectivity to the outer shells. Within the interior, one finds the branch-cell amplification region, which defines the type and volume of interior void space that may be enclosed by the terminal groups as the dendrimer is grown. The interior composition and volume of these internal cavities determine the extent and nature of guest-host properties that are possible within a particular dendrimer family and generation.

Finally, the surface consists of reactive or passive terminal groups that may perform several functions. Maybe the most exploited property of dendrimers is their multivalency. Unlike in linear polymers, when the molecular weight and generation of the dendrimer increase, the terminal units become more closely packed. The highly congested branching can have interesting effects on its conformation. At low generations, a dendrimer has a floppy, disc-like structure, but at higher generations, it adopts a more globular conformation. And this behaviour has a huge impact on their thermal, mechanical and rheological properties.

Dendrimers are almost exclusively amorphous materials, so the glass transition temperature T_g is one of the most important thermal properties. Van der berg and Meijer³⁹ found that the T_g for dendrimers of generation four or higher is almost independent of the molecular weight but strongly dependent on the kind of

functional end groups. In other words, T_g of dendrimers, as for hyperbranched polymers, is independent of the macromolecular architecture or shape, but dependent on the nature of the chain ends.

Like hyperbranched polymers, the configuration of dendrimers is coined by the lack of entanglements, and this leads to a particular viscosity behaviour. Dendrimer solutions have significantly lower viscosity than linear polymers⁴⁰. When the molecular mass of dendrimers increases, their intrinsic viscosity goes through a maximum at the fourth generation and then begins to decrease²¹. This behaviour is unlike that of linear polymers because for classical polymers the intrinsic viscosity increases continuously with molecular mass. Hawker and Devonport explained this behaviour by the globular, almost spherical structure of dendrimers, resulting in an increase in volume according to $V = 4\pi r^3/3$, while the dendrimers' mass doubles at each generation and thus increases exponentially in accordance with $M_w \sim 2^{(\text{generation}-1)}$. As their molecular weights increase, the rheological behaviour of dendrimers is dominated not by chain entanglement, but by interdigitation or interpenetration of the globular macromolecules, and this leads to the direct proportionality between intrinsic viscosity η and viscosity-average molecular weight M_η ⁴¹. Moreover linear polymers experience a dramatic increase in melt viscosity after a critical molecular weight. However, as for hyperbranched polymers, dendrimers show a continuous slope of 1.1 up to 100000 a.m.u with no critical weight limit being observed. Once more, this behaviour can be explained by the different macromolecular architecture of linear polymers vs. dendrimers. For low molecular weights, linear polymers consist of random coil chains, which, as the molecular weight increases, start to entangle at a critical molecular size, leading to a sharp increase in melt viscosity. In contrast, the globular, highly branched architecture of dendrimers seems to prevent chain entanglement, resulting in a continuous slope of melt viscosity. The properties of dendrimers depend more on the chain length between the branching points than on the total molecular weight. Therefore, regardless of the total molecular weight, a dendrimer behaves like a low molecular weight polymer as long as the chain length between the branching point is less than the critical molecular weight for chain entanglements¹⁴.

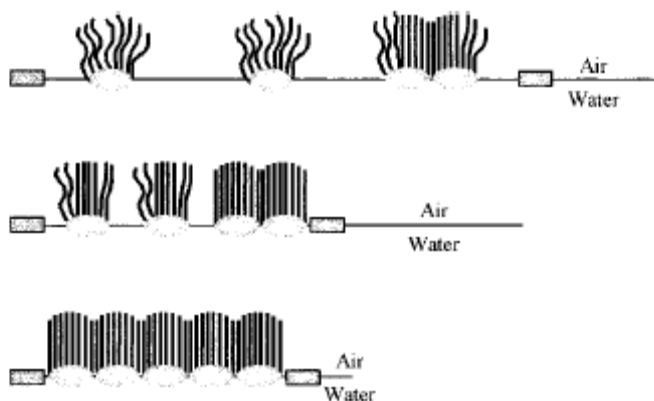
The presence of many terminal groups is responsible for the high solubility, miscibility and for high reactivity of dendrimers⁴⁰. The solubility of a dendrimer can be modulated by these peripheral end groups. Hydrophilic terminal groups can make

water soluble, a dendrimer with a hydrophobic core⁴² and hydrophobic peripheral groups can make a dendrimer with a hydrophilic interior, soluble in oil.

1.1.4 Applications

As mentioned earlier, due to their multistep syntheses, dendrimers have a uniform well-defined architecture, which can be tailored in terms of properties according to the desired applications. The possibilities of designing these appealing macromolecules, for example by choosing specific functional end groups or certain multifunctional monomers, is a very powerful tool that enables the exploration and development of a wide variety of applications. Dendrimers can be tailored with functional building blocks for the creation of self-organizing, so-called self-assembled, nanostructures. Self-assembling dendrimers are considered to be model compounds for biological systems as vesicles and micelles¹. Newkome et al. raised the idea of constructing three-dimensional dendrite networks linked by supramolecular interactions, especially by hydrogen bonding and metal complexation^{34,43}.

Based on this self-assembling nature, the formation of supramolecular amphiphilic assemblies at the air-water interface in the form of stable Langmuir-Blodgett monolayers has been reported⁴⁴ and can be seen in **Scheme 6**.



Scheme 6: Schematic representation of the organization of amphiphilic dendrimers in a monolayer on the water surface⁴⁴. (Reproduced by permission of The American Chemical Society)

Together with the ability of dendrimers to form nanostructures, these surface characteristics proved to be suitable for dendrimer applications as templating agents for nanoporous materials, as well as surface-active antibody conjugates with enhanced

detection capability for biological components⁴⁵. Wang et al. demonstrated the use of a novel type of biosensor⁴⁶, consisting of dendritic DNA surface layers and mass-selective piezoelectric transducers, which allows detection and monitoring of hybridization as shown in **Figure 1**.

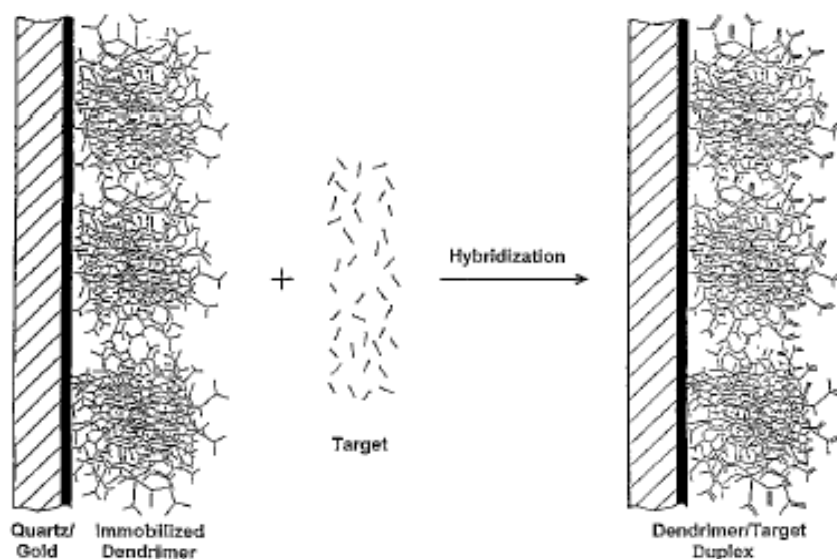


Figure 1: Schematic drawing showing the hybridization detection at the dendrimer/quartz-crystal microbalance (QCM) biosensor⁴⁶. (Reproduced by permission of The American Chemical Society)

Self-organization of dendrimers in liquid-crystalline phases has also been investigated. Liquid crystal polymers are of considerable interest for specific applications such as electronic components, housings for light-wave conductors, and filaments. Due to their highly branched, globular structure, dendrimers were first believed to be amorphous macromolecules. However, various research groups presented a variety of approaches for the assembly of dendritic architectures showing liquid-crystalline mesophases.⁴³ Moreover, their unique structural features, such as monodispersity, internal cavities, and well-defined, three-dimensional architecture, coupled with possibilities to tailor their physical and chemical properties, suggest that dendrimers may function as synthetic analogues of enzymes, proteins and viruses. Since several dendrimers possess a low *in-vivo* toxicity, their applications as diagnostic imaging contrast agents, gene-therapy vectors, vaccines and drug-delivery agents have been studied intensively⁴⁷. According to chemical structure, flexibility, and number of branches at junction points, higher generation dendrimers tend to develop controlled cavities. This characteristic was exploited by Meijer et al.³⁵. They

have described experiments in which they had trapped four molecules of Rose Bengal or eight to ten molecules of p-nitrobenzoic acid in one dendrimer. **Figure 2** shows the principle of encapsulation/release process of guest molecules. Two guests of different sizes are encapsulated in the dendrimer. Dialysis is a common procedure used to remove excess guest. Then, the shell is partially perforated, liberating the smaller guest. Subsequent removal of the shell liberates the larger guests, with recovery of the starting poly(propylene imine) dendrimer. Success of this study made it very promising for drug delivery applications.

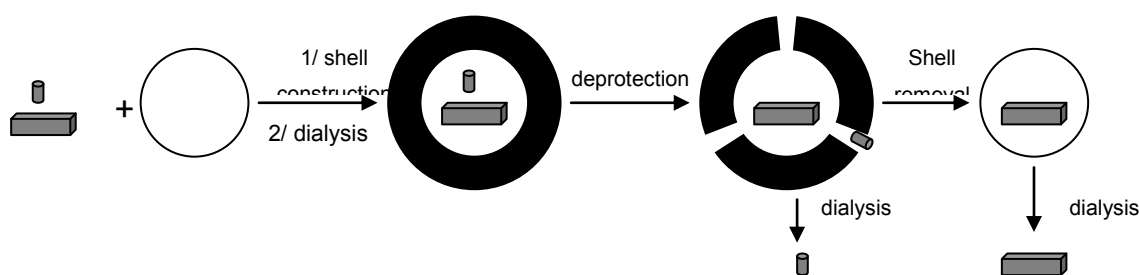


Figure 2: Schematic presentation of the principle of encapsulation and shape-selective liberation.³⁵

Archut and co-workers⁴⁸ developed a method in which boxes could be opened photochemically. A fourth generation propylene imine dendrimer with 32 terminal groups was terminated with azobenzene groups. The latter undergoes fully reversible photoisomerisation reaction. Photochemical modifications of the dendritic surface cause encapsulation and release of guest molecules.

An important area of research on dendrimers is the preparation of dendrimer-based catalysts. They consist of catalytic sites coupled with dendritic wedges, which function as an auxiliary for the enhancement of rate and selectivity. The catalytic sites can be introduced at the central core and or/ on the surface of the dendritic architecture⁴⁹, as shown in **Figure 3**.

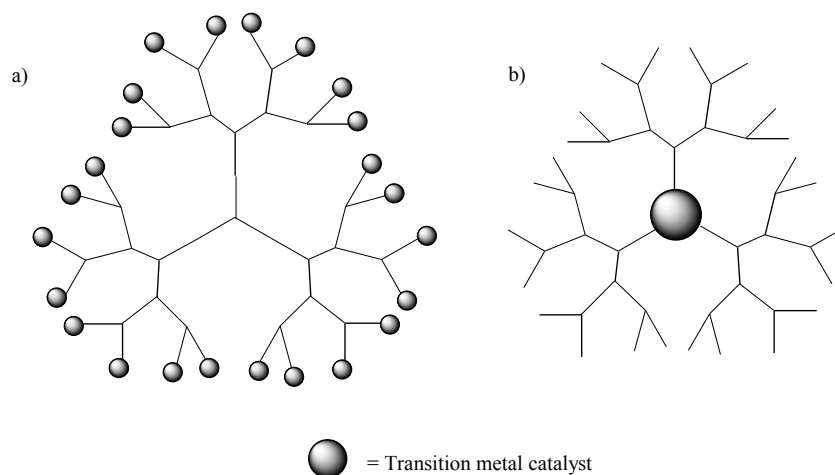


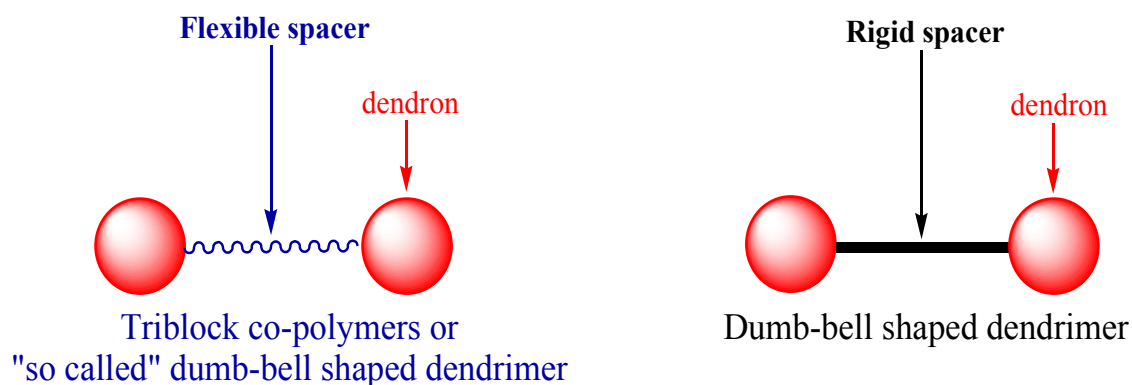
Figure 3: Transition metal catalyst fragment can be attached at the periphery (a) or at the core (b).⁴⁹

For example, Brunner demonstrated the preparation of an enantio- and size-selective catalyst, which consists of diphenyl-phosphine ligands substituted with chiral-surface dendritic wedges⁵⁰. Chiral catalysts permit the combination of advantages of homogeneous and heterogeneous catalysis since they could be employed in a homogeneous catalysis and then removed by means of ultrafiltration⁵¹. To conclude, dendrimers exhibit unique structures and properties, and the large interdisciplinary research on dendritic polymers has culminated in a remarkable variety of applications.

1.1.5 Dumbbell Shaped dendrimers

As mentioned above, the globular shape of dendrimers leads to interesting properties. Star-shaped dendrimers, such as PAMAM, have been widely studied over the past 20 years. Chemists have begun to develop different designs and shapes of dendrimers by modulating the central core of these macromolecules. Among them exist the dumbbell-shaped macromolecules with a bifunctional focal point but they are much less known and only a few studies have been performed so far^{52,53}. Since the characteristic properties are shape driven, this is only recently that the interest in these molecules of particular shape has grown.

Two categories of dumbbell-shaped molecules can be distinguished: the so called “dumbbell” shaped and the real dumb-bell macromolecules, as shown in **Scheme 7**.

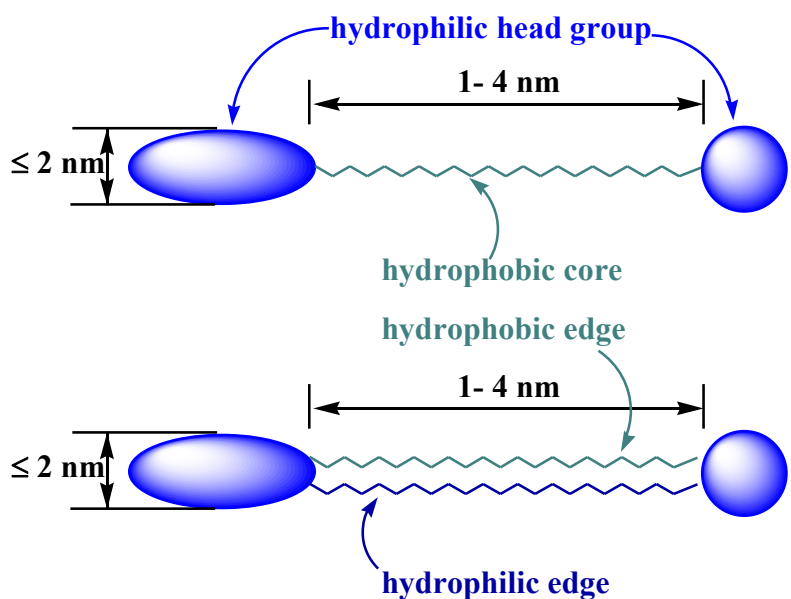


Scheme 7: Description of dumbbell shaped dendrimers

The so called “dumbbell” shaped macromolecules are made of a flexible chain as a core to which are attached dendrons on its ends. These triblock copolymers show interesting chemical and physical properties^{52,54,55}. Among these types of macromolecules exist the bolaamphiphiles.

a) Bolaamphiphiles

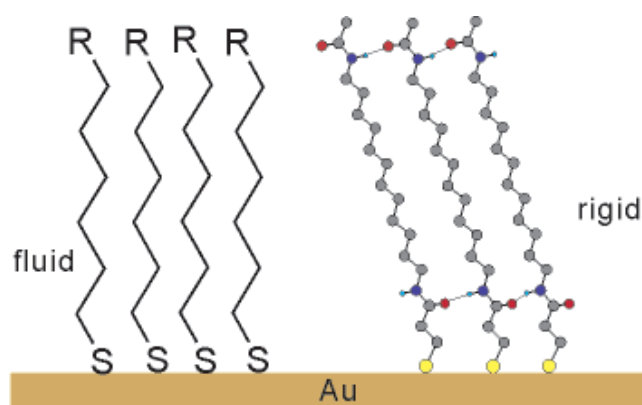
Bolaamphiphiles (or bolas) are defined as molecules in which two or more hydrophilic groups are connected by hydrophobic functionalities⁵⁶⁻⁶³ (Fuoss and Edelson, 1951), as described in **Scheme 8**. Other terms such as bolaform amphiphile⁶³ or arborol⁶⁴ have been used to describe molecules having this architecture. Since Fuhrhop and Mathieu^{56,57} reported the synthesis and self-assembly of several bolaamphiphiles, other researchers have explored applications of this architecture. The classical application of bolas is the formation of monolayer membrane (MLM) vesicles. These vesicles are robust with respect to fusion and flip-flop head groups, and their membrane may be one-half as thick as a bilayer⁵⁹.



Scheme 8: Schematic drawings of a bolaamphiphile

Synthetic bolaamphiphiles try to reproduce the unusual architecture of monolayered membranes found in archaebacteria but they don't use the same building blocks, which are difficult to synthesize⁶⁵. The ester bonds found in membrane lipids of most other organisms are replaced by ether bonds, which let the archaebacteria survive in a volcanic environment. Usually, the hydrophobic core possesses chiral methine groups with methyl substituents. They provide stiffness to the membrane by helix formation within the macrocycles.

Synthetic bolas tend also to form extended planar monolayers on the surface of water or of smooth solids⁶⁶ as shown in **Scheme 9**.



Scheme 9: Representation of a monolayer lipid membrane of a vesicle with charged headgroups^{60b,66}. (Reproduced by permission of The American Chemical Society)

Multilayers may be formed by the combination of two bolas with two cationic or two anionic headgroups or by combination of a dianionic bola and a cationic polymer or vice versa. Ultrasonication of aqueous dispersions of bola monolayers leads to spherical lipid particles made of monolayer lipid membranes (MLMs). Long-chain bolas produce vesicles. Short-chain, water-soluble bolas give micelles.

Bolas are very useful as coatings of smooth solid materials: one end of the bolas is covalently attached to the surface of electrodes⁶⁶ (**Scheme 9**), polyelectrolytes, or nanoparticles (**Figure 4**) whereas the other headgroups are used for the solubilization in water and for interactions with solutes.

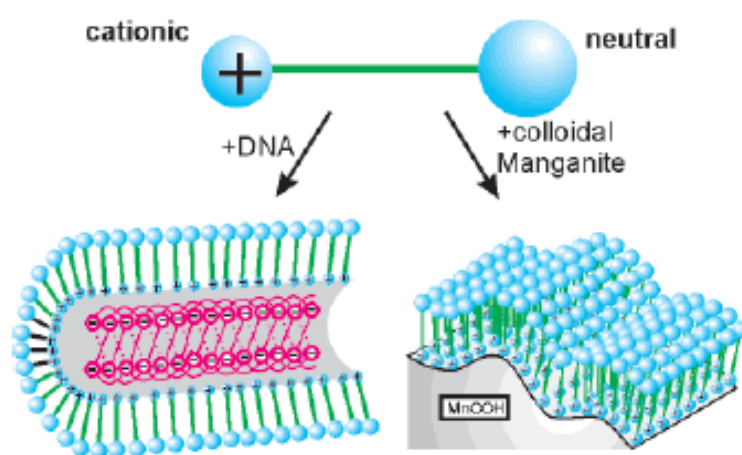


Figure 4: Bolas with an electroneutral and a positively charged head group used to neutralize surface charges of polyelectrolytes or a solvent for hydrophobic molecules^{60b,66}. (Reproduced by permission of The American Chemical Society)

Fluid or rigid monolayers covered with reactive end groups are thus obtained to yield electron-conducting materials⁶⁶.

Intra- and Intermolecular arrangements of bola headgroups are used to build monolayered lipid membranes (MLMs) in bulk aqueous media or on smooth solid surfaces. For these purposes the width of the bola's headgroups should be smaller or about the same as that of the hydrophobic core. The smallest hydrophilic headgroup is the primary amino group with a diameter of about 0.3 nm and a volume of 0.03 nm³. The largest known headgroups were made of a ruthenium-tris(bipyridyl) complex with a diameter of 1.0 nm and a volume of 1 nm³. Larger hydrophilic headgroups are usually polymeric and transform bolas into copolymers. The width of the hydrophobic core in known bolas lies between 0.5 and 3 nm. The third dimension or the thickness

of bolas units, is limited to less than 1 nm. More bulky molecules tend to arrange in crystals rather than in isolated monolayers. Bolas can be used also for the inclusion of functional groups into membranes, and the disruption of biological membranes, which could lead to therapeutic agents⁶⁷, as well as catalysts in reactions⁶⁸.

The bolamphiphiles are not limited to assemblies such as membranes and vesicles; specific “two-directional” arborols can form gels⁶⁹⁻⁷¹, rods and tubules are formed by α -L-Lysine- ω -aminobolaphiles⁷². When polymerizable functionalities are included either in the head groups or within the hydrophobic spacer, routes to extended covalently linked domains are opened⁷³. Nontraditional structures (e.g., aqueous gels) result when noncovalent forces are coupled with a proper molecular architecture. The series of two-directional arborols synthesized by Newkome et al. demonstrate this variation on the theme of self-assembly⁶⁹. In the proposed model of the aggregated structure one arborol is stacked with the next; the hydrophobic chains overlap and the hydrophilic hydroxyl groups are oriented toward the aqueous solution. Hydrogen bonding between the polar end groups and water results in solid matrix. This model is supported by the long fiberlike structures seen in electron micrographs of these assemblages⁷⁴. As with micelle formation, there is a minimum spacer length needed for gelation to occur; for saturated spacer this length is eight methylene units⁶⁹.

Use of Fréchet-type wedges has been reported through their attachment to other materials in order to modify their chemophysical properties. As one early example of such attachment, Gibsov et al.⁷⁵⁻⁷⁸ reported the synthesis of dendritic polyethereal copolymers (**Figure 5**). Similar linear-dendritic architectures, using “well-defined” blocks of poly(ethylene oxide), poly(ethylene glycol), polyester and also polystyrene have been reported.⁷⁹

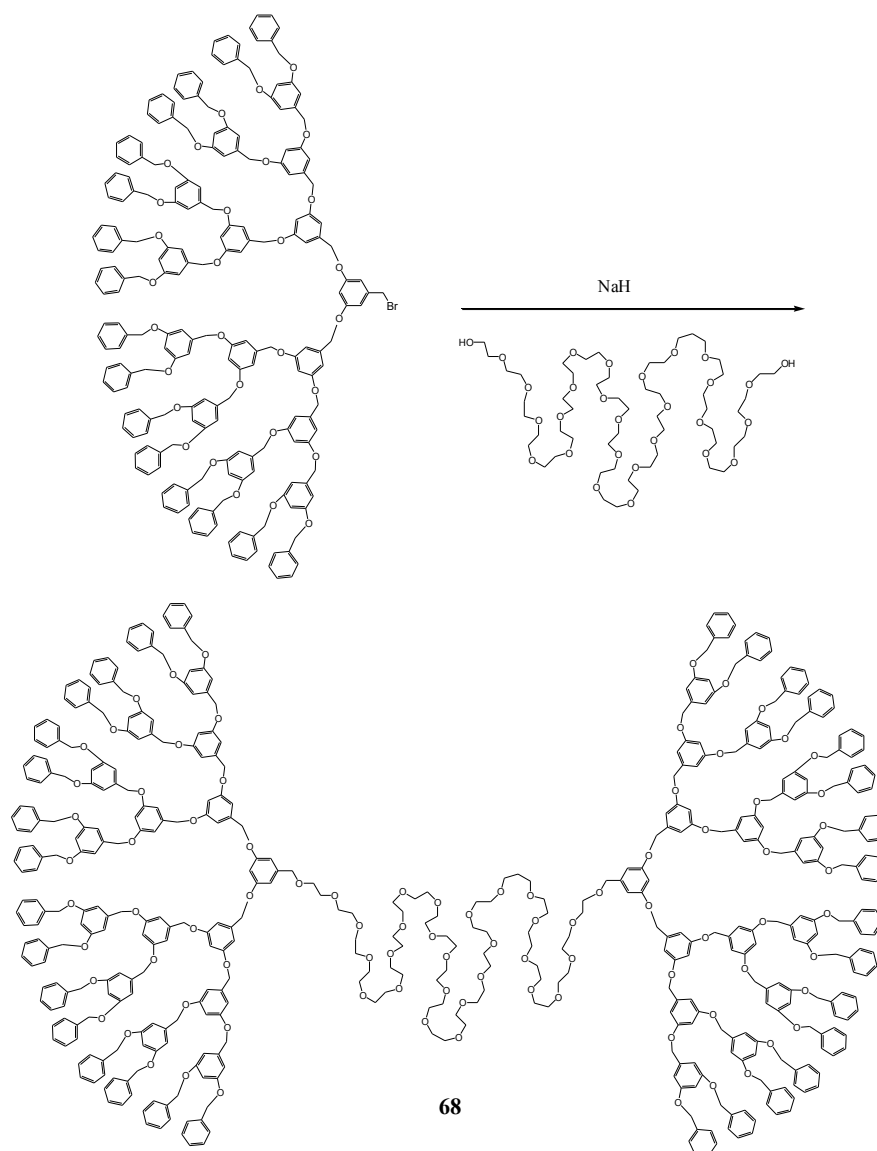


Figure 5: Attachment of Fréchet-type wedges to poly(ethylene oxide).⁷⁵⁻⁷⁸

Hirst and co-workers⁸⁰⁻⁸² have demonstrated that symmetric dendrimers based on building blocks constructed from L-Lysine form gel-phase materials with dendritically controlled physical properties. Moreover Suzuki and co-workers⁸³ have investigated new L-Lysine-based, low molecular-weight gelators in which two L-Lysine derivatives are linked by alkylene spacers. The gelators created a three-dimensional network by entanglement of self-assembled nanofibers *via* hydrogen bonding and van der Waals interactions. The hydrogel-broken temperatures (T_{gel}) depended on the carbon numbers of the alkylene spacers and showed an odd-even effect.

Cho and co-workers have prepared extended amphiphilic dendrons in the shape of macromolecular dumbbells with identical hydrophilic volume fractions but with branched second and third generation based amphiphilic dendrons⁵⁵ (**Figure 6**).

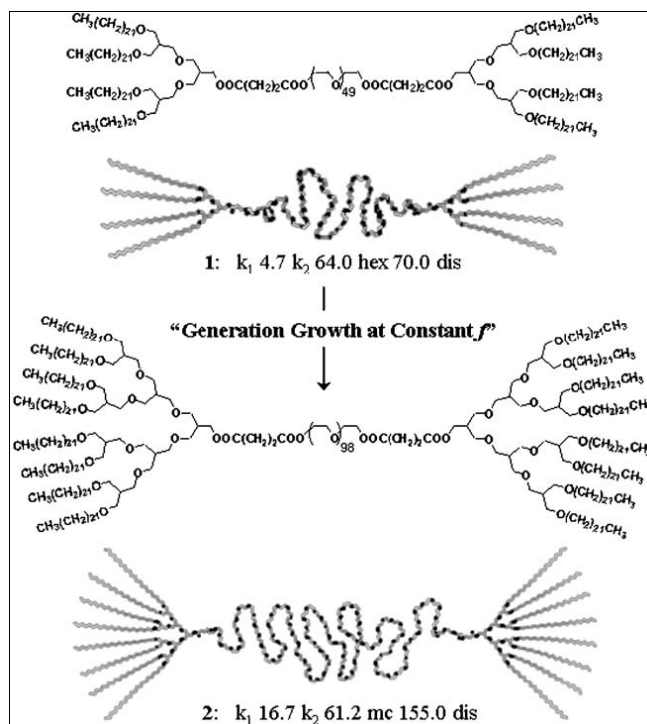


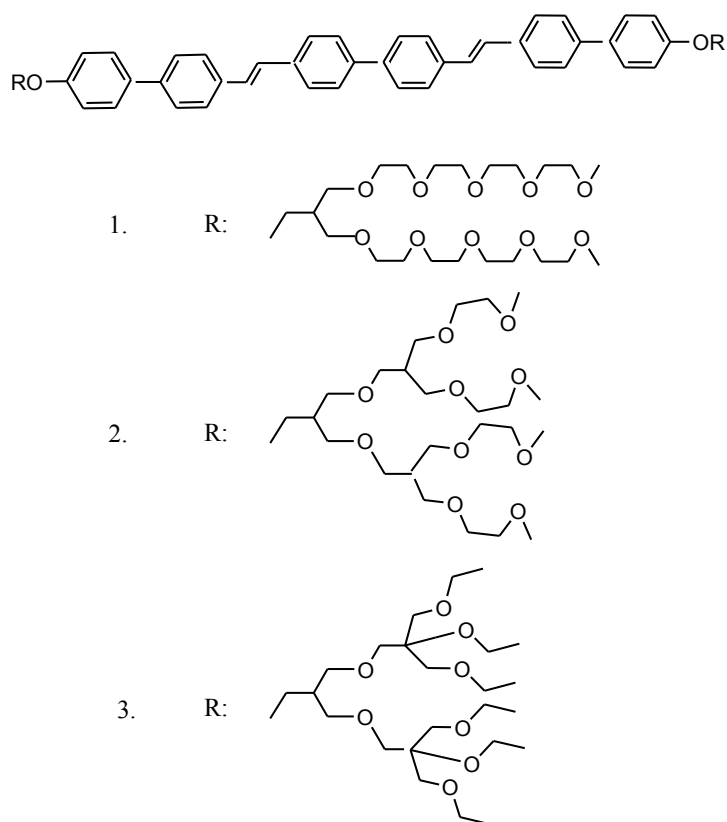
Figure 6: Molecular structures of ABA-extended amphiphilic dendrons 1 and 2⁵⁵. (Reproduced by permission of The Royal Society of Chemistry)

Second generation based species are consistent with a 2-D hexagonal columnar mesophase, while those of the third generation based compounds are consistent with a micellar cubic mesophase. Thus, compared to linear block copolymers, self-assembly can be tuned in more detail since, in addition to volume fraction, generation dependent molecular shape, is an independent parameter to tailor bulk supramolecular architecture.

b) Dumbbell shaped dendrimers

The real dumbbell-shaped dendrimers consist of dendritic wedges attached covalently to both ends of a rigid rod segment. Self-assembling molecules based on *p*-conjugated rods are receiving increased attention as building blocks for electrooptically active supramolecular structures, such a discrete bundles, ribbons, and vesicles⁸⁴⁻⁸⁸.

Lee and co-workers⁵³ have synthesized and investigated the self-assembling behaviour of dumbbell-shaped molecules consisting of three biphenyls connected through vinyl linkages as a conjugated rod segment and aliphatic dendritic wedges with different cross-sections, that is dibranch (1), tetrabranch (2) and hexabranch (3) (**Scheme 10**). They self-assemble into discrete bundles of tunable size that organize into three-dimensional superlattices. The size control of the bundles assembled from the rod building blocks was determined by the cross-section of the flexible segment attached to the rod ends.

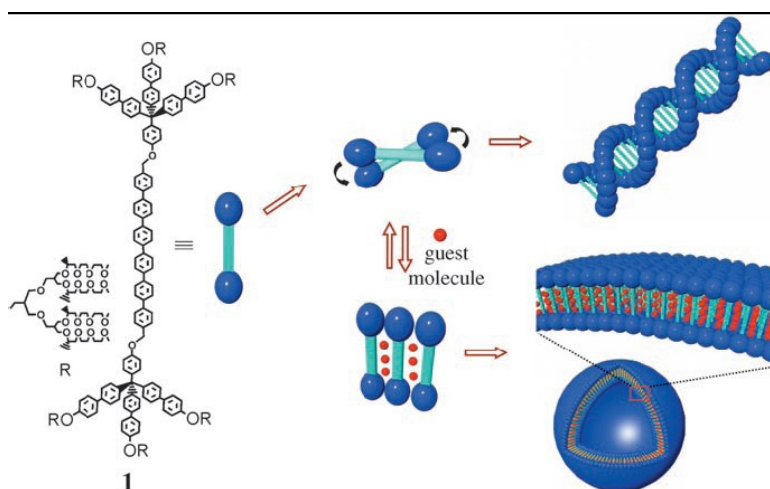


Scheme 10: Chemical structure of dumbbell-shaped molecules 1-3⁵³.

Another interesting property in this type of macromolecules is the formation of helical structures. Again Lee's group found that dumbbell-shaped molecules based on dodeca-*p*-phenylene⁸⁹ and *n*-hexa-phenylene⁹⁰ rods and bulky dendritic segments self-assemble into well-defined helical cylinders with the diameter of approximately the length of a molecule. The primary driving force responsible for the helical arrangement of the conjugated rods is believed to be the energy balance between

repulsive interaction among the adjacent bulky dendritic segments and π - π stacking interactions.

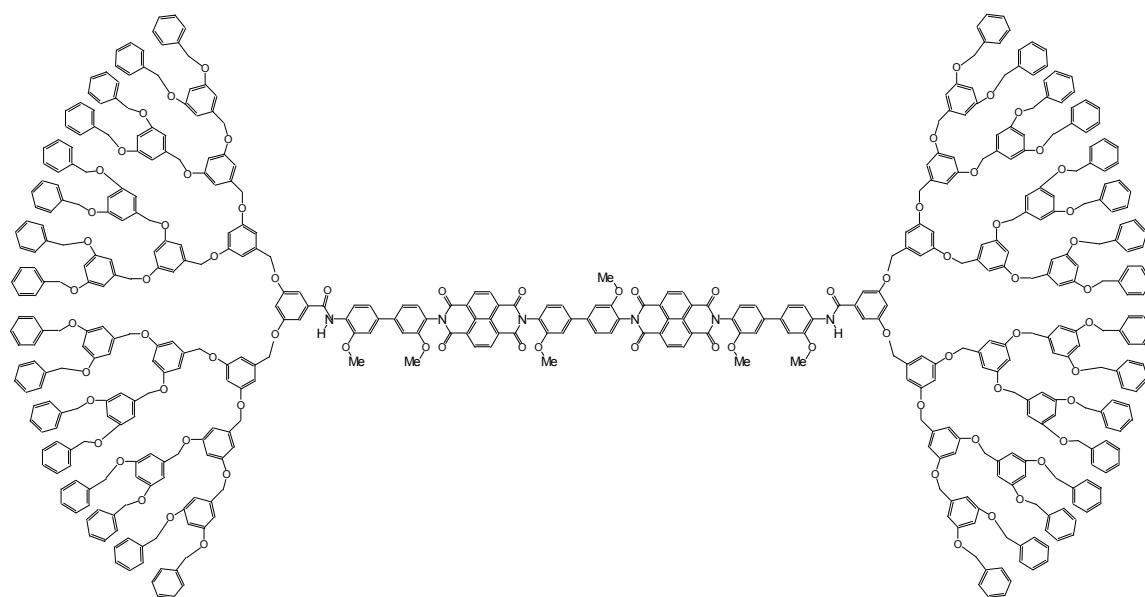
For the molecular dumbbells based on a n-hexa-phenylene rod, the helical structure transforms into a capsule- like structure on addition of guest molecules (**Scheme 11**). This reversible transformation between helical strands and nanocages in response to the addition of guest molecules is attributed to the intercalation of aromatic substrates within the rod segments and subsequent packing change of the rod segments from a twisted to a parallel arrangement to allow more space for guest molecules.



Scheme 11: Representation of the reversible transformation of helical fibers into a spherical capsule⁹⁰. (Copyright Wiley-VCH Verlag GmbH & Co. KGaA. Reproduced with permission)

This dynamic structural variation triggered by external stimuli may find useful applications in many areas including the development of responsive supramolecular materials. Moreover Malenfant and co-workers have studied the redox states of a series of well-defined hybrid dendrimers based on oligothiophene cores and poly(benzyl ether) dendrons⁹¹. The oxidation potentials and the electronic transitions of the neutral, singly oxidized, doubly oxidized states of these hybrid materials have been determined as a function of oligothiophene conjugation length. The attachment of poly(benzyl ether) dendritic wedges at both ends of these lengthy oligothiophenes considerably enhances their solubility. And it has been found that the effect on the properties of the redox states vary with the oligothiophene length and dendron size.

Another group, Miller and co-workers^{79,92} also synthesised polyether dendrons, generations 1-4, but in this case, they were connected to naphthalene diimides and rigid rod naphthalene diimide-benzidine oligomers (**Scheme 12**). The electrochemical reduction provided anion radicals on each diimide of the rigid rod. It was also found that larger dendrons slowed the electrochemical reaction, and had slightly larger effects when the rod was shorter. It was proposed that the bulky dendrons prevent access of the diimide groups to the electrode.



Scheme 12: Chemical structure of dumbbell-shaped macromolecule D_4 -BABAB- D_4 ⁹².

Dendrimers are aesthetically pleasing and chemically intriguing macromolecules. This appeal has been, and remains, mostly dictated by their globular structural build-up. Shape-driven application of dendrimers demand that more studies into non-spherical dendrimers have to be investigated.

1.1.6 Characterization

Dendrimers that are monodisperse and hyperbranched macromolecules are characterized by a variety of complimentary techniques. A brief description of some of these techniques and those that are more relevant to characterize dendrimers reported in this thesis, is given below.

A) FT-IR Spectroscopy

Infra-red radiation in the range of 666-4000 cm^{-1} is absorbed by organic molecules, and is converted into energy of molecular vibrations. These vibrations, that are of two types, *stretching* and *bending*, induce a rhythmical change in the dipole moment of the molecule to be observed. It is a “fingerprint technique” that allows to detect characteristic functional groups of the analysed molecules.

FT-IR technique can also easily detect hydrogen bonds that are generally formed when H is bonded to a small highly electronegative element (X-H, X = O, N, F). Hydrogen bonding alters the force constant, shifting the X-H stretching bands to lower frequencies.

B) Matrix Assisted Laser Desorption Ionization - Time of Flight (MALDI-TOF) Mass Spectroscopy

Common mass spectrometer apparatus measure the mass-to-charge ratio (m/z) of analyte ions, and require gas-phase ions for a successful analysis. It makes this technique incompatible with the study of polymers and dendrimers. However, by mixing a dilute solution of the analyte (dendrimer or hyperbranched polymer) to a more concentrated matrix solution and using a laser desorption method, analyte ions can be created. This laser desorption method is assisted by the matrix, hence the acronym MALDI, has been introduced by Tanaka⁹³ and Hillenkamp.^{94,95}

When a sample is irradiated by laser (nitrogen laser light, $\lambda = 337 \text{ nm}$), the matrix crystallises by instant evaporation of the solvent and captures the energy provided by the laser source. After that, follows the desorption of the analytes, cationized by protons or metal ions in gas phase (**Figure 7**). Typical MALDI-TOF matrices are aromatic organic acids that can readily absorb heat energy. The best compatibility between the dendritic systems reported in this thesis and organic matrices was found with dithranol or α -cyano-hydroxy-cinnamic acid. Sodium and potassium, even found in small amounts in the solution mixture, easily generate large amounts of Na^+ and K^+ . KBr and LiBr (found with dithranol) can also be added to the matrix solution to generate metal ions. This technique constitutes the most essential one for dendrimers.

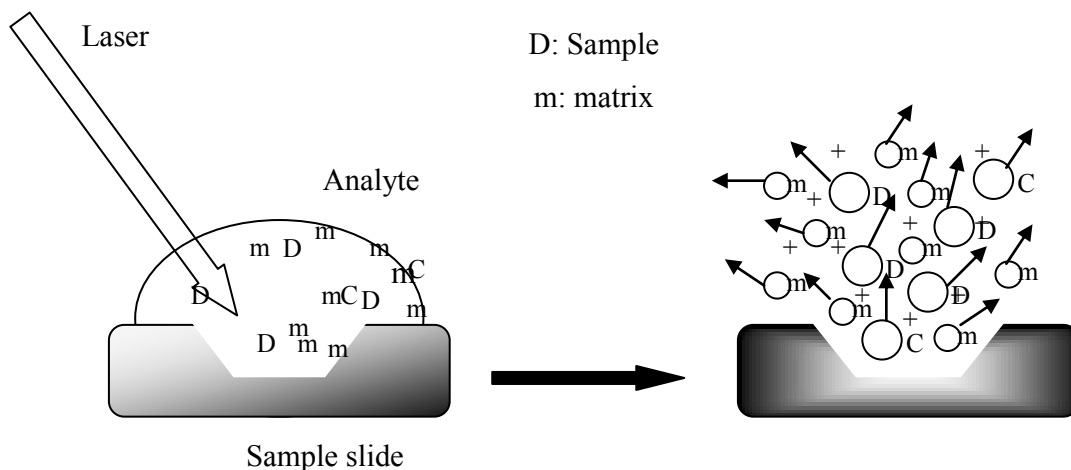


Figure 7: Ionization using the MALDI technique.

C) Transmission Electron Spectroscopy

The transmission electron microscope (TEM) was used to obtain essential information on a phenomenon of high interest in this thesis, the formation of aggregates. The image that can be seen on the screen is the result of differential loss of electrons from a beam transmitted through a thin-film sample. Electrons from a source (electron gun) are focused by a condenser lens, passed through the sample, and then to the objective lens to be finally imaged onto a fluorescent screen, or an image converter plate. These lenses are electromagnetic coils that focus the electrons as glass lenses would do with a ray of light. To create images of the specimen, the electrons are channeled and focused through a series of different lenses. The objective lens and the intermediate lens are the most important lenses of the TEM. Since variations in the current passing through the objective lens produce changes in the focal length, bringing the final magnified image into focus. The role of the intermediate lens is to produce changes in magnification.^{96,97}

D) UV-Visible Absorption Spectroscopy

Molecular absorption in the near UV (200-380 nm) and visible (380-780 nm) region of the spectrum is dependent on the electronic structure of the molecule. Energy absorbed in the ultraviolet region produces transitions of the valence electrons in the molecule. Changes in the electronic energy results in the excitation of an electron from a filled molecular orbital in the ground state (non bonding p or bonding π -orbital) to the next higher energy orbital (antibonding π^* orbital). The relation

between the absorbance and the concentration of the absorbing species is established by the Beer-Lambert's law:

$$A = \epsilon bc \quad \text{eqn. 2.1}$$

where A is the absorbance, ϵ the molar extinction coefficient, b the path length through the sample and c the concentration of the solute (in mol/L).

UV-visible spectroscopy can be a useful tool to study the *turbidity* of a solution^{96,97}. Turbidity can be defined as a decrease in the intensity of a beam of light because of scattering. By analogy to the Beer-Lambert's law, we can write

$$I = I_0 e^{-\tau l} \quad \text{eqn. 2.2}$$

where I_0 is the incident light intensity, I the transmitted light intensity, l the length of the light path and τ the turbidity coefficient. A connection can be made between the turbidity and the molecular weight of a solute featuring an ideal single molecular weight.⁹⁸

In summary, measuring the turbidities of solutions of varying concentration leads to a linear relation in which extrapolation to zero concentration results in determining the molecular weight inverse. By analogy to this method, it is possible to determine the *critical aggregation concentration (cac)* of the dendrimers. The scattering region of our UV spectra at varying concentrations as the differences in absorption are dependent on i) concentration, and on ii) formation of aggregates in solution. Plot of the absorption versus the concentration of the solute can be done at a chosen wavelength. Above *cac*, differences in absorption are pronounced leading to a linear relation when plotting A Vs c . Below *cac*, differences in absorption are smaller (only the result of difference in concentration) and lead to a another linear relation of a much lower slope when plotting A Vs c . Intercept of both linear relations occurs at *cac*.

1.2 Goals

The first goal of this thesis was to explore the synthesis of dendrimers with a shape that is different than typical spheres. Dumb-bell shaped dendrimers, containing a central linear core with an acetylenic moiety, were thus envisioned being synthesized by following a procedure that has been well developed in our laboratory. We planned to elaborate a divergent methodology that was based on simple and

versatile acid-base hydrolytic chemistry. This requires commercially available reagents, 2-butyne-1,4-diol, 3,5-dihydroxybenzyl alcohol (the acidic component) and bis(dimethylamino)dimethylsilane (the basic component). The formation of dendritic hyperbranched structures was subsequently investigated by the reaction of 2-butyne-1,4-diol with dimethylsilylamine to form the bifunctional focal point of the dumbbell shaped dendrimer. Then, repetition of a sequential addition of 3,5-dihydroxybenzyl alcohol and dimethylsilylamine, under controlled reaction conditions, will lead to the growth of the dendritic wedges. These dendrimers will be characterized using a combination of techniques to understand their structure-property relationships, in particular their self-assembly in different solvents. Finally, dumbbell shaped dendrimers will be used as templates in a one-step synthesis for the formation of silver nanoparticles. We will investigate their evolving morphologies by using complementary techniques. But, in order to understand the importance of metal particles and the evolving morphology in these nanoparticles, it is essential to include a brief introduction to metal nanoparticles that is provided in Chapter 2.

1.3 References

- [1] Zeng, F.; Zimmerman, S. C. *Chem. Rev.* **1997**, *97*, 1681.
- [2] Kawa, M.; Fréchet, J. M. J. *Chem. Mater.* **1998**, *10*, 286.
- [3] Fischer, M.; F. Vögtle, F. *Angew. Chem. Int. Ed.* **1999**, *38*, 884.
- [4] Adranov, A.; Fréchet, J. M. J. *Chem. Comm.* **2000**, 1701.
- [5] Chardac, F.; Astruc, D. *Chem. Rev.* **2001**, *101*, 2991.
- [6] Van Heerbeek, R.; Kamer, P. C. J.; Van Leeuwen, P. W. N. M.; Reek, J. N. H. *Chem. Rev.* **2002**, *102*, 3717.
- [7] Morgan, M.T.; Carnahan, M.A.; Immoos, C.E.; Ribeiro, A.A.; Finkelstein, S.; Lee, S.J.; Grinstaff, M.W. *J. Am. Chem. Soc.* **2003**, *125*, 15485.
- [8] Ooe, M.; Murata, M.; Mizugaki, T.; Ebitani, K.; Kaneda, K. *J. Am. Chem. Soc.* **2004**, *126*, 1604.
- [9] Flory P.J. *J. Am. Chem. Soc.* **1952**, *74*, 2718.
- [10] Stockmayer, W.H. *J. Chem. Phys.* **1943**, *11*, 45.
- [11] Stockmayer, W.H. *J. Chem. Phys.* **1944**, *12*, 125.
- [12] Kim, H.Y.; Webster, O.W. *J. Am. Chem. Soc.* **1990**, *112*, 4592.
- [13] Hawker, C.J.; Lee, R.; Fréchet J.M.J. *J. Am. Chem. Soc.* **1991**, *113*, 4583.
- [14] Kim, Y. H. *J. Polym. Sci. A: Polym. Chem.* **1998**, *36*, 1685.
- [15] Sunder, A.; Hanselmann, R.; Frey, H.; Mühlhaupt, R. *Macromolecules* **1999**, *32*, 4240.
- [16] Fréchet, J.M.J.; Henmi, M.; Gitsov, I.; Aoshima, S.; Leduc, M.R.; Grubbs, R.B. *Science* **1995**, *269*, 1080.
- [17] Yates, C.R.; Hayes, W. *Eur. Polym. J.* **2004**, *40*, 1257.
- [18] Wooley, K.L.; Hawker, J.M.; Pochan, J.M.; Fréchet, J.M.J. *Macromolecules* **1993**, *26*, 1514.
- [19] Hult, A.; Johansson, M.; Malström, E. *Adv. Polym. Sci.* **1999**, *143*, 1.
- [20] Rogunova, M.; Lynch, T.-Y.S.; Pretzer, W.; Kulzick, M.; Hiltner, A.; Baer, E. *J. Appl. Polym. Sci.* **2000**, *77*, 1207.
- [21] Mourey, T.H.; Turner, S.R.; Rubinstein, M.; Fréchet, J.M.J.; Hawker, C.J.; Wooley, K.L. *Macromolecules* **1992**, *25*, 2401.
- [22] Wooley, K.L.; Fréchet, J.M.J.; Hawker, C.J. *Polymer* **1994**, *35*, 4489.
- [23] Voit, B. *J. Polym. Sci. A: Polym. Chem.* **2000**, *38*, 2505.
- [24] Voit, B. *J. Polym. Sci. A: Polym. Chem.* **2005**, *43*, 2679.

- [25] Gao, C.; Yao, D. *Prog. Polym. Sci.* **2004**, *29*, 183.
- [26] Buhleier, E.; Wehner, W.; Vögtle, F. *Synthetic (Mass)* **1978**, 155.
- [27] Tomalia, D. A.; Baker, H. ; Dewald, J. R.; Hall, M.; Kallos, G.; Martin, S. ; Roeck, J; Ryder, J.; Smith, P. *Polym. J.* **1985**, *17*, 117.
- [28] Newkome, G.R., Yao, Z., Baker, G.R.; Gupta, V.K. *J. Org. Chem.* **1985**, *50*, 2003.
- [29] Bourrier, O.; Kakkar, A.K. *J. Mater. Chem.* **2003**, *13*, 1.
- [30] Hourani, R.; Kakkar, A.K. *J. Mater. Chem.* **2005**, *15*, 2106.
- [31] Hawker, C.J.; Fréchet, J.M.J. *J. Chem. Soc., Chem. Comm.* **1990**, 1010.
- [32] De Brabander-van den Berg, E.M.M.; Meijer, E.W. *Angew. Chem. Int. Edn. Engl.* **1993**, *32*, 1308.
- [33] Hawker, C.J.; Fréchet, J.M.J. *J. Am. Chem. Soc.* **1990**, *112*, 7638.
- [34] Newkome, G. R.; Moorefield, C. N.; Vögtle, F. Dendrimers and Dendrons: Concepts, Syntheses, Applications, 1st edn; Wiley-VCH:Weinheim, **2001**.
- [35] Jansen, J. F. G. A. ; De Brabander-van den Berg, E. M. M.; E. W. Meijer, E. W. *Science* **1994**, *266*, 1226.
- [36] Jansen, J. F. G. A.; Meijer, E. W. *J. Am. Chem. Soc.* **1995**, *117*, 4417.
- [37] Miller, T. M.; Neenan, T. X. *Chem. Mater.* **1990**, *2*, 349.
- [38] Miller, T. M.; Neenan, T. X.; Zayas, R.; Blair, H. E. *J. Am. Chem. Soc.* **1992**, *114*, 1018.
- [39] De Branbender van der Berg, E.; Meijer, E. *Angew. Chem.* **1993**, *105*, 1370.
- [40] Fréchet, J.M.J. *Science* **1994**, *263*, 1710.
- [41] Hawker, C. J. *Curr. Opin. Colloid Interface Sci.* **1999**, *4*, 117.
- [42] Liu, M.; Kono K.; Fréchet J.M.J. *J. Control. Release* **2000**, *65*, 121.
- [43] Inoue, K. *Prog. Polym. Sci.* **2000**, *25*, 453.
- [44] Schenning, A.; Roman, C.; Weener, J.; Baars, M.; van der Gaat, S.; Meijer, E. *J. Am. Chem. Soc.* **1998**, *120*, 8199.
- [45] Durst, D. *Proc. 50th SERMACS Conf.* **1998**, *50*, 234.
- [46] Wang, J.; Jiang, M.; Nilsen, T.; Getts, R. *J. Am. Chem. Soc.* **1998**, *120*, 8281.
- [47] Matthews, O. A.; Shipway, A.N.; Stoddart, J. F. *Prog. Polym. Sci.*, **1998**, *23*, 1.
- [48] Archut, A.; Azzelini, G.C.; Balzani, V.; Cola, L.D.; Vögtle, F. *J. Am. Chem. Soc.* **1998**, *120*, 12187.
- [49] Oosterom, G. E.; Reek, J. N. H.; Kamer, P. C. J.; Van Leeuwen, P. W. N. M. *Angew. Chem. Int. Ed.* **2001**, *40*, 1828.

- [50] Brunner H. *J. Organomet. Chem.* **1995**, *500*, 39.
- [51] Vögtle, F.; Gestermann, S.; Hesse, R.; Schwierz, H.; Windisch, B. *Prog. Polym. Sci.* **2000**, *25*, 987.
- [52] Gitsov, I.; Fréchet J.M.J. *Macromolecules* **1994**, *27*, 7309.
- [53] Lee, M.; Jeong, Y.-S.; Cho, B.-K.; Oh, N.-K.; Zin, W.-C. *Chem. Eur. J.* **2002**, *8*, 876.
- [54] Tang, X.-D.; Fan, X.-H.; Zhang, Q.-Z.; Chen, X.-F.; Li, A.-X.; Zhou, Q.F. *Chin. J. Chem.* **2005**, *23*, 11.
- [55] Cho, B.-K.; Jain, A.; Gruner, S.M.; Wiesner, U. *Chem. Commun.* **2005**, 2143.
- [56] Fuhrhop, J.-H.; Mathieu, J. *Angew. Chem.* **1984**, *96*, 124.
- [57] Fuhrhop, J.-H.; Mathieu, J. *Angew. Chem., Int. Ed. Engl.* **1984**, *23*, 100.
- [58] Fuhrhop, J.-H.; Fritsch, D. *Acc. Chem. Res.* **1986**, *19*, 130.
- [59] Escamilla, G.H.; Newkome, G.R. *Angew. Chem., Int. Ed. Engl.* **1994**, *33*, 1937.
- [60] a) Fuhrhop, J.-H.; Koenig, J. Molecular Assemblies and Membranes, Monographs in Supramolecular Chemistry, Stoddart, J.F., Ed.; Royal Society of Chemistry; London, **1994**; Vols. *i-xiii*, pp 1-227. b) Fuhrhop, J.-H.; Wang, T. *Chem. Rev.* **2004**, *104*, 2901.
- [61] a) Zahna, R. Specialist Surfactants, Robb, I.D., Ed.; Chapman & Hall; Glasgow, **1996**, p 81.
- [62] Fuhrhop, J.-H.; Endlisch, C. Molecular and Supramolecular Chemistry of Natural Products and Model Compounds; Marcel Dekker; New York, **2000**; p 606.
- [63] Fuoss, R.M.; Edelson, D.J. *J. Am. Chem. Soc.*, **1951**, *73*, 269.
- [64] Newkome, G.R.; Baker, G.R.; Arai, S.; Saunders, M.J.; Russo, P.S.; Gupta, V.K.; Yao, Z.-Q.; Miller, J.E.; Bouillon, K. *J. Chem. Soc., Chem. Commun.* **1986**, 752.
- [65] Yamauchi, K.; Kinoshita, M. *Prog. Polym. Sci.* **1993**, *18*, 763.
- [66] Ulman, A. An Introduction to Ultrathin Organic Films, from Langmuir-Blodgett to Self-Assembly; Jovanovich, H. B., Ed.; Academic Press: New York, **1991**.
- [67] Hudson, R.H.E.; Damha, M.J. *J. Am. Chem. Soc.* **1993**, *115*, 2119.
- [68] Fornasier, R.; Scrimin, P.; Tecilla, P.; Tonellato, U. *J. Am. Chem. Soc.* **1989**, *111*, 224.
- [69] Newkome, G.R.; Lin, X.; Yaxiong, C.; Escamilla, G.H. *J. Org. Chem.* **1993**, *58*, 3123.
- [70] Newkome, G.R.; Moorefield, C.N.; Baker, G.R.; Behera, R.K.; Escamilla, G.H.; Saunders, M.J. *Angew. Chem.* **1992**, *104*, 901.

- [71] Newkome, G.R.; Moorefield, C.N.; Baker, G.R.; Behera, R.K.; Escamilla, G.H.; Saunders, M.J. *Angew. Chem., Int. Ed. Engl.* **1992**, *31*, 917.
- [72] Fuhrhop, J.-H.; Spiroski, D.; Boettcher, C. *J. Am. Chem. Soc.* **1993**, *115*, 1600.
- [73] Fendler, J.-H.; Tundo, P. *Acc. Chem. Res.* **1984**, *17*, 3.
- [74] Newkome, G.R.; Baker, G.R.; Arai, S.; Saunders, M.J.; Russo, P.S.; Theriot, K.J.; Moorefield, C.N.; Miller, J.E. Bouillon, K. *J. Am. Chem. Soc.* **1990**, *112*, 8458.
- [75] Gitsov, I.; Wooley, K. L.; Fréchet, J. M. J. *Angew. Chem. Int. Ed.* **1992**, *31*, 1200.
- [76] Gitsov, I.; Wooley, K. L.; Hawker, C. J.; Fréchet, J. M. J. *Macromolecules* **1993**, *26*, 5621.
- [77] Gitsov, I.; Fréchet, J. M. J. *Macromolecules* **1993**, *26*, 6536.
- [78] Gitsov, I.; Fréchet, J. M. J. *Polym. Mater. Sci. Eng.* **1995**, *73*, 129.
- [79] Miller, L. L.; Zinger, B.; Schlechte, J. S. *Chem. Mater.* **1999**, *11*, 2313.
- [80] Love, C.S.; Hirst, A.R.; Chechik, V.; Smith, D.K.; Ashworth, I.; Brennan, C. *Langmuir* **2004**, *20*, 6580.
- [81] Hirst, A.R.; Smith, D.K.; Feiters, M.C.; Geurts, H.P.M. *Langmuir* **2004**, *20*, 7070.
- [82] Hirst, A.R.; Smith, D.K. *Org. Biomol. Chem.* **2004**, *2*, 2965.
- [83] Suzuki, M.; Nanbu, M.; Yumoto, M.; Shirai, H.; Hanabusa, K. *New. J. Chem.* **2005**, *29*, 1439.
- [84] Leclere, P.; Calderone, A.; Marsitzky, D.; Francke, V.; Geertz, Y.; Müllen, K.; Bredas, J.L.; Lazzaroni, R. *Adv. Mater.* **2000**, *12*, 1042.
- [85] Wang, H.; You, W.; Jiang, P.; Yu, L.; Wang, H.H. *Chem. Eur. J.* **2004**, *10*, 986.
- [86] Kilbinger, A.F.M.; Schenning, A.P.H.J.; Goldoni, F.; Feast, W.J.; Meijer, E.W. *J. Am. Chem. Soc.* **2000**, *122*, 1820.
- [87] Zahn, S.; Swager, T.M. *J. Am. Chem. Soc.* **2002**, *41*, 4225.
- [88] Lee, M.; Kim, J.-W.; Hwang, I.-W.; Kim, Y.-R.; Oh, N.-K.; Zin, W.-C. *Adv. Mater.* **2001**, *13*, 1363.
- [89] Bae, J.; Choi, J.-H.; Yoo, Y.-S.; Oh, N.-K.; Kim, B.-S.; Lee, M. *J. Am. Chem. Soc.* **2005**, *127*, 9668.
- [90] Ryu, R.-H.; Kim, H.-J.; Huang, Z.; Lee, E.; Lee, M. *Angew. Chem., Int. Ed.* **2006**, *45*, 5304.

- [91] Apperloo, J. J.; Janssen, R. A. J.; Malenfant, P. R. L.; Groenendaal, L.; Fréchet, J. M. J. *J. Am. Chem. Soc.* **2000**, *122*, 7042.
- [92] Miller, L. L.; Schlechte, J. S.; Zinger, B.; Burrell, C. J. *Chem. Mater.* **2002**, *14*, 5081.
- [93] Tanaka, K.; Waki, H.; Ido, Y.; Akita, S.; Yoshida, Y.; Yoshida, T. *Rapid Comm. Mass Spectrom.* **1988**, *2*, 151.
- [94] Karas, M.; Hillenkamp, F. *Anal. Chem.* **1988**, *60*, 2299.
- [95] Bahr, U.; Deppe, A.; Karas, M.; Hillenkamp, F.; Giessman, U. *Anal. Chem.* **1992**, *64*, 2866.
- [96] Swift, J. A. Electron Microscopes, Kogan Page London, **1970**.
- [97] Marcus, R. B.; T. T. Sheng, T. T. Transmission Electron Microscopy of Silicon VLSI Circuits and Structures, 1st edn., John Wiley & Sons Inc., New York, **1983**.
- [98] Allcock, H. R.; Lampe, F. W. Contemporary Polymer Chemistry, 2nd edn., Prentice-Hall Inc., New Jersey, **1990**.

CHAPTER 2

Metal Nanoparticles: Building Nanodevices by Atom Assembly

2. Metal Nanoparticles

2.1 Introduction

A metal nanoparticle is a finely dispersed material, characterized by a high surface area to volume ratio, in the sub-micrometer particles size range^{1a}. Particles from approximately 5 nm to 100 nm size, just above atomic dimensions, exhibit physicochemical properties that differ from those of both the constituent atoms or molecules and the macroscopic material. The differences in composition, structure, and interactions between the surface atoms or molecules, and those in the interior of a colloidal particle lead to the unique character of the finely divided material.

The surface plasmon band (SPB) is a strong and broad band observed in absorption in the UV-visible spectrum for metallic nanoparticles (NPs) bigger than 2 nm^{1b}. These surface plasmon resonance peaks observed in the spectra originate from the collective oscillation of the conduction electron cloud relative to the ionic background. For smaller clusters, quantum effects are predominant and no SPB is observed, and all metals feature this property^{1b}. However, gold, silver and copper exhibit very intense SPBs that explains, with the ease of their synthesis and their robustness, the success of gold and silver NPs in this field. The position, shape and intensity of the SPB strongly depends on factors such as the dielectric constant of the surrounding medium, the electronic interactions between the stabilizing ligands and the nanoparticle, which modify the electron density inside the nanoparticle, and the size, shape and monodispersity of the NPs^{1b-e}.

2.2 Synthesis

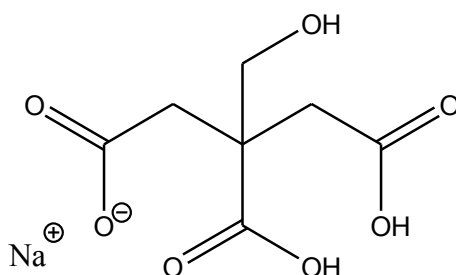
There is current interest in the synthesis of nanostructures for next-generation (opto)electronics², sensors³, catalysts⁴, battery electrolytes⁵ and biomedical applications⁶. However, nanomaterials have been used for a very long time and date back to the 16th century from the colloidal gold potions reported by Paracelsus^{1a}. The first application for nanoparticles was colored glass, pioneered by Cassius and Kunchel in the 17th century⁷. These early applications used nanoparticles with an extremely large polydispersity. Faraday's work in the 19th century represents the first chemical route to nanoparticulate metals, through phosphorus reduction of gold

chloride mixtures. However, it was not possible to control the diameters of the nanostructures using these early synthetic approaches.

While gold particles of nanometer size have been formed since Faraday used surface-active molecules as stabilizers⁸, templating approaches have come into focus over the past few years⁹. In these structures, polymers or preformed surfactant assemblies control size and shape of inorganic nanocomposites. Metal nanoparticles could be formed by using a well-established methodology: micelles of molecules, either surfactants or amphiphilic block copolymers where precursors are solubilized inside a self-assembled template^{10,11}.

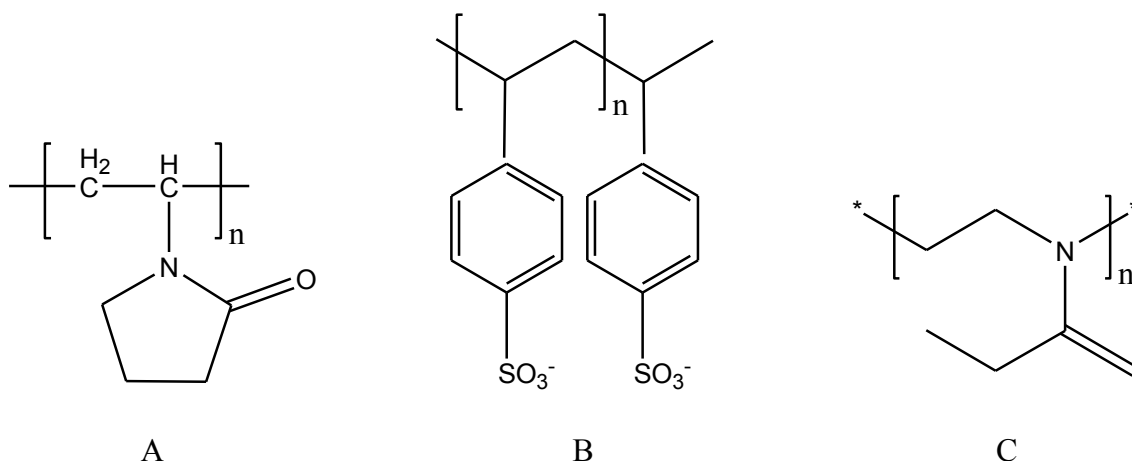
Metal particles in the size range of 1 to 10 nm dispersed in a liquid matrix can be prepared by chemical reduction of metal salts¹². This reduction of metal salts is usually done by using NaBH₄, H₂ or hydrazine as reducing agents. In theory, any metal with a larger standard reduction potential (E°) than the reducing agent is a candidate for reduction to its metal form.

The presence of surfactant molecules prevents the coagulation and precipitation of the colloidal particles. It means that the colloidal nanoparticles are stabilized by surrounding organic ligands. Most of the early work employed polydispersed organic polymers and ionic species to stabilize colloidal suspensions (e.g., the Turkevich process¹³ using sodium citrate (**Scheme 13**)).



Scheme 13: Chemical structure of sodium citrate

A wide variety of other species have been used to control the growth of metal nanostructures. Schaak et al.¹⁴ have used polymers such as poly(vinylpyrrolidone) (PVP, A), polystyrenesulfonic acid) sodium salt (PSS, B), and poly(2-ethyl-2-oxazoline) (PEO, C) (**Scheme 14**) to form nanoparticles, including nanoalloy formation at temperatures of ca. 200°C.



Scheme 14: Chemical Structure of A) PVP, B) PSS and C) PEO

The PVP architecture has also shown to facilitate the growth of Au@Ag core-shell nanostructures¹⁵, as well as Ag nanowires and nanocubes¹⁶.

For the formation of monodisperse nanoclusters of a form useful for applications, a stabilizing agent should be:

- chemically unreactive toward the growing nanocluster, forming an unpassivated nanocluster surface.
- structurally well-defined (size/shape), which allows controlled growth of the encapsulated nanocluster.
- comprised of light elements (organic-based), so its structure doesn't interfere with the characterization of the nanocluster, and
- surface-modifiable, to allow the tunable solubility and selective interactions with external stimuli.

These requirements¹⁷ are fulfilled through the use of dendritic architectures. Indeed, dendrimers are not only able to control the diameter of the formed nanocluster through structural variations (core and periphery), but their solubility and surface reactivity may also be tuned through the variation of peripheral groups.

PAMAM dendrimers were first applied to form Cu nanoclusters in 1998, as reported by Crooks¹⁸ and then shortly later by Tomalia and co-workers¹⁹. Three years later, the poly(propyleneimine) dendrimer (PPI) was first introduced by Crooks *et al.*^{20,21} for Cu⁰ and Pd⁰ nanoclusters formation, as shown in **Figure 8**.

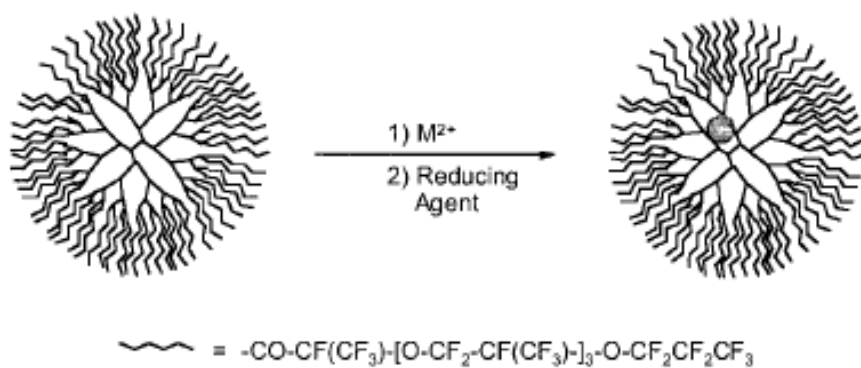


Figure 8: Schematic representation of the Dendrimer/ Pd^{2+} chemically reduced to yield dendrimer-encapsulated Pd^0 nanoparticles²⁰. (Reproduced by permission of The American Chemical Society)

The earliest examples of dendrimer-encapsulated nanoclusters growth featured the use of amine-terminated dendrimers, particularly for metal ions (Au, Ag, Cu, Pd, Pt) that readily form complexes with primary amine ligands. But the size of the resultant nanostructure is relatively large, with a higher degree of agglomeration^{22,23}. This is especially the case for hyperbranched polymers that exhibit random structure, resulting in a much higher polydispersity²⁴.

Surface complexation (inter-dendrimer stabilization) yields nanoparticles/nanoclusters (nanoparticulate gold, silver, platinum metals^{25,26}, iron oxide^{27,28} (**Figure 9**) and II-VI semiconductors (*e.g.*, CdS ^{29,30,31}).

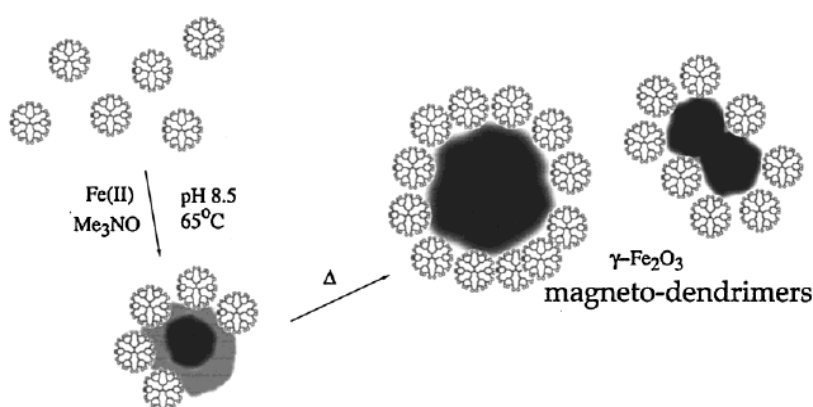


Figure 9: Schematic representation of the stabilization of maghemite nanoparticles by carboxyl-terminated poly(amidoamine) dendrimer (generation 4.5)²⁷. (Reproduced by permission of The American Chemical Society)

For these structures, dendrimers act as colloidal stabilizers much like linear polymers or surfactants, resulting in less control over resultant nanocluster size/properties. Complexation effects also result from varying the solution pH^{32,33}, which affects the protonation of surface and interior amine groups with pKa values of 7-9 and 3-6, respectively, as shown in **Figure 10**. At a pH of 2, the exterior primary amine groups are preferentially protonated relative to the interior tertiary amines^{34,35}.

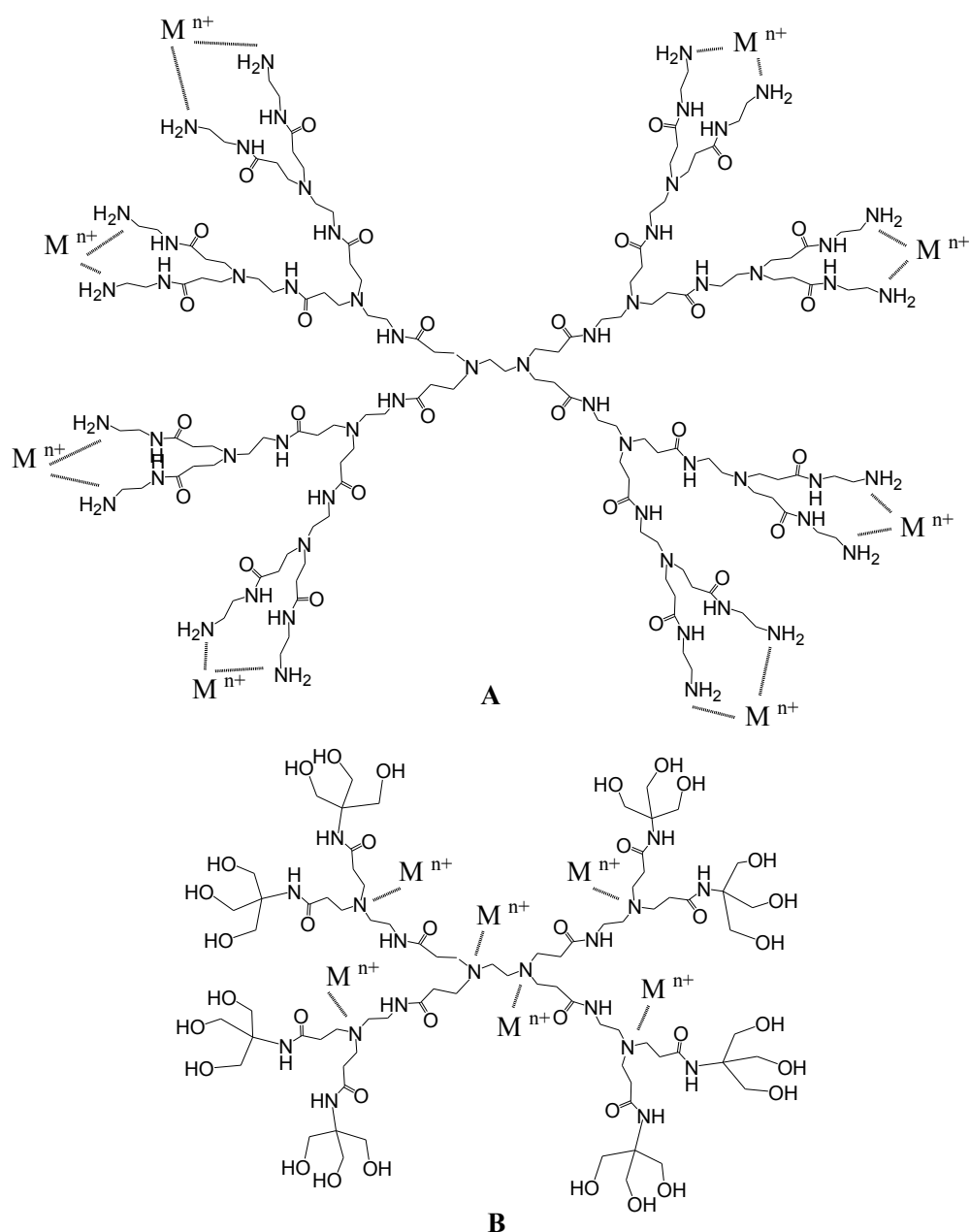
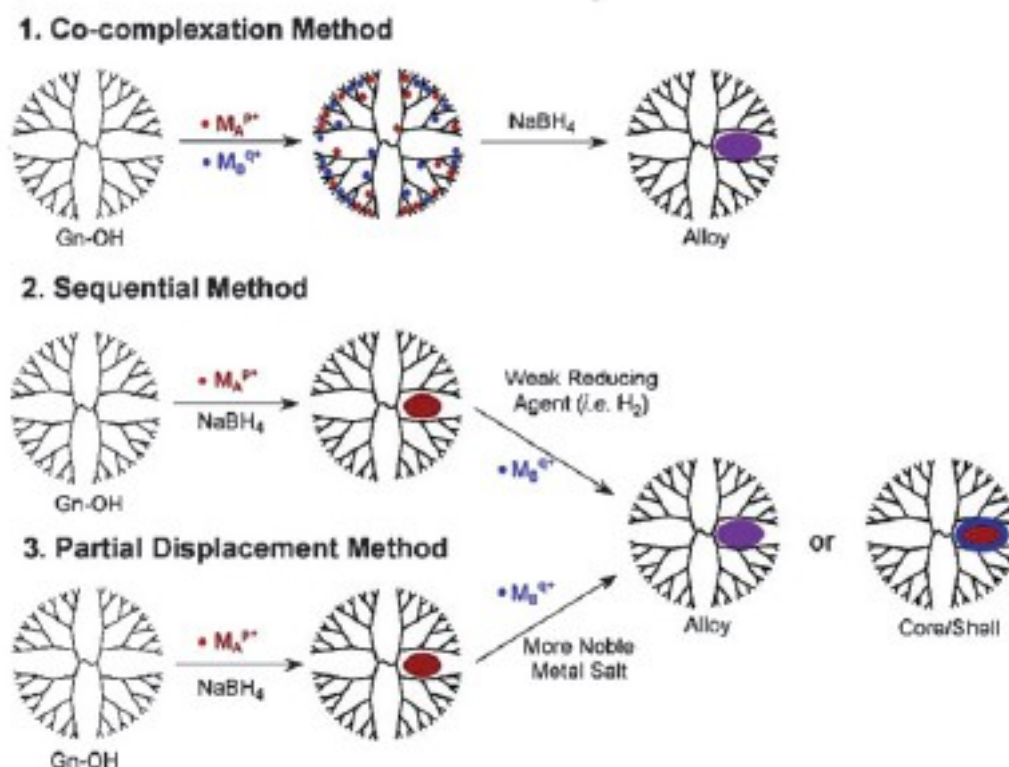


Figure 10: Molecular structure of a second generation (G2) amine-terminated PAMAM dendrimer where the metal ions chelated to the primary amine groups (**A**) and G2 hydroxyl-terminated PAMAM dendrimer, with the metal ions chelating to the interior tertiary amine groups (**B**).

Metal ions compete with protons for amine chelation to the interior of the dendritic structure within highly acidic solutions. Tuning the solution pH for dendrimers containing primary and tertiary amine groups may lead to either intra-dendrimer encapsulation, or inter-dendrimer stabilization, with the former resulting in much smaller diameters and extremely narrow polydispersities for the reduced metal nanoclusters.

In addition to isolated metal nanoclusters, complex intermetallic species have also been synthesized through the introduction of more than one metal to the dendritic structure. As shown in **Scheme 15**, there exist three routes for the solution-phase synthesis of bimetallic nanoclusters within a dendrimer³⁶⁻⁴⁰. These methods should also be amenable for the synthesis of trimetallic nanoclusters for interesting catalytic applications⁴¹.



Scheme 15: Schematic representation of the three methods used to generate bimetallic nanoparticles within a dendritic host⁴⁰. (Reproduced by permission of The Royal Society of Chemistry (RSC) on behalf of the Centre National de la Recherche Scientifique (CNRS))

2.3 Characterization

Complementary techniques are used to characterize these metal nanoparticles. The most important and useful ones are transmission electron microscopy (TEM), UV-Visible absorption spectroscopy (UV-Vis) and X-Ray Powder Diffraction (XRPD).

Principles of the TEM and UV-Vis techniques are explained in Chapter 1. In the case of metal nanoparticles, TEM gives information about their size and morphology, UV-Vis is commonly employed to describe the coordination environment of encapsulated metal ions.

XRPD is one of the most powerful techniques for analyzing the crystalline nature of solids. Diffraction experiments require X-ray wavelengths of the order of the interatomic spacing (0.07-0.2 nm) to produce building interference patterns⁴². Powder diffraction is performed with a powder diffractometer⁴³. The beam intensity is measured with a position sensitive detector with a wide angular (2θ) range of 0° to 120° . The cobalt $K_{\alpha 1}$ radiation ($\lambda = 0.178897$ nm) is one of the probing rays used. The measurements are performed at room temperature. The colloidal particle diameter along the normal to a plane of reflection can be calculated from the broadening of the reflection peak according to equation:

$$d = \frac{K\lambda}{B \cos \theta}$$

where K is the Scherrer constant which depends on the form of the particle, λ is the wavelength of the X-ray beam, θ is the diffraction angle, and B is the corrected line breadth at half-maximum in radians. The diffraction pattern is a fingerprint of each crystalline substance.

Other techniques can be very helpful for specific analysis such as atomic force microscopy (AFM), scanning electron microscopy (SEM) and near edge X-ray absorption fine structure (NEXAFS). A detailed description of Cu²⁺/nanocomposites was recently reported by Bubeck et al.⁴⁴, using near edge X-ray absorption fine structure (NEXAFS). This study showed that the metal ions interact with both tertiary amine groups and oxygens from neighbouring carbonyl groups. It was also shown that the interaction of the metal ion with the dendritic host on the counter ion present. Counter Cl⁻ ions resulted in a two-fold reduction in Cu²⁺/dendrimer complexation strength relative to SO₄²⁻ ions. Thus, during complexation of a metal salt with a

dendrimer, it is possible that the counterions may exist as both free spectator anions and M^{n+} -coordinated ligands.

2.4 Applications

2.4.1 Catalysis

The primary application for metallic nanoclusters is homogeneous/heterogeneous catalysis. Crooks has distinguished the two by referring to dendrimer-encapsulated nanoclusters (DENs) dissolved to solution as homogeneous catalysts, and those attached to a support as heterogeneous⁴⁵.

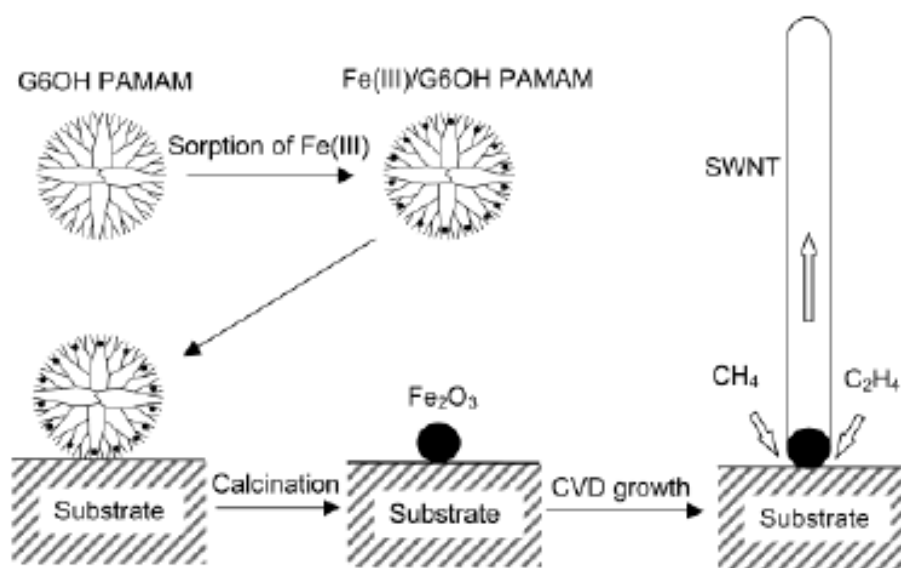
The dendritic architecture is especially suited for catalytic applications because the nanoclusters are extremely small (< 5 nm) resulting in extraordinary surface area, precluding surface saturation through inter-dendrimer interactions. Since the surface of the dendrimer may be modified with a host of different groups, the solubility of the dendrimer can be varied for different solvents. The structural and compositional tunability of the dendritic architecture allows the DENs to be selective toward different reactants and products⁴⁶.

Heterogeneous catalysis using DENs involves immobilizing them on solid supports such as gold⁴⁷, silica⁴⁸, and titania⁴⁹ surfaces, or a polymer matrix⁵⁰. The advantage of using dendrimers for this application is that nanoparticles can be synthesized and dispersed with minimal post-aggregation. Most frequently, surface chemisorption occurs through the strong interaction of many surfaces with $-NH_2$ and $-OH$ groups, as featured in commercially-available PAMAM and PPI structures.

2.4.2 Carbon Nanotubes

A recent application for dendrimer-encapsulated nanoclusters is for the controlled growth of carbon nanotubes (CNTs). It has been demonstrated that the diameters of catalytically grown CNTs can be varied through changing the diameter and/or nature of the catalytic sites⁵¹.

Dai and co-workers⁵² used dendrimers as carriers for the delivery of catalytic iron species onto a substrate surface (**Scheme 16**). After the pyrolysis of the polymeric matrix, uniformly arranged iron oxide nanoparticles having a narrow size distribution allowed the synthesis of single-walled nanotubes (SWNTs) with a narrow diameter distribution.



Scheme 16: Schematic process for carbon nanotube synthesis by Chemical Vapor Deposition (CVD) on a catalytic nanoparticle derived from PAMAM dendrimer template⁵². (Reproduced by permission of The American Chemical Society)

2.4.3 Films/ Coatings

Polyelectrolyte-facilitated layer-by-layer (LbL) thin film growth remains an exciting area of investigation for the design of multifunctional coatings on a variety of substrates⁵³. Tomalia and co-workers⁵⁴ used alternating layers of poly(sodium-4-styrenesulfonate) and Au@PAMAM nanoclusters. Bimetallic multilayer films consisting of alternating layers of positively charged Au@PAMAM (pH 3) and negatively-charged Ag@PAMAM (pH 11) was recently reported⁵⁵.

2.4.4 Quantum Dots

Though quantum dots are thought of as semiconductor nanocrystals⁵⁶, the electronic structure of a metal nanocluster is also critically dependent on its size. Though the size-tunable color of metallic nanoclusters arises from surface plasmon resonance effects, this phenomenon become significantly reduced for very small nanoclusters (diameters < 3 nm). Through the use of dendritic stabilizers, it is possible to form the smallest of metal nanoclusters, within the range where quantum confinement occurs. Dendrimer-encapsulated Au₈ nanoclusters were synthesized⁵⁷, emitting light in the blue spectral region with quantum yield of 41%. The high level of intra-dendritic stabilization was thought to facilitate the pronounced quantum efficiency, through the isolation of the nanoclusters from quenchers in solution.

2.4.5 Biomedical Applications

Dendrimers are currently being investigated for a number of biomedical applications⁵⁸, most notably drug delivery⁵⁹. However, DENs find applications as antimicrobial and imaging agents. PAMAM dendrimer-based silver complexes and nanocomposites have been reported⁶⁰ to be effective antimicrobial agents *in vitro* against *Staphylococcus aureus*, *Pseudomonas aeruginosa*, and *Escherichia coli*.

Specifically regarding imaging applications, dendrimers containing chelated Gd³⁺ have been used in MRI studies and dendrimer nanocomposites with gold and silver have shown promise as cell biomarkers. Balogh and co-workers have reported that silver⁶¹ and gold⁶² nanocomposites are non-toxic, fluorescent, water soluble, and stable at biologic pH levels. Characteristics such as size, surface charge, and toxicity are tunable functions of the surface of the dendrimer templates.

2.5 Importance of Size and Shape of Metal Nanoparticles

The size and shape of noble metal nanocrystals can have a significant influence on their physical properties. In the last decade, numerous studies concerning the growth mechanisms of nanocrystals have been investigated⁶³. But controllable nanocrystallization still has to be understood and predicting the conditions to obtain nanocrystals of a desired size and shape is highly challenging.⁹⁵

Numerous theoretical and computational studies have been undertaken to calculate the characteristic shape of objects at equilibrium over a range of sizes from a few atoms (clusters) up to 3 nm (nanocrystals)⁶⁴. The most widely used model for shape control of crystals is given by the Gibbs-Curie-Wulff theorem⁶⁵. Each facet of the crystal was described by its free surface and interfacial energies and the crystal shape was the result of the minimization of these energies for a certain volume. However, the model was valid only at thermal equilibrium, and the resulting shape is the equilibrium shape of the crystal. A pseudo “Wulff construction”⁶⁶ was proposed and it was based on the fact that the driving parameter was not the equilibrium surface but the growth rate of each facet. Then, the nucleation stage for the growth of various shapes plays a significant role to determine the size and shape of the formed nanocrystals.

As mentioned earlier, noble metals exhibit characteristic surface plasmon resonance peaks. This surface plasmon resonance was found to be highly sensitive to

the size and shape of the nanocrystals⁶⁷ and this has been demonstrated by simulations^{67b,c,f}. Indeed, two methods are needed to indicate changes in the shape of noble metal nanocrystals: numeric optical simulations of the surface plasmon calculations by discrete dipolar approximation (DDA) and the chemical method.

In the DDA method, for a finite array of point dipoles, the scattering issue may be solved exactly, so the only approximation in the DDA is the replacement of the continuum target by an array of N -point dipoles. When, the object studied is represented as a simple cubic lattice of N -polarizable point dipoles localized at r_i , $i=1, 2, \dots, N$, each one characterized by a polarizability α_i . The dipoles interact with one another via their electric field. After solving equations and matrices, this method gave very good theoretical results about scattering and absorption of surface plasmon resonance^{67b,c,f,68}, as shown in **Figure 11**.

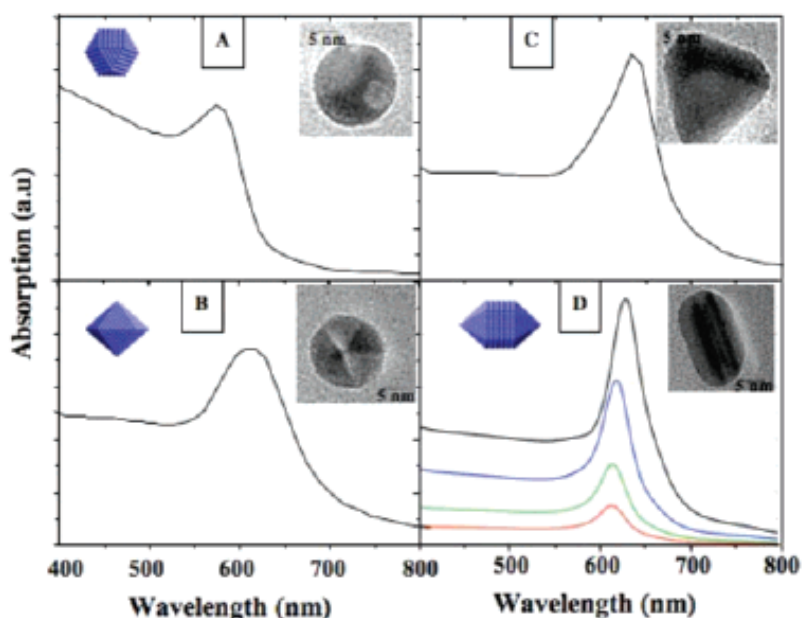


Figure 11: Simulated absorption spectra of copper nanocrystals differing by their shapes 3 nm cuboctahedron (A), 3 nm decahedron (B), 23 nm flat nanodisks (C), and 1.5 nm (red), 3 nm (green), 5 nm (blue), and 6 nm (black), ellipsoidal particles with an aspect ratio of 2 (D)⁹⁵. (Reproduced by permission of The American Chemical Society)

The advantages of the DDA approach, compared to the other theoretical approaches⁶⁹ was that each parameter (size, shape,...) was chose independently from the others.

For the chemical method, the oldest technique used was chemical vapour deposition (CVD)⁷⁰ and by using this method, it was possible to form clusters in the range of a few nanometers with the same shape as clusters^{71,72}.

Soft chemistry was carried out at room temperature in solution in the presence of various organic molecules, polymers, and/or surfactants as mentioned earlier. This is now the most widely used technique because it can be scaled to industrial applications.

Specific adsorptions of polymers⁷³, surfactants⁷⁴, molecules⁷⁵, and ions⁷⁶ on facets of clusters lead to the formation of nanocrystals with distinct shapes such as cubes, polyhedra, nanodisks, rods, prisms, plates, and spherical nanocrystals.

At the atomic level Kepler described in 1611 the arrangement of hard spheres packed in a face-centered cubic (*fcc*) arrangement, having the maximum density⁷⁷. The densest possible packing of four spheres was a tetrahedron. For *fcc* materials⁷⁸, the clusters were cubooctahedra (**Figure 12 A**), decahedra (**Figure 12 B**), and icosahedra (**Figure 12 C**).

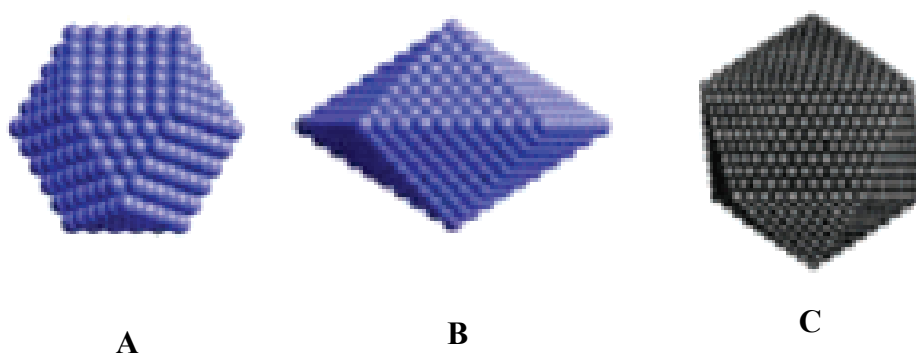


Figure 12: Different shapes of clusters: cubooctahedra (**A**), decahedra (**B**), icosahedra (**C**)⁹⁵.- Reproduced by permission of The American Chemical Society.

The shape of the primary clusters determined the shape of the crystals. In a recent review by Pileni⁹⁵, the formation of different shapes of atomic clusters has been described. Thus:

- As shown in **Figure 13 I**, the elongated particles were formed with additional intermediate (110) planes and were attributed to truncated large decahedra with 5-fold symmetry⁷⁹.
- Nanocubes (**Figure 13 II**) corresponded to cubooctahedral precursors⁸⁰.
- Triangular nanocrystals were nanoprisms and nanodisks⁸¹ (**Figure 13 III**).

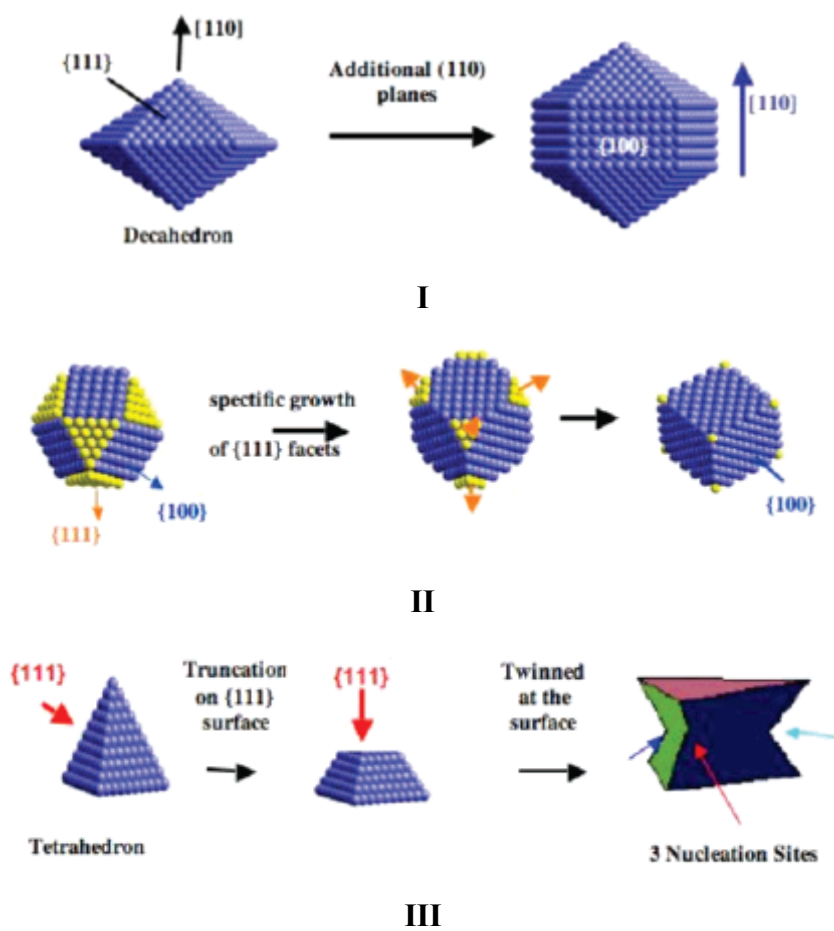


Figure 13: Scheme of the growth mechanism from clusters to a given shape of nanocrystals **I**) truncated decahedral nanocrystals, **II**) cubic nanocrystals, **III**) nanodisks⁹⁵. (Reproduced by permission of The American Chemical Society)

This thesis will focus on silver metal nanoparticles in particular, and a brief introduction to these is provided below.

2.6 Silver Nanoparticles

Silver metal nanoparticles are of great current interest because of their unique catalytic, electronic, optical, fungicidal properties, and their potential in designing materials for metal nanoparticles^{1b,c}.

This latter application is strongly dependent on the size and shape of the nanoparticles. Monodispersed metal colloids are usually formed in the presence of a protective agent, which can be organic molecule, linear polymer, and surfactant⁸².

During the past few decades, many methods including both chemical and physical⁸³ have been reported in the literature for the synthesis of silver nanoparticles. These nanostructures of different shapes seem to be particularly interesting to synthesize and study because bulk silver exhibits the highest electrical and thermal conductivities among all metals.

Moreover, of the three metals (Ag, Au, Cu) that display plasmon resonance in the visible spectrum, Ag exhibits the highest efficiency of plasmon excitation⁸⁴. Optical excitation of plasmon resonances in nanosized Ag particles is the most efficient mechanism by which light interacts with matter. A single Ag nanoparticle interacts with light more efficiently than a particle of the same dimension composed of any organic or inorganic chromophore. Silver is also the only material whose plasmon resonance can be tuned to any wavelength in the visible spectrum.

Numerous methods for the synthesis of Ag nanoparticles have been reported in the literature. Most of the solution-phase synthesis techniques are based on various modifications of the Lee-Meisel method, which uses AgNO₃ as the metal source⁸⁵. For Ag nanoparticle suspensions, a common method is the Lee-Meisel method as mentioned earlier, but this method produces a broad distribution of particle sizes. The other common method for the synthesis of nanosized Ag particles is the reduction of AgNO₃ with NaBH₄. Referred to as the Creighton method, this methodology generally yields about 10 nm size particles with a narrow distribution⁸⁶. Due to the large positive reduction potential of Ag, nanoparticle oxidation is thermodynamically unfavourable, resulting in stable aqueous and alcoholic suspensions without the aid of capping ligands. Aggregation can be avoided by the thick electrical double layers that form around metal nanoparticles in low-ionic-strength suspensions. For high ionic strength suspensions, capping agents such as self-assembled monolayers⁸⁷, surfactants^{75,85a,b}, polymers^{85e,88}, and dendrimers^{25,36} can be used to protect the particles from aggregation. If the synthesis occurs in the presence of capping agents, however, anisotropic particles may result due to the differing affinities of the ligands to the exposed crystal faces. This is sometimes a desired effect and several researchers have shown that various shapes can be produced by the judicious use of stabilizing agent^{75,89}. Nanoparticles can be capped with desired molecules after the synthesis to facilitate their transfer into nonpolar phases or to tailor their surface chemistry.

With these solution-phase synthesis techniques, the major problem is a limited flexibility of the size of the nanoparticles that can be formed and these methods are

sold on their ability to produce <10 nm particles. Small particles are desirable in catalysis, where the emphasis is on surface-to-volume ratio, but larger particles are often needed for optical applications. Small silver nanoparticles do not interact with light as efficiently as particles that are in the 50-100 nm range and do so only through energy absorption. The plasmon resonances in larger Ag nanoparticles have an important light-scattering component that can be greatly used in applications that require efficient optical labels, such as chemical assays.

There are also other methods that include high temperature reduction in porous solid matrices⁹⁰, vapour-phase condensation of a metal onto a solid support⁹¹, laser ablation of a metal target into a suspending liquid⁹², photoreduction of Ag ions⁹³ and electrolysis of a Ag salt solution⁹⁴. The problem with these methods is a wide size distribution, lack of particle crystallinity, cost, and the scalability of the production. The best synthetic method should address all of those problems and also yield particles with no chemicals that can alter the optical properties and the surface chemistry of the particle.

As mentioned earlier, control over the size and shape of noble metal nanoparticles is still challenging. A brief summary of efforts in the area of silver nanoparticles, is provided below. By using reverse micelles and various experimental conditions, Pileni and co-workers⁹⁵ were able to obtain silver nanoparticles of different sizes and shapes with a *fcc* structure: nanospheres of 5 nm size and nanoprisms or nanodisks of 30 nm to 120 nm size.

Mixed reverse micelles were formed from an appropriate mixture of Na(AOT) and Ag(AOT) (AOT: Sodium bis(2-ethylhexyl)sulfosuccinate) and hydrazine was used as reducing agent⁹⁶. Two parameters, w (the ratio of water to total surfactant concentration) and R (the ratio of hydrazine to functionalized surfactant concentration) were varied. Silver nanocrystals with 5 nm average diameter were produced from reverse micelles ($R= 2.4$, $w=2$). At the end of the synthesis, the nanocrystals were coated with dodecanthiol and extracted from the micelles⁹⁶. Dodecanthiol formed a well-packed self-assembled monolayer on the surface of the silver nanoparticles, attached by covalent S-Ag bonds⁹⁷. The electron diffraction pattern showed the characteristic distances of a *fcc* structure.

The cluster shapes were retained as decahedral nanocrystals, icosahedrons, and cubooctahedrons with a *fcc* structure. The Ag nanoparticles appeared to be highly crystalline. No transformation such as facets occurred during the growth process and

exclusively spherical nanocrystals were produced⁹⁸. Similar shapes were formed by using an inert gas aggregate source yielding distributions of silver clusters including icosahedra in the 1-2 nm size range and both cubooctahedra and icosahedra in the 4-8 nm range⁹⁹. Whereas decahedra were not formed and were then considered to be unstable above 3 nm. Using techniques highly diverse from each other, such as reverse micelles and inert gas evaporation, the resulting silver nanocrystal shape was similar to the that of the original *fcc* clusters et the atomic level.

Silver nanodisks^{71c,75,100} were also produced from reverse micelles. However, the required concentration of hydrazine is such that a phase transition takes place. The silver nanodisk size increased with the *R* value. At *R*=15, the average nanodisk size was 30 nm, whereas it was 120 nm at *R*=39.

Spherical polycrystalline nanoparticles were also formed. There were some differences in the silver nanodisks produced at various *R* values: at low *R* values, the silver nanodisk edges were not well-defined with very small truncatures as seen in **Figure 14G**, and the best fit between experiments and simulations was obtained at a given aspect ratio and zero truncation. At *R*= 39, the edges of the silver nanodisks were straight and there was a distribution of shape as shown in **Figure 14H**.

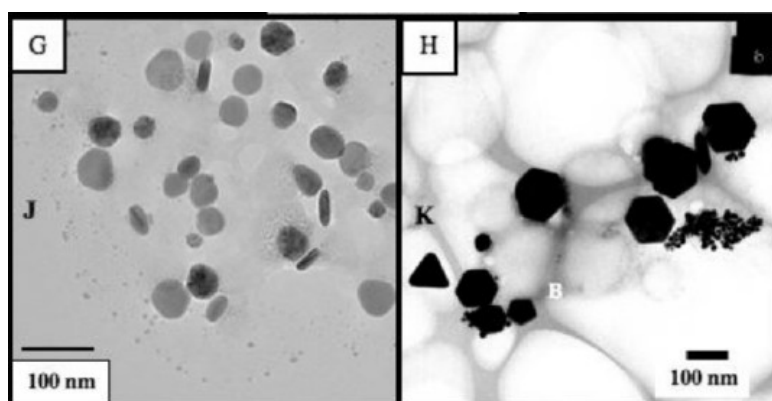


Figure 14: TEM images of silver nanodisks at various hydrazine contents⁹⁵.

(Reproduced by permission of The American Chemical Society)

These structures manifested a significant change in their optical properties¹⁰¹. A large quantity of nanospheres were converted into triangular nanoprisms or nanodisks by photolysis^{68a,102}. The excitation wavelength seemed to be a key parameter to develop such photo fragmentation^{73,68a,102}.

In conclusion, the degree of crystallinity and shape of the resulting metal nanoparticles are two important criteria that determine the suitability of their use in electrical and optical nanodevices or as catalysts. Thus, the controlled nucleation and growth of defect-free and specifically shaped nanocrystals is a key challenge in nanoscience research today.

In this thesis, we aim to develop a methodology to synthesize silver metal nanoparticles using dendrimers as templates in the role of nanoreactor as well as nanostabilizers. In addition, efforts related to developing an understanding of size and shape control of silver metal nanoparticles using these dendrimers as templates will be presented in Chapter 3.

2.7 References

- [1] a) http://www.en.wikipedia.org/wiki/Colloidal_gold. b) Kreibig, U.; Vollmer, M. *Optical Properties of Metal Clusters*, Springer, Berlin, **1995**. c) Liz-Marzan, L.M. *Mater. Today* **2004**, 7, 26. d) Kreibig, U.; Genzel, L. *Surf. Sci.* **1985**, 156, 678. e) Hutter, E.; Fendler, J.H. *Chem. Mater.* **2004**, 16, 1685.
- [2] Stankic, S.; Sterrer, M.; Hofmann, P.; Bernardi, J.; Diwald, O.; Knozinger, E. *Nano Lett.* **2005**, 5, 1889.
- [3] Huang, C.-C.; Chang, H.-T. *Anal. Chem.* **2006**, 78, 8332.
- [4] Hoover, N.N.; Auten, B.J.; Chandler, B.D. *J. Am. Chem. Soc.* **2006**, 110, 8606.
- [5] Prabhuram, J.; Zhao, T.S.; Tang, Z.K.; Chen, R.; Liang, Z.X. *J. Phys. Chem.* **2006**, 110, 5245.
- [6] Choi, J.-S.; Jun, Y.-W.; Yeon, S.-I.; Kim, K.C.; Shin, J.-S., Cheon, J. *J. Am. Chem. Soc.* **2006**, 128, 15983.
- [7] Rao, C. N. R.; Kulkarni, G. U.; Thomas, P.J.; Edwards, P.P. *Chem. Soc. Rev.* **2000**, 29, 27.
- [8] Faraday, M. *Phil. Trans. R. Soc.* **1857**, 147, 145.
- [9] Li, M.; Schnablegger, H.; Mann, S. *Nature*, **402**, 393, 1999.
- [10] Liveri, V.T. *Curr. Top. Colloid Interface Sci.* **1999**, 3, 65.
- [11] Bae, D.-S.; Han, K.-S.; Adair, J.H. *J. Am. Chem. Soc.* **2002**, 85, 1321.
- [12] Kooij, S.; Wormeester, H.; Martin Brouwer, E.A.; Van Vroonhoven, E.; Van Silfhout, A. Optical characterization of thin colloidal gold, *Bene Poelsema*, **2002**.
- [13] Turkevich, J.; Stevenson, P.S.; Hillier, J. *Discuss. Faraday Soc.*, **1951**, 11, 58.
- [14] Schaak, R.E., Sra, A.K.; Leonard, B.M.; Cable, R.E.; Bauer, J.C.; Han, Y.-F.; Means, J.; Teizer, W.; Vasquez, Y.; Funck, E.S. *J. Am. Chem. Soc.* **2005**, 127, 3506.
- [15] Tsuji, M.; Miyamae, N.; Lim, S.; Kimura, K.; Zhang, X.; Hikino, S.; Nishio, M. *Cryst. Growth Des.* **2006**, 6, 1801.
- [16] Chen, M.; Wang, L.-W.; Han, J.T.; Zhang, J.-Y.; Li, Z.-Y.; Qian, D.-J. *J. Phys. Chem. B* **2006**, 110, 11224.
- [17] Fahlman, B.D. *Materials Chemistry*, Springer, New York, in press.
- [18] Zhao, M.; Sun, L.; Crooks, R.M. *J. Am. Chem. Soc.* **1998**, 120, 4877.
- [19] Balogh, L.; Tomalia, D.A. *J. Am. Chem. Soc.* **1998**, 120, 7355.
- [20] Crooks, R.M. ; Yeung, L.K. *Nano. Lett.*, **2001**, 1, 14.

- [21] Floriano, P.N.; Noble, C.O.; Schoonmaker, J.M.; Poliakoff, E.D.; McCarley, R.L. *J. Am. Chem. Soc.* **2001**, *123*, 10545.
- [22] Ottaviani, M.F.; Montalti, F.; Turro, N.J.; Tomalia, D.A. *J. Phys. Chem. B* **1997**, *101*, 158.
- [23] Sun, X.; Dong, S.; Wang, E. *Macromolecules* **2004**, *37*, 7105.
- [24] Mecking, S.; Thomann, R.; Frey, H.; Sunder, A. *Macromolecules* **2000**, *33*, 3958.
- [25] Esumi, K.; Suzuki, A.; Yamahira, A.; Torigoe, K. *Langmuir* **2000**, *16*, 2604.
- [26] Torigoe, K.; Suzuki, A.; Esumi, K. *J. Colloid. Interface. Sci.* **2001**, *241*, 346.
- [27] Strable, E.; Bulte, J. W. M.; Moskowitz, B.; Vivekanandan, K.; Allen, M.; Douglas, T. *Chem. Mater.* **2001**, *13*, 2201.
- [28] Frankamp, B.L.; Boal, A.K.; Tuominen, M.T.; Rotello, V.M. *J. Am. Chem. Soc.* **2005**, *127*, 9731.
- [29] Hanus, L.H.; Sooklal, K.; Murphy, C.J.; Ploehn, H.J. *Langmuir* **2000**, *16*, 2621.
- [30] Lackowics, R.; Gryczynski, I.; Gryczynski, Z.; Murphy, C.J. *J. Phys. Chem. B* **1999**, *103*, 7613.
- [31] Huang, J.; Sooklal, K.; Murphy, C.J.; Ploehn, H.J. *Chem. Mater.* **1999**, *11*, 3595.
- [32] Zheng, J.; Stevenson, M.S.; Hikida, R.S.; Van Patten, P.G. *J. Phys. Chem. B* **2002**, *106*, 1252.
- [33] Kleinman, M.H.; Flory, J.H.; Tomalia, D.A.; Turro, N.J. *J. Phys. Chem. B* **2000**, *104*, 11472.
- [34] Tomalia, D.A.; Naylor, A.M.; Goddard, W.A. *Angew. Chem., Int. Ed. Engl.* **1990**, *29*, 138.
- [35] Niu, Y.; Sun, L.; Crooks, R.M. *Macromolecules* **2003**, *36*, 5725.
- [36] Crooks, R.M.; Zhao, M.; Sun, L.; Chechik, V.; Yeung, L.K. *Acc. Chem. Res.* **2001**, *34*, 181.
- [37] Scott, R.W.J.; Datye, A.K.; Crooks, R.M. *Catal. Lett.* **2003**, *125*, 3708.
- [38] Chung, Y.-M.; Rhee, H.K. *Catal. Lett.* **2003**, *85*, 159.
- [39] Chung, Y.-M.; Rhee, H.K. *J. Mol. Catal. A: Chem.* **2003**, *206*, 291.
- [40] Scott, R.W.J.; Wilson, O.M.; Crooks, R.M. *J. Phys. Chem. B* **2004**, *109*, 692.
- [41] Henglein, A. *J. Phys. Chem. B* **2000**, *104*, 6683.
- [42] Encyclopedia of Materials: Science and Technology. <http://www.elsevier.com>
- [43] Pathmamanoharan, C.; Philipse, A.P. *J. Colloid Int. Sci.* **1998**, *205*, 340.

- [44] Bubeck, R.A.; Dvornic, P.R.; Hu, J.; Hexemer, A.; Li, X.; Keinath, S.E.; Fischer, D.A. *Macromol. Chem. Phys.*, **2005**, *206*, 1146.
- [45] Scott, R.W.J.; Wilson, O.M.; Crooks, R.M. *J. Phys. Chem. B* **2005**, *109*, 692.
- [46] Yeung, L.K.; Lee, C.T.; Johnston, K.P.; Crooks, R.M. *Chem. Commun.* **2001**, 2290.
- [47] Ye, H.; Scott, R.W.J.; Crooks, R.M. *Langmuir* **2004**, *20*, 2915.
- [48] Lang, H.; May, R.A.; Iversen, B.L.; Chandler, B.D. *J. Am. Chem. Soc.* **2003**, *125*, 14832.
- [49] Liu, S.; Zhu, T.; Hu, R.; Liu, Z. *Phys. Chem. Chem. Phys.* **2002**, *4*, 6059.
- [50] Alvarez, J.; Sun, L.; Crooks, R.M. *Chem. Mater.* **2002**, *14*, 3995.
- [51] Cheung, C.L. *J. Phys. Chem. B* **2002**, *106*, 2429.
- [52] Choi, C.H.; Kim, W.; Wang, D.; Dai, H. *J. Phys. Chem. B* **2002**, *106*, 12361.
- [53] Hammond, P.T. *Adv. Mater.* **2004**, *16*, 1271.
- [54] He, J.-A.; Valluzzi, R.; Yang, K.; Dolikhanyan, T.; Sung, C.; Kumar, J.; Tripathy, S.K.; Samuelson, L.; Balogh, L.; Tomalia D.A. *Chem. Mater.* **1999**, *11*, 3268.
- [55] Esumi, K.; Akiyama, S.; Yoshimura, T. *Langmuir* **2003**, *19*, 7679.
- [56] Lemon, B.I.; Crooks, R.M. *J. Am. Chem. Soc.* **2000**, *122*, 12886.
- [57] Zheng, J.; Petty, J.T.; Dickson, R.M. *J. Am. Chem. Soc.* **2003**, *125*, 7780.
- [58] Svenson, S.; Tomalia, D.A. *Adv. Drug Delivery Rev.* **2005**, *57*, 2106.
- [59] a) Boas, U.; Heegaard, P.M.H. *Chem. Soc. Rev.* **2004**, *33*, 43. b) Fréchet, J.M.J. *Pharm. Sci. Technol. Today* **2000**, *2*, 393.
- [60] Balogh, L. Swanson, D.R., Tomalia, D.A., Hagnauer, G.L., McManus, A.T. *Nano. Lett.* **2001**, *1*, 18.
- [61] Lesniak, W.; Bielinska, A.U.; Sun, K.; Janczak, K.W.; Shi, X.; Baker, J.R.; Balogh, L.P. *Nano. Lett.* **2005**, *5*, 2123.
- [62] a) Bielinska, A.; Eichman, J.D.; Lee, I.; Baker, J.R.; Balogh, L.P. *J. Nanopart. Res.* **2002**, *4*, 395. b) Shi, X., Ganser, T.R.; Sun, K.; Balogh, L.P.; Baker, J.R. *Nanotechnology* **2006**, *17*, 1072.
- [63] a) Pileni, M.P. *J. Phys. Chem.* **1993**, *97*, 6961. b) Fendler, J.; Meldrum, F.C. *Adv. Mater.*, **1995**, *7*, 607; c) Gardea-Torresday, L.J.; Tiemann, K.J.; Gamez, G.; Dokken, K.; Tehuacanero, S.; Yacaman, M.J. *J. Nanopart. Res.* **1999**, *1*, 397. d) Mann, L.; Scher, E.C.; Alivisatos, A.P. *J. Am. Chem. Soc.* **2000**, *122*, 12700. e) Pileni, M.P. *Langmuir*, **2001**, *17*, 7476. e) Pileni, M.P. *Nat. Mater.*, **2003**, *2*, 145. g) Murphy, C.J.; Sau, T.K.; Gole, A.M.; Orendorff, C.J.; Gao, L.; Gou, L.;

- Hunyadi, S.E.; Lin, T. *J. Phys. Chem. B* **2005**, *109*, 13857. h) Burda, C.; Chen, X.; Narayanan, R.; El Sayed, M.A. *Chem. Rev.* **2005**, *105*, 1025.
- [64] Pyykkö, P. *Angew. Chem., Int. Ed.* **2004**, *43*, 4412.
- [65] Mullin, J.W. *Crystallization*, 4th ed.; Butterworth Heinemann: Boston, **2001**.
- [66] Bühler, J.; Prior, Y. *J. Cryst. Growth* **2000**, *209*, 779.
- [67] Pipino, A.C.R.; Schatz, G.C.; Van Duyne, R.P. *Phys. Rev. B* **1996**, *53*, 4162. b) Kelly, K.L.; Lazarides, A.A.; Schatz, G.C. *Comput. Sci. Eng.* **2001**, *3*, 67. c) Kelly, K.L.; Coronado, E.; Zhao, L.L.; Schatz, G.C. *J. Phys. Chem. B* **2003**, *107*, 668. d) Hutter, E.; Fendler, J.H. *Adv. Mater.* **2004**, *16*, 1685. e) Salzemann, C.; Lisiecki, I.; Brioude, A.; Urban, J.; Pileni, M.P. *J. Phys. Chem. B* **2004**, *108*, 13242. f) Germain, V.; Brioude, A.; Ingert, D.; Pileni, M.P. *J. Chem. Phys.* **2005**, *122*, 124707. g) Salzemann, C.; Brioude, A.; Pileni, M.P. *J. Phys. Chem. B* **2006**, *110*, 7208.
- [68] a) Jin, R.; Cao, Y. W.; Mirkin, C.A.; Kelly, K.L.; Chatz, G.C.; Zheng, J.G. *Science* **2001**, *294*, 1901. b) Jin, R.; Cao, Y. W.; Hao, E.; Metraux, G.S.; Schatz, G.C.; Mirkin, C.A. *Nature* **2002**, *425*, 487.
- [69] a) Novotny, L.; Pohl, D.W.; Hecht, B. *Optical Letters* **1995**, *20*, 970. b) Kahnert, F.M. *J. Quant. Spectrosc. Radiat. Transfer* **2003**, *79-80*, 775. c) Futumata, M.; Maruyama, Y.; Ishikawa, M. *J. Phys. Chem. B* **2003**, *107*, 7607.
- [70] Reinhard, D.; Hall, B.D.; Berhoud, P.; Valkealahti, S.; Monot, R. *Phys. Rev.* **1998**, *58*, 4917.
- [71] a) Reinhard, D.; Hall, B.D.; Berthoud, P.; Valkealahti, S.; Monot, R. *Phys. Rev. Lett.* **1997**, *79*, 1459. b) Urban, J. *Cryst. Res. Technol.* **1998**, *33*, 1009. c) Maillard, M.; Giorgio, S.; Pileni, M.P. *Adv. Mater.* **2002**, *14*, 15.
- [72] Yacaman, M.J.; Ascension, J.A.; Liu, H.B.; Gardea-Torrese, J. *J. Vac. Sci. Technol. B.* **2001**, *19*, 1091.
- [73] Jun, Y.; Choi, I.; Cheon, J. *Angew. Chem., Int. Ed.* **2006**, *45*, 3414.
- [74] Manna, L.; Scher, E.C.; Alivisatos, A.P. *J. Am. Chem. Soc.* **2000**, *122*, 12700.
- [75] Maillard, M.; Giorgio, S.; Pileni, M.P. *J. Phys. Chem. B* **2003**, *107*, 2466.
- [76] a) Tanori, J.; Pileni, M.P. *Adv. Mater.* **1995**, *7*, 862. b) Filankembo, A.; Pileni, M.P. *J. Phys. Chem.* **2000**, *104*, 5867.
- [77] Kepler, J. *Strena seu de nive sexangule*, Caspar, M., Hammer, F., Eds.; Clarendon Press : Oxford, 1966 ; p 46.

- [78] Kirkland, A.I.; Jefferson, D.A.; Duff, D.G.; Edwards, P.P.; Gameson, I.; Johnson, B.F.G.; Smith, D. *J. Proc. R. Soc. Lond., Ser. A* **1993**, *440*, 589.
- [79] Lisiecki, I.; Filankembo, A.; Sack-Kongehl, H.; Weiss, K.; Pileni, M.P.; Urban, J. *Phys. Rev. B* **2000**, *61*, 4968.
- [80] a) Ahmadi, T.S.; Wang, Z.L.; Henglein, A.; El-Sayed, M.A. *Chem. Mater.*, **1996**, *8*, 1161. b) Salzemann, C.; Lisiecki, I.; Urban, J.; Pileni, M.P. *Langmuir*, **2004**, *20*, 11772.
- [81] a) Hamilton, D.R.; Seidensticker, R.G. *J. Appl. Phys.*, **1960**, *31*, 1165. b) Hamilton, J.F.; Brady, L.E. *J. Appl. Phys.*, **1964**, *35*, 414. c) Salzemann, C.; Urban, J.; Lisiecki, I.; Pileni, M.P. *Adv. Funct. Mater.*, **2005**, *15*, 1277.
- [82] Esumi, K.; Suzuki, A.; Aihara, N.; Usui, K.; Torigoe, K. *Langmuir* **1998**, *14*, 3157.
- [83] Chou, K.S.; Reh, C.Y. *Mater. Chem. Phys.* **2000**, *64*, 241.
- [84] Kreibig, U.; Vollmer, M.; Optical Properties of Metal Clusters, Springer Series in Materials Science 25, New York, Springer-Verlag, 1995, p50.
- [85] a) Sondi, I.; Goia, D.V.; Matijević, E. *J. Colloid Interface Sci.* **2003**, *260*, 75. b) Cason, J.P.; Khambaswadkar, K.; Roberts, C.B. *Ind. Eng. Chem. Res.* **2000**, *39*, 4749. c) Li, X.; Zhang, J.; Xu, W.; Jia, H.; Wang, X.; Yang, B.; Zhao, B.; Li, B.; Ozaki, Y. *Langmuir* **2003**, *19*, 4285. d) Shirtcliffe, N.; Nickel, U.; Schneider, S. *J. Colloid Interface Sci.* **1999**, *211*, 122. e) Tan, Y.; Dai, X.; Li, Y.; Zhu, D. *J. Mater. Chem.* **2003**, *13*, 1069. f) Caswell, K.K.; Bender, C.M.; Murphy, C.J. *Nano. Lett.* **2003**, *3*, 667. g) Rodriguez-Gattorno, G.; Diaz, D.; Rendón, L.; Hernandez-Segura, G.O. *J. Phys. Chem. B* **2002**, *106*, 2482.
- [86] Creighton, J.A.; Blatchford, C.G.; Albrecht, M.G. *J. Chem. Soc. Farad. Trans. II* **1979**, *75*, 790.
- [87] He, S.; Yao, J.; Jiang, P.; Shi, D.; Zhang, H.; Xie, S.; Pang, S.; Gao, H. *Langmuir* **2001**, *17*, 1571.
- [88] Velikov, K.P.; Zegeres, G.E.; van Blaaderen, A. *Langmuir* **2003**, *19*, 1384.
- [89] Sun, Y.; Yin, Y.; Mayers, B.T.; Herricks, T.; Xia, Y. *Chem. Mater.* **2002**, *14*, 4736.
- [90] a) Plyuto, Y.; Berquier, J.-M.; Jacquiod, C.; Ricolleau, C. *Chem. Commun.* **1999**, *17*, 1653. b) Wang, T.C.; Rubner, M.F.; Cohen, R.E. *Langmuir* **2002**, *18*, 3370.

- [91] a) Zhao, Y.-P.; Ye, D.-X.; Wang, G.-C.; Lu, T.-M. *Nano. Letters* **2002**, *2*, 351. b) Jensen, T.R.; Malinsky, M.D.; Haynes, C.L.; Van Duyne, R.P. *J. Phys. Chem. B* **2000**, *104*, 10549.
- [92] Mafuné, F.; Kohno, J.-Y.; Takeda, Y.; Kondow, T.; Sawabe, H. *J. Phys. Chem. B* **2000**, *104*, 8333.
- [93] Abid, J.P.; Wark, A.W.; Brevet, P.F.; Girault, H.H. *Chem. Commun.* **2002**, *7*, 792.
- [94] Zhu, J.; Liu, S.; Palchik, O.; Kolytyn, Y.; Gedanken, A. *Langmuir* **2000**, *16*, 6396.
- [95] Pileni, M.P. *J. Phys. Chem. C* **2007**, *111*, 9019.
- [96] Petit, C.; Lixon, P.; Pileni, M.P. *Langmuir* **1991**, *7*, 2620.
- [97] Fendler, J.; Meldrum, F.C. *Adv. Mat.* **1995**, *7*, 607.
- [98] Courty, A.; Lisiecki, I.; Pileni, M.P. *J. Chem. Phys.* **2002**, *116*, 8074.
- [99] Giorgio, S.; Urban, J. *J. Phys. F: Met. Phys.* **1988**, *18*, L147-L152.
- [100] Germain, V.; Li, J.; Inger, D.; Wang, Z.L.; Pileni, M.P. *J. Phys. Chem. B* **2003**, *107*, 34.
- [101] a) Brioude, A.; Jiang, X.C.; Pileni, M.P. *J. Phys. Chem. B* **2005**, *109*, 13138. b) Brioude, A.; Pileni, M.P. *J. Phys. Chem. B* **2005**, *109*, 23371.
- [102] a) Maillard, M.; Huang, P.; Brus, L. *Nanoletters* **2003**, *3*, 1611. b) Bastys, V.; Pastoriza-Santos, I.; Rodriguez-Gonzalez, B.; Vaisnoras, R.; Liz-Marán, L.M. *Adv. Funct. Mat.* **2006**, *16*, 766.

CHAPTER 3

Synthesis and Self-Assembly of Dumbbell Shaped Dendrimers

3. Synthesis and Self-assembly of Dumbbell Shaped Dendrimers

3.1 Introduction

As highlighted in Chapter 1, dendrimers that are hyperbranched and monodisperse macromolecules, are becoming increasingly important in designing smart and efficient nanomaterials for a variety of applications in medicine, catalysis and electronics¹. A significant effort in the design and syntheses of these globular architectures has been invested, that has led to inside-out (divergent) or outside-in (convergent) methodologies². Many different types of structural variations in these dendrimers are possible by changing the central core, and it can provide access to novel type of morphologies upon their aggregation³. We have been investigating the role of central core, the backbone, and the linking units on the evolving morphology of the dendrimers, and have established a simple and efficient divergent synthetic route to such dendritic macromolecules⁴, based on the acid-base hydrolytic chemistry of amino-silanes and -stannanes with organic acids⁵. We were intrigued by the possibility of developing hyperbranched structures that will evolve using symmetric growth on either side of a bifunctional linear core, and give rise to dumbbell shape type dendrimers. Compared with the globular dendrimers, the synthetic elaboration and a detailed investigation of the properties of the latter class have been much less explored⁶.

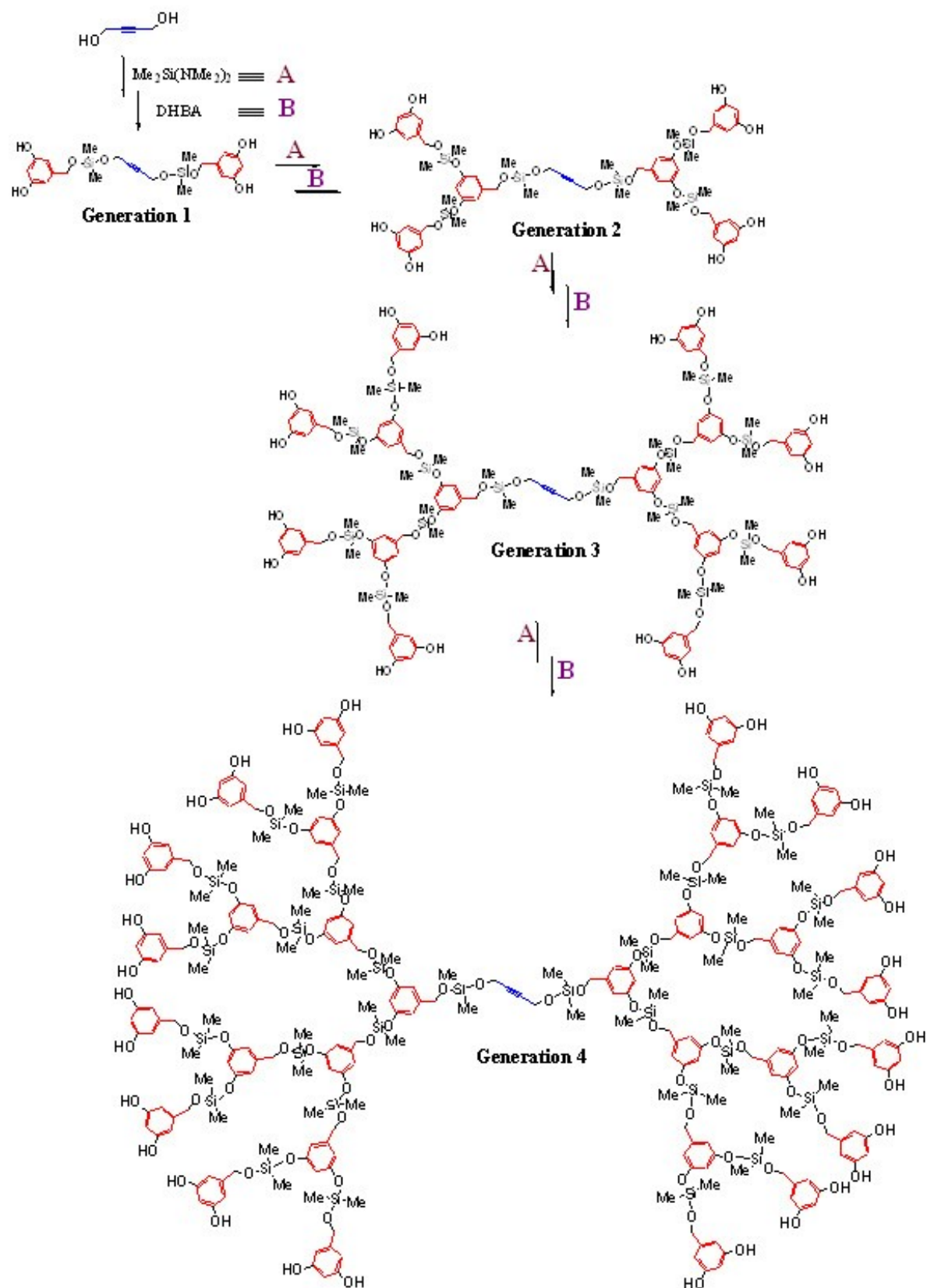
We report herein a simple divergent synthetic route to dumbbell shaped dendrimers that are constructed from the bifunctional core, 2-butyne-1,4-diol, and 3,5-dihydroxybenzyl alcohol (DHBA) as wedges. The synthetic elaboration is based on the controlled addition of bis(dimethylamino)dimethylsilane ($\text{Me}_2\text{Si}(\text{NMe}_2)_2$) to the bifunctional core, followed by addition of DHBA. The process is then repeated with $\text{Me}_2\text{Si}(\text{NMe}_2)_2$ and DHBA, in sequence, with amine as the only by-product, and the purification of dendrimers can be easily achieved by simple extraction into deuterium oxide. Self-organization of dendrimers through suitable peripheral groups continues to be an area of much significance, and provides opportunities in designing nanomaterials for molecular encapsulation and delivery^{4,7,8}. The dumb-bell shaped dendrimers, reported here, have suitably placed OH groups for inter-dendrimer interactions, and we have examined their self-assembly through such interactions in

THF and water, using UV-Vis spectroscopy and transmission electron microscopy. Generations 1-3 form aggregates at a higher critical aggregation concentration (*cac*) compared to generation 4 in THF. This behavior is related to the open structure in the lower generations with a linear core becoming important in their self-assembly, while in generation 4, more globular architecture with more prominent hydrogen bonding sites, facilitates self-assembly at lower concentrations.

3.2 Results and Discussion

3.2.1 Synthesis of Dumbbell Shaped Dendrimers

Dendrimers were synthesized using a quantitative acid-base hydrolytic reaction of aminosilanes with molecules containing terminal OH groups⁵. The choice of the linear core around which dendrons are built, was based on its rigidity, solubility and commercial availability, and 2-butyne-1,4-diol was considered to be an ideal candidate for developing the desired dendrimers. The dendron backbone was chosen to be 3,5-dihydroxybenzyl alcohol since it has been successfully employed in our laboratory to synthesize globular dendritic architectures⁴. For synthesizing the first generation dendrimer, 1 molar equivalent of 2-butyne-1,4 diol was added dropwise over a period of 2 h, to an ice-bath cooled solution of 2 equivalents of bis(dimethylamino)dimethylsilane in THF. The solution was stirred at ice-bath temperature for additional 6 hours, and then left to warm to room temperature. The latter was transferred to an addition funnel, and added slowly to a solution of 2 equivalents of DHBA in THF, and stirred overnight. After removal of the solvent in vacuo, the product was extracted into deuterium oxide D₂O. The solution was filtered and D₂O was then removed under vacuum, to afford a light pink powder. Continuation of this methodology by carrying out reactions under controlled conditions, led to the synthesis of generation 2-4 dendrimers in very good yields. Dendrimers were characterized using a combination of ¹H- and ¹³C- NMR spectroscopy, matrix-assisted laser desorption/ionization time of flight (MALDI-TOF) techniques, FT-IR, and elemental analyses. These data confirmed the identity of these dendrimers as shown in **Scheme 17**.



Scheme 17: Preparation of dumbbell shaped dendrimers, following the acid base hydrolytic divergent methodology.

3.2.2 Self-Assembly of Dumbbell Shaped Dendrimers

Self-assembly of dendrimers via intermolecular interactions between peripheral groups, is a topic of current interest^{7,8}, and we have also investigated aggregation behaviour of globular DHBA based dendrimers in solution and at interfaces⁴. We were intrigued by the self-assembly behaviour of dendrimers in which the linear core as well as the evolving shape of the dendrimers could influence their association. In addition, dendrimer generations 1-4 contain peripheral hydroxyl groups that increase exponentially from 4 to 32, and are expected to contribute to enhanced inter-dendrimer interactions as the generation number increases.

The aggregation behaviour of dendrimers was first investigated using UV-Vis spectroscopy at concentrations of 1 to 10 mg/mL in THF. The dendrimers generally depict three peaks around 240, 260 and 290 nm at 1 mg/mL (**Figure 15 A**), which become broad as the concentrations are increased and the solutions become turbid. The *cac* for each generation was calculated by plotting the intensity of scattered light at a given wavelength against concentration (**Figure 15 B**), and it was found to be 4.9 mg/mL for generations 1-3. The latter is much higher than the globular DHBA based dendrimers of generations 1-3, that was calculated to be 3.7 mg/mL (4g). This suggests that more open structure of dendrimers, constructed around the linear core, allows more freedom for these molecules. In addition, the central core in these open structures might also participate in packing via π - π interactions, and these competing interactions might create an association/dissociation equilibrium which will delay aggregation.

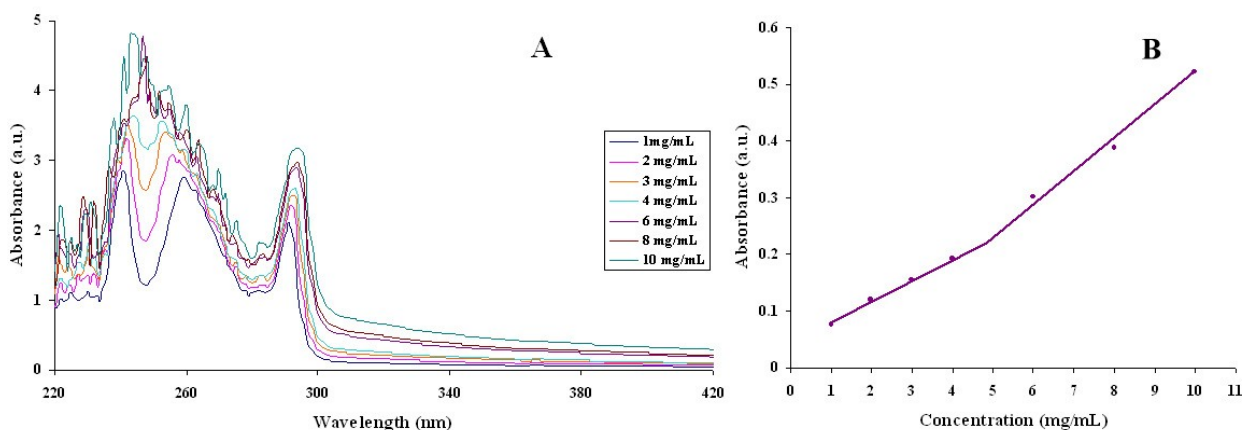


Figure 15: (A) UV-Vis absorption spectra of dendrimer generation 1 at concentrations of 1 to 10 mg/mL in THF, and (B) plot of absorbance vs concentration of dendrimers 1 in THF at 340 nm.

The generation 4 dendrimer showed a *cac* of 4.1 mg/mL which was quite comparable to the DHBA based dendrimers, suggesting clearly that the structure was becoming more globular at this generation. The aggregation of dendrimers through participation of terminal OH groups in hydrogen bonding, was also confirmed by FT-IR that showed a broad peak at approximately 3300 cm^{-1} for the terminal OH groups. The latter clearly suggested that terminal OH groups in these dendrimers are strongly hydrogen bonded at concentrations above *cac*, as below this concentration, a peak at around 3500 cm^{-1} is commonly observed, which is indicative of the absence of hydrogen bonds.

Transmission electron microscopy is a useful technique to examine self-assembly of macromolecules, and can provide essential information related to the morphology of the resulting aggregates⁹. We first studied aggregation behaviour of dendrimers of generations 1-4 in THF at concentrations of 4 and 8 mg mL⁻¹ (concentrations below and above *cac*). At 4 mg mL⁻¹, a general globular morphology for the aggregates (**Figure 16**) was observed for dendrimer generations 1-4. Upon examining particle size distribution in these aggregates, it was noted that, in general, dumb-bell dendrimers of generations 2-4 form mostly small aggregates of 5 to 25 nm in size (**Figure 16 B-D**). In contrast, the size distribution for generation 1 dendrimer aggregates was found to range between 30-135 nm (**Figure 16 A**), whereas the largest aggregates for those from generation 4, for example, were 55 nm in size. This type of behavior has also been observed earlier¹⁰, and can be explained by considering that,

generally, dendrimers of lower generations tend to exist in relative open forms. Their peripheral OH groups are therefore more easily accessible to interact *via* hydrogen bonding with the other surrounding molecules, and lead to the formation of larger aggregates.

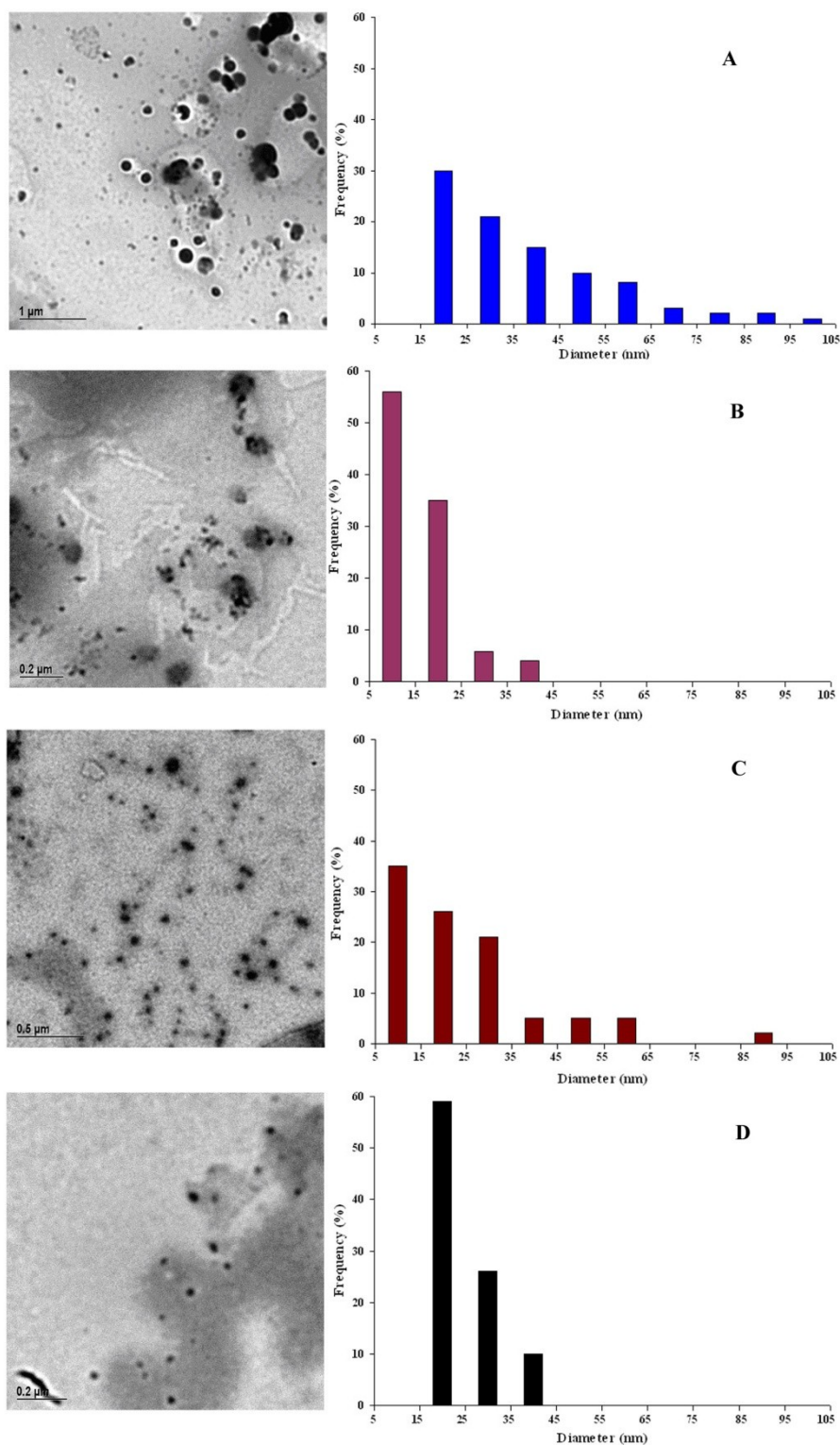


Figure 16: Transmission electron micrographs and particle size distributions of dendrimer generations 1 (A), 2 (B), 3 (C) and 4 (D) in THF at 4 mg/mL.

On the other hand, in higher generation dendrimers with a more spherical structure, peripheral OH groups can backfold, and become less available for hydrogen bonding with other molecules. We were also intrigued to notice that small aggregates in higher generations tend to cluster together to form linear assemblies of about 200 nm in size.

Upon increasing the concentration to 8 mg/mL in THF, it was observed that the globular shape of dumbbell dendrimer generations 1-4 was generally retained. However, there were quite significant differences in particle size distribution of the aggregates with those at 4 mg/mL. For example, generation 1 dendrimer formed smaller aggregates, with a larger population now in the range of 5-15 nm in size (**Figure 17**). This can be explained considering that at much higher concentrations, large aggregates can collapse, yielding small size clusters.

We also studied aggregation of these dendrimers in a more polar solvent at a concentration of 4 mg/mL, and aggregation behaviour changed significantly with the change in the solvent from THF to water. The dumb-bell shaped dendrimers possess a hydrophobic interior with polar OH groups at the periphery. In smaller generations, there may be hydrophobic-hydrophilic repulsion between dendrimers which will enhance their coagulation in water. Water will also compete with interdendritic hydrogen bonding, and it is expected that much smaller aggregates will emerge. TEM study was in compliance, and these effects were quite evident especially in generation 1 and 2 dendrimers, which seem to avoid any contact with water, and yield random assemblies of various confirmations (**Figure 18**). In addition, the sizes of these aggregate assemblies were much smaller than in THF at 4 mg/mL

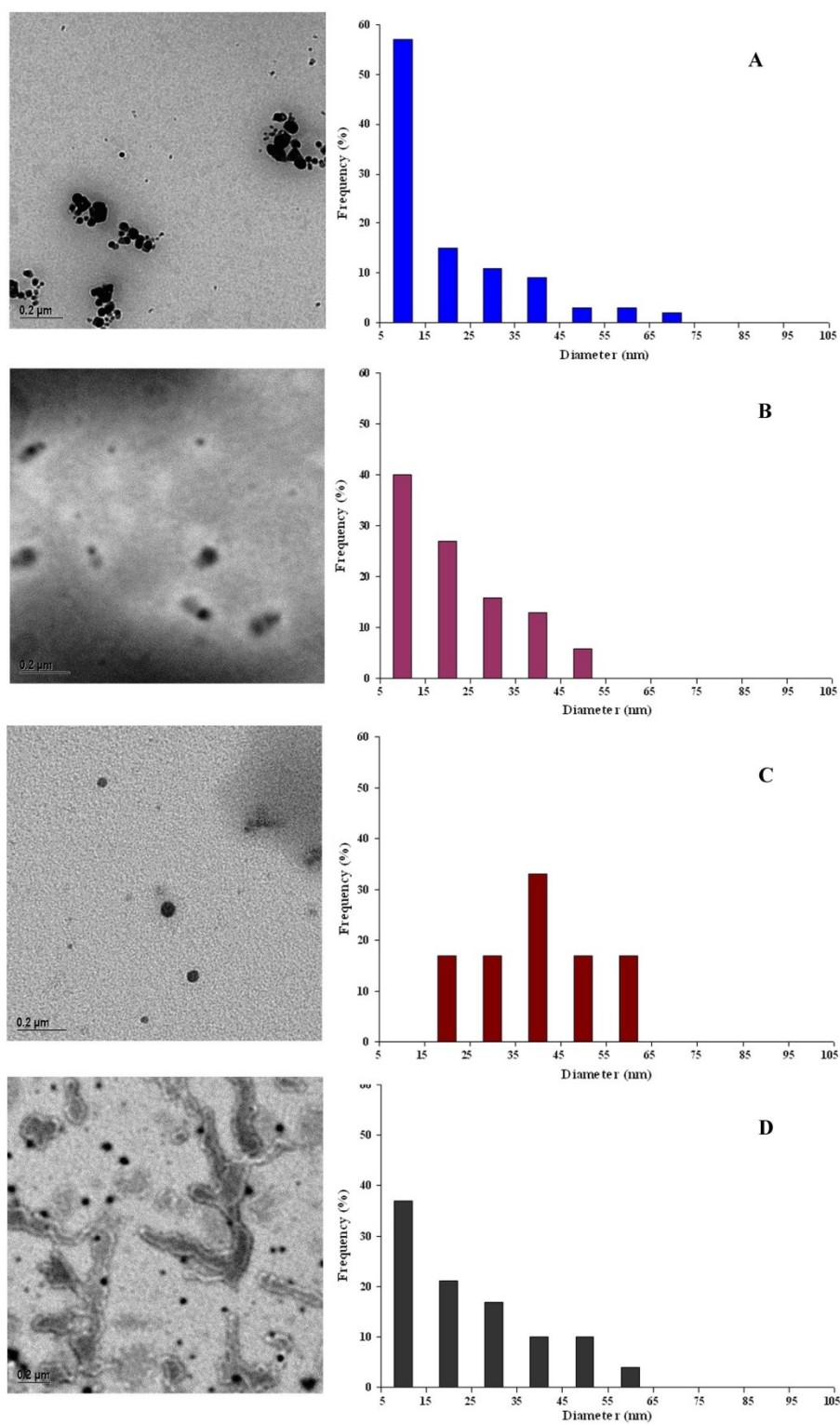


Figure 17: Transmission electron micrographs and particle size distributions of dendrimer generations 1 (A), 2 (B), 3 (C) and 4 (D) in THF at 8 mg/mL.

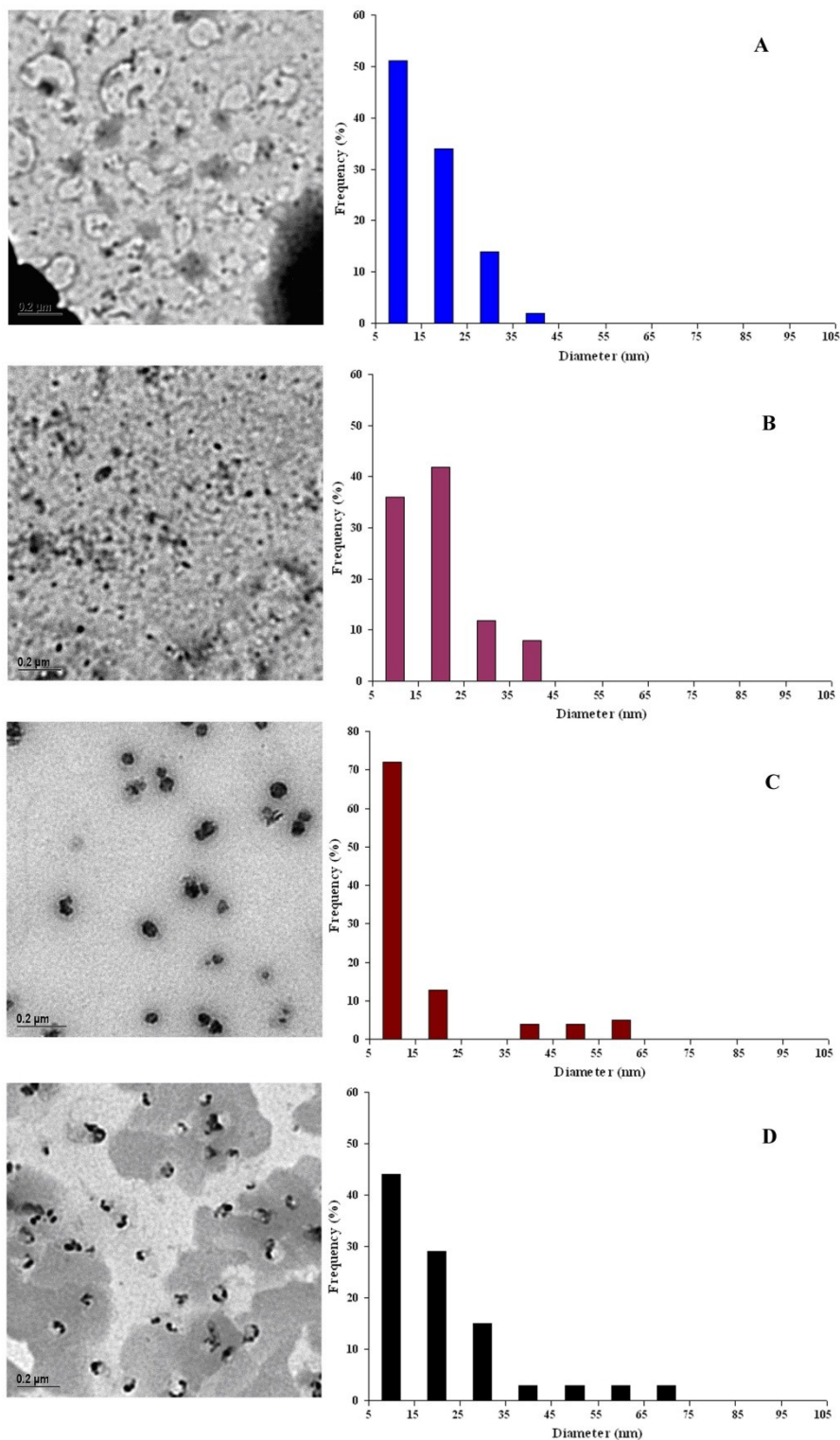


Figure 18: Transmission electron micrographs and particle size distributions of dendrimer generations 1 (A), 2 (B), 3 (C) and 4 (D) in H₂O at 4 mg/mL.

Self-assembly of dendrimer generations 3 and 4 in water was found to be quite different from that of first and second generation dendrimers. It suggested that small aggregates of 5 to 25 nm size are first formed, which then assemble into larger

clusters of 55 to 75 nm size (Figure **18 D**). This can be explained by considering that generation 3 and 4 dendrimers start to adopt a more globular structure, and there is much less hydrophobic interior and hydrophilic exterior contact which reduces repulsion.

3.3 Conclusions

Symmetric growth of DHBA based dendrons on a linear core has been successfully carried out to construct dumb-bell shaped dendrimers of generations 1-4. These dendrimers evolve from a very open structure in lower generations to that resembling a globular architecture in higher generations. Molecular self-assembly of these dendrimers is influenced by their backbone structure, as indicated by much higher critical aggregation concentration of generations 1-3, compared with that of globular dendrimers counterparts, and generation 4. The influence of solvent in their self-assembly was studied using THF and water, and in lower generations, the inability of more polar solvents to interact with their backbones, leads to aggregates that are formed by minimizing the repulsive forces. In higher generations, the major interaction of the solvent with the dendrimer is at the periphery which has a higher concentration of polar OH groups, and it does not interfere significantly with their ability to self-associate. The influence of the solvent in controlling morphology and sizes of aggregates, is of interest, as it allows one to tailor their properties for molecular encapsulation and release.

Addendum:

This chapter has been submitted as a full paper to Canadian Journal of Chemistry for a special issue dedicated to Professor Robert H. Marchessault. Subsequent to that, generation 5 and 6 dumbbell shaped dendrimers were also synthesized but their characterization was impeded by their poor solubility in D₂O. It was also noted using the available data that their structure contained defects of minor nature. This is due to exponential increase of OH groups at the periphery that cause steric congestion. Indeed, there are 32 OH peripheral groups in dendrimer generation 4 that need to react with small diaminosilane, followed by a bulkier monomer 3,5-dihydroxybenzyl alcohol. Due to incomplete reactions, even a few unreacted OH groups will cause a

defect in the otherwise monodisperse dendrimers. We are continuing to evaluate the validity of these arguments, and the synthesis of these dendrimers is currently being pursued in our laboratory.

3.4 Experimental section

Materials and Measurements

2-butyne-1,4-diol (Aldrich), 3,5-dihydroxybenzyl alcohol (Aldrich), and bis(dimethylamino)dimethylsilane (Gelest) were used as received. All manipulations were performed under a nitrogen atmosphere using either standard schlenk line techniques or an Innovative Technology (Braun) Labmaster MB-150-M dry box. All solvents were stored under nitrogen and used after distillation over sodium/benzophenone. NMR spectra were measured on a 270 MHz JEOL spectrometer at ambient temperature. The samples were prepared inside the dry box using deuterated solvents (Cambridge Isotope laboratories, Inc.), and the chemical shifts in ppm are reported relative to tetramethylsilane as an internal standard for ^1H and ^{13}C spectra. Mass spectra were obtained on a Hewlett Packard 5973 mass spectrometer, and MALDI-TOF spectra on a Kratos Kompact Maldi 3.v.4.0.0 spectrometer using LiBr/dithranol as the matrix. Elemental analysis were performed by Laboratoire d'Analyse Elementaire de l'Université de Montréal. Infrared spectra were measured on a Bruker IFS-48 Fourier transform infrared spectrometer using a standard resolution of 4 cm^{-1} for transmission. UV-Visible spectra were recorded in water on a Hewlett Packard 8453 with a resolution of 2 nm. Transmission electron microscopy (TEM) measurements were carried out on a JEOL 2000FX microscope operating at an acceleration voltage of 80 kV.

First generation dumbbell shaped dendrimer [G-1]-(OH)₄:

A solution of 2-butyne-1,4-diol (0.200 g, 2.32 mmol) dissolved in 5 mL of dry THF, was added dropwise to a solution of 2 equivalents of bis(dimethylamino)dimethylsilane (0.852 mL, 4.65 mmol) in 5 mL of dry THF, cooled to 0°C. Stirring at ice bath temperature was maintained for additional 6 hours, and the resulting solution was subsequently warmed to room temperature. The latter was then added dropwise to a solution of 2 equivalents of DHBA (0.651 g, 4.65 mmol) in 10 ml of dry THF. The resulting solution was stirred overnight, and THF

was then removed under vacuum to afford a sticky gel. 2-3 mL of deuterium oxide D₂O were added to the gel and was stirred for 5-10 minutes. The solution was filtered and D₂O was then removed under vacuum to afford a light pink powder (778 mg, 70%). ¹H NMR (270 MHz, D₂O-d₂): δ (ppm) 0.05 (s, 12H, OSiMe₂O), 4.11 (s, 4H, OCH₂C), 4.36 (s, 4H, C₆H₃-CH₂O), 6.18 (s, 2H, C₆H₂ para), 6.30 (t, 4H, C₆H₂ ortho). ¹³C NMR (68 MHz, D₂O-d₂): δ -1.7, -0.7 (SiCH₃), 49.7 (OCH₂C), 63.6 (C₆H₃-CH₂), 83.6 (OCH₂C), 101.9, 106.4, 143.8, 157.1 (C₆H₃). FT-IR (KBr, cm⁻¹): 3243 (ν_{OH}), 2896 (ν_{C-H arom.}), 1242 (δ_{Si-CH₃}), 1041 (ν_{Si-O}). Mass spectrum (EI-MS) *m/z* 479.1 (Expected: 478.6). Elemental analysis: C₂₂H₃₀O₈Si₂: Calcd.: C, 55.21; H, 6.32. Found: C, 55.36; H, 5.96.

Second generation dumbbell shaped dendrimer [G-2]-(OH)₈:

A solution of 1 equivalent of 2-butyne-1,4-diol (50 mg, 0.581 mmol) in 10 mL of THF, was added to a solution of 2 equivalents of bis(dimethylamino)dimethylsilane (0.213 mL, 1.161 mmol) in 5 mL of THF, and stirred for 6 hours at ice bath temperature. The resulting solution was added dropwise over a period of 1h to 2 equivalents of DHBA (163 mg, 1.161 mmol) dissolved in 10 mL of THF. After stirring overnight, the mixture was then added dropwise (1h) to a solution of 4 equivalents of bis(dimethylamino)dimethylsilane (0.426 mL, 2.323 mmol) in 5 mL of THF. The resulting solution was added dropwise (1h) to 4 equivalents of DHBA (325 mg, 2.323 mmol) dissolved in 15 mL of THF, and stirred overnight. The removal of the solvent under vacuum afforded a sticky gel. 4-5 mL of deuterium oxide D₂O were added to the gel and stirred for 5-10 minutes. The solution was filtered and D₂O was then removed under vacuum to afford a light pink powder (455 mg, 62%). ¹H NMR (270 MHz, D₂O-d₂) δ 0.05 (m, 36H, OSiMe₂O), 4.15 (s, 4H, OCH₂C), 4.36 (s, 12H, C₆H₃-CH₂O), 6.18 (s, 6H, C₆H para), 6.30 (m, 12H, C₆H₂ ortho). ¹³C NMR (68 MHz, D₂O-d₂): δ (ppm) -1.7, -0.1 (SiCH₃), 50.3 (OCH₂C), 64.3 (C₆H₃-CH₂), 83.6 (OCH₂C), 102.6, 107.0, 144.5, 157.8 (C₆H₃). FT-IR (KBr, cm⁻¹): 3378 (ν_{OH}), 2962 (ν_{C-H arom.}), 1262 (δ_{Si-CH₃}), 1084, 890 (ν_{Si-O}). Mass spectrum (MALDI-TOF) *m/z* 1261.3 (including *m/z* Li⁺, Expected 1263.7).

Third generation dumbbell shaped dendrimer [G-3]-(OH)₁₆:

A similar procedure as described above for the second generation was used to prepare the third generation. A solution of 1 equivalent of 2-butyne-1,4-diol (20 mg, 0.232 mmol) in 10 mL of THF was added to a solution 2 equivalents of bis(dimethylamino)dimethylsilane (0.085 mL, 0.465 mmol) in 5 ml THF, and stirred for 6 hours at ice bath temperature. The above mixture was added dropwise (1h) to a solution of 2 equivalents of DHBA (65,1 mg, 0.465 mmol) in 10 mL of THF, and stirred overnight at room temperature. It was then added dropwise (1h) to a solution of 4 equivalents of bis(dimethylamino)dimethylsilane (0.170 mL, 0.929 mmol) in 5 mL of THF, and stirred overnight at room temperature. The latter was added dropwise (1h) to a solution of 4 equivalents of DHBA (130 mg, 0.929 mmol) in 10 mL of THF, and after stirring overnight, it was added dropwise (1h) to a solution of 8 equivalents of bis(dimethylamino)dimethylsilane (0.341 mL, 1.858 mmol) in 5 mL of THF, and stirred for 14 hours. Finally it was added to a solution of 8 equivalents of DHBA (260 mg, 1.858 mmol) in 15 mL of THF, and stirred overnight. THF was removed under vacuum to afford a gel. 4-5 mL of deuterium oxide D₂O were added to the gel and was stirred for 5-10 minutes. The solution was filtered and D₂O was then removed under vacuum to afford a light pink powder (402 mg, 61%). ¹H NMR (270 MHz, D₂O-d₂): δ 0.01, 0.05 (m, 84H, OSiMe₂O), 4.10 (s, 4H, OCH₂C), 4.34 (s, 28H, C₆H₃-CH₂O), 6.18 (s, 14H, C₆H para), 6.30 (m, 28H, C₆H₂ ortho). ¹³C NMR (68 MHz, D₂O-d₂): δ (ppm) -1.7, -0.77 (SiCH₃), 49.6 (OCH₂C), 63.6 (C₆H₃-CH₂), 83.5 (OCH₂C), 101.8, 106.3, 143.7, 157.0 (C₆H₃). FT-IR (KBr, cm⁻¹): 3378 (ν_{OH}), 2892 (ν_{C-H arom.}), 1154 (δ_{Si-CH₃}), 1042, 954 (ν_{Si-O}). Mass spectrum (MALDI-TOF) *m/z* 2837.9 (including *m/z* Li⁺, Expected 2833.9).

Fourth generation dumbbell shaped dendrimer [G-4]-(OH)₃₂:

A solution of 1 equivalent of 2-butyne-1,4-diol (20 mg, 0.232 mmol) in 10 mL of THF, was added to a solution 2 equivalents of bis(dimethylamino)dimethylsilane (0.085 mL, 0.465 mmol) in 5 ml THF, and stirred for 6 hours at ice bath temperature. The above mixture was added dropwise (1h) to a solution of 2 equivalents of DHBA (65,1 mg, 0.465 mmol) in 10 mL of THF, and stirred overnight at room temperature. It was then added dropwise (1h) to a solution of 4 equivalents of bis(dimethylamino)dimethylsilane (0.170 mL, 0.929 mmol) in 5 mL of THF, and stirred overnight at room temperature. The latter was added dropwise (1h) to a

solution of 4 equivalents of DHBA (130 mg, 0.929 mmol) in 10 mL of THF, and after stirring overnight, it was added dropwise (1h) to a solution of 8 equivalents of bis(dimethylamino)dimethylsilane (0.341 mL, 1.858 mmol) in 5 mL of THF, and stirred for 14 hours. Then it was added to a solution of 8 equivalents of DHBA (260 mg, 1.858 mmol) in 15 mL of THF, and stirred overnight. The resulting solution was added dropwise to 16 equivalents of bis(dimethylamino)dimethylsilane (0.681 mL, 3.717 mmol) in 10 mL of THF. Stirring was continued overnight at room temperature. The resulting solution was then added dropwise (1h) to a solution of 16 equivalents of DHBA (521 mg, 3.717 mmol) in 10 mL of THF. The reaction mixture was stirred for 36 hours at room temperature. Solvent removal under vacuum afforded a sticky gel. 4-5 mL of D₂O were added to the gel and was stirred for 5-10 minutes. The solution was filtered and D₂O was then removed under vacuum to afford a pink powder (833 mg, 60%). ¹H NMR (270MHz, D₂O-d₂): δ -0.06, 0.00, 0.22 (m, 180H, OSiMe₂O), 4.10 (s, 4H, OCH₂C), 4.31 (s, 60H, C₆H₃-CH₂O), 6.15 (s, 30H, C₆H para), 6.25 (m, 60H, C₆H₂ ortho). ¹³C NMR (68 MHz, D₂O-d₂): δ (ppm) -1.54, -1.033, 0.40 (SiCH₃), 49.5 (OCH₂C), 63.9 (C₆H₃-CH₂), 83.7 (OCH₂C), 100.5, 105.9, 143.1, 158.8 (C₆H₃). FT-IR (KBr, cm⁻¹): 3379 (ν_{OH}), 2889 (ν_{C-H arom.}), 1263 (δ_{Si-CH₃}), 1042, 970 (ν_{Si-O}). Mass spectrum (MALDI-TOF) *m/z* 5978.8 (including *m/z* Li⁺, Expected: 5974.3). Elemental analysis: C₂₇₄H₃₆₆O₉₂Si₃₀: Calcd.: C, 55.14; H, 6.18. Found: C, 55.26; H, 6.31.

Fifth generation dumbbell shaped dendrimer [G-5]-(OH)₆₄:

A solution of 1 equivalent of 2-butyne-1,4-diol (20 mg, 0.232 mmol) in 10 mL of THF was added to a solution 2 equivalents of bis(dimethylamino)dimethylsilane (0.085 mL, 0.465 mmol) in 5 ml THF, and stirred for 6 hours at ice bath temperature. The above mixture was added dropwise (1 hr) to a solution of 2 equivalents of DHBA (65,1 mg, 0.465 mmol) in 10 mL of THF, and stirred overnight at room temperature. It was then added dropwise (1 hr) to a solution of 4 equivalents of bis(dimethylamino)dimethylsilane (0.170 mL, 0.929 mmol) in 5 mL of THF, and stirred overnight at room temperature. The latter was added dropwise (1 hr) to a solution of 4 equivalents of DHBA (130 mg, 0.929 mmol) in 10 mL of THF, and after stirring overnight, it was added dropwise (1 hr) to a solution of 8 equivalents of bis(dimethylamino)dimethylsilane (0.341 mL, 1.858 mmol) in 5 mL of THF, and

stirred for 14 hours. Then it was added to a solution of 8 equivalents of DHBA (260 mg, 1.858 mmol) in 15 mL of THF, and stirred overnight. The resulting solution was added dropwise to 16 equivalents of bis(dimethylamino)dimethylsilane (0.681 mL, 3.717 mmol) in 10 mL of THF. Stirring was continued overnight at room temperature. The resulting solution was then added dropwise (1hr) to a solution of 16 equivalents of DHBA (521 mg, 3.717 mmol) in 10 mL of THF. The reaction mixture was stirred for 36 hours at room temperature. The resulting solution was then added dropwise (1hr) to 32 equivalents of bis(dimethylamino)dimethylsilane (1.363 mL, 7.434 mmol) in 10 mL of THF and stirred overnight at room temperature. Finally, the resulting solution was added dropwise to 32 equivalents of DHBA (1.042 g, 7.434 mmol) in 10 mL of THF. The reaction mixture was let to stir for 3 days at room temperature. Solvent removal under vacuum afforded a sticky gel. 5-6 mL of D₂O were added to the gel and was stirred for 5-10 minutes. The solution was filtered and D₂O was then removed under vacuum to afford a dark pink powder (1.651 g, 58%).

¹H NMR (270MHz, D₂O-d₂): δ -0.06, 0.00, 0.22 (m, 20H, OSiMe₂O), 4.10 (s, 2H, OCH₂C), 4.31 (s, 10H, C₆H₃-CH₂O), 6.15 (s, 10H, C₆H para), 6.25 (m, 20H, C₆H₂ ortho). FT-IR (KBr, cm⁻¹): 3377 (ν_{OH}), 2958 (ν_{C-H arom.}), 1198 (δ_{Si-CH₃}), 1042, 967 (ν_{Si-O}). Mass spectrum (MALDI-TOF) *m/z* 12,266.2 (including *m/z* Li⁺, expected mass 12,255.3).

Sixth generation dumbbell shaped dendrimer [G-6]-(OH)₁₂₈ :

A solution of 1 equivalent of 2-butyne-1,4-diol (20 mg, 0.232 mmol) in 10 mL of THF was added to a solution 2 equivalents of bis(dimethylamino)dimethylsilane (0.085 mL, 0.465 mmol) in 5 ml THF, and stirred for 6 hours at ice bath temperature. The above mixture was added dropwise (1 hr) to a solution of 2 equivalents of DHBA (65,1 mg, 0.465 mmol) in 10 mL of THF, and stirred overnight at room temperature. It was then added dropwise (1 hr) to a solution of 4 equivalents of bis(dimethylamino)dimethylsilane (0.170 mL, 0.929 mmol) in 5 mL of THF, and stirred overnight at room temperature. The latter was added dropwise (1 hr) to a solution of 4 equivalents of DHBA (130 mg, 0.929 mmol) in 10 mL of THF, and after stirring overnight, it was added dropwise (1 hr) to a solution of 8 equivalents of bis(dimethylamino)dimethylsilane (0.341 mL, 1.858 mmol) in 5 mL of THF, and stirred for 14 hours. Then it was added to a solution of 8 equivalents of DHBA (260

mg, 1.858 mmol) in 15 mL of THF, and stirred overnight. The resulting solution was added dropwise to 16 equivalents of bis(dimethylamino)dimethylsilane (0.681 mL, 3.717 mmol) in 10 mL of THF. Stirring was continued overnight at room temperature. The resulting solution was then added dropwise to a solution of 16 equivalents of DHBA (521 mg, 3.717 mmol) in 10 mL of THF. The reaction mixture was stirred for 36 hours at room temperature. The resulting solution was then added dropwise (1hr) to 32 equivalents of bis(dimethylamino)dimethylsilane (1.363 mL, 7.434 mmol) in 10 mL of THF and stirred overnight at room temperature. The resulting solution was added dropwise to 32 equivalents of DHBA (1.042 g, 7.434 mmol) in 10 mL of THF. The reaction mixture was let to stir for 3 days at room temperature. The reaction mixture was added dropwise to 64 equivalents of bis(dimethylamino)dimethylsilane (2.726 mL, 0.0148 mol) in 15 mL of THF. Stirring was continued overnight at room temperature. Finally, the resulting solution was then added dropwise to a solution of 64 equivalents of DHBA (2.084 g, 0.0148 mol) in 30 mL of THF. The reaction mixture was stirred for 36 hours at room temperature. 5-8 mL of D₂O were added to the gel and was stirred for 10 minutes. The solution was filtered and D₂O was then removed under vacuum to afford a dark pink powder (3.171 g, 55%). ¹H NMR (270MHz, D₂O-d₂): δ -0.06, 0.00, 0.22 (m, 30H, OSiMe₂O), 4.10 (s, 2H, OCH₂C), 4.31 (s, 15H, C₆H₃-CH₂O), 6.15 (s, 15H, C₆H para), 6.25 (m, 20H, C₆H₂ ortho). FT-IR (KBr, cm⁻¹): 3379 (ν_{OH}), 2963 (ν_{C-H arom.}), 1193 (δ_{Si-CH₃}), 1052, 965 (ν_{Si-O}). Mass spectrum (MALDI-TOF) *m/z* 24,861.8 (including *m/z* Li⁺, expected mass 24,817.1).

3.5 References

- [1] a) Antoni, P.; D. Nystrom, D.; Hawker, C. J.; Hulta, A.; Malkoch, M. *Chem. Comm.*, **2007**, 2249. b) Vohsa, J.K.; Fahlman, B. D. *New J. Chem.*, **2007**, *31*, 1041. c) Gingras, M.; Raimundo, J-M.; Chabre, Y. M. *Angew. Chem. Int. Ed.*, **2007**, *46*, 1010. d) Helms, B.; Meijer, E. W. *Science*, **2006**, *313*, 929. e) Newkome, G. R.; Moorefield, C. N.; Vögtle, F. Dendrimers and Dendrons, Concepts, Syntheses and Applications, Wiley-VCH, 135 Weinheim, **2002**. f) Grayson, S. M.; Fréchet, J. M. J. *Chem. Rev.*, **2001**, *101*, 3819. g) Jiang, D.-L.; Aida, T. *Nature*, **1997**, *388*, 454. h) Sayed-Sweet, Y.; Hedstrand, D. M.; Spinder, R.; Tomalia, D. A. *J. Mater. Chem.*, **1997**, *7*(7), 1199.
- [2] a) Smith, D. K. *Chem. Comm.*, **2006**, 34. b) Fréchet, J. M. J.; Tomalia, D. A. Dendrimer and Other Dendritic Polymers; Eds. John Wiley & Sons: West Sussex, UK, **2001**. c) Astruc, D.; Chardac, F. *Chem. Rev.*, **2001**, *101*, 2991. d) Ishida, Y.; Jikei, M.; Kakimoto, M. *Macromolecules*, **2000**, *33*, 3202.
- [3] Washio, I.; Shibasaki, Y.; Mitsuru, U. *Macromolecules*, **2005**, *38*, 2237.
- [4] a) Czerniewski, A. A.; Liu, X. J.; Rolland, O.; Hourani, R.; Four, M.; Kakkar, A.K. *J. Mater. Chem.*, **2007**, *17*, 2737. b) Hourani, R.; Kakkar, A.K.; Whitehead, M.A. *Journal of Molecular Structure: THEOCHEM*, **2007**, *807*, 101. c) Vassilieff, T.; Quist, F.; Kakkar, A.K. *J. Colloid and Interface Science*, **2006**, *297*, 455. d) Hourani, R.; Kakkar, A.K.; Whitehead, M.A. *J. Mater. Chem.*, **2005**, *15*, 2106. e) Bourrier, O.; Butlin, J.; Hourani, R.; Kakkar, A.K. *Inorganica Chimica Acta*, **2004**, *357*, 3836. f) Bourrier, O.; Kakkar, A.K. *Macromolecular Symposia*, **2004**, *209*, 97. g) Bourrier, O.; Kakkar, A.K. *J. Mater. Chem.*, **2003**, *13*, 1306. h) Kakkar, A.K. *Macromolecular Symposia*, **2003**, *196*, 145. i) Dasgupta, M.; Peori, M.B.; Kakkar, A.K. *Coord. Chem. Rev.*, **2002**, *233-234*, 223. j) Peori, M.B.; Kakkar, A.K. *Organometallics*, **2002**, *21*, 3860. k) Petrucci, M.G.L.; Guillemette, V.; Dasgupta, M.; Kakkar, A.K. *J. Am. Chem. Soc.*, **1999**, *121*(9), 1968.
- [5] a) Jones, K.; Lappert, M.F. *J. Organometal. Chem.*, **1965**, *3*, 295. b) Jones, K.; Lappert, M.F. *J. Chem. Soc.*, **1965**, 1944. c) Sawyer, A.K. Organotin Compounds, Vol. 2, New York, **1971**. d) Davies, A.G. Organotin Chemistry, 2nd Ed., **2004**.
- [6] a) Ge, Z.; Chen, D.; Zhang, J.; Rao, J.; Yin, J.; Wang, D.; Wan, X.; Shi, W.; Liu, S. *J. Polym. Sci. Part A: Polymer Chemistry*, **2007**, *45*, 1432. b) Huang, B.; Hirst, A.R.; Smith, D.K.; Castelletto, V.; Hamley, I.W. *J. Am. Chem. Soc.*, **2005**, *127*,

7130. c) Tang, X.-D.; Zhang, Q.-Z.; Li, A.-X.; Fan, X.-H.; Chen, X.-F.; Zhou, Q.-F. *Chinese Journal of Chemistry*, **2005**, *23*, 11. d) Lee, M.; Jeong, Y.-S.; Cho, B.-K.; Oh, N.-K.; Zin, W.-C. *Chem. Eur. J.*, **2002**, *8*, 876. e) Newkome, G. R.; Lin, X.; Yaxiong, C.; Escamilla, G.H. *J. Org. Chem.*, **1993**, *58*, 3123.
- [7] a) Bosman, A.W.; Janssen, H.M.; Meijer, E.W. *Chem. Rev.*, **1999**, *99*, 1665. b) Laufersweiler, M.J.; Rhode, J.M.; Chaumette, J.-L.; Sarazin, D.; Parquette, J.R. *J. Org. Chem.*, **2001**, *66*, 6440. c) Percec, V.; Ahn, C.-H.; Bera, T.K.; Ungar, G.; Yeardley, D.J.P. *Chem. Eur. J.*, **1999**, *5*, 1070. d) Sebastian, R.-M.; Margo, G.; Caminade, A.-M.; Majoral, J.-P. *Tetrahedron*, **2000**, *56*, 6269. e) Brettreich, M.; Burghardt, S.; Bottcher, C.; Bayerl, T.S.; Hirsch, A. *Angew. Chem. Int. Ed.*, **2000**, *39*, 1845.
- [8] a) Tanaka, K.; Dai, S.; Kajiyama, T. *Langmuir*, **2003**, *19*, 1196. b) Tsukruk, V. V.; Shulha, H.; Zhai, X. *Appl. Phys. Lett.*, **2003**, *82*, 907. c) Sano, M.; Okamura, J.; Ikeda, A.; Shinkai, S. *Langmuir*, **2001**, *17*, 1807. d) Schenning, A. P. H. J.; Elissen-Roman, C.; Weener, J.-W.; Baars, M. W. P. L.; van der Gaast, S. J.; Meijer, E. W. *J. Am. Chem. Soc.*, **1998**, *120*, 8199. e) Laufersweiler, M. J.; Rohde, J. M.; Chaumette, J. L.; Sarazin, D.; Parquette, J. R. *J. Org. Chem.*, **2001**, *66*, 6440. f) Zhang, W.; Simanek, E. E. *Tet. Lett.*, **2001**, *42*, 5355.
- [9] Spence, J. C. H. *Materials Science & Engineering Reports*, **1999**, *26*, 1.
- [10] a) Esumi, K.; Suzuki, A.; Yamahira, A.; Torigoe, K. *Langmuir*, **2000**, *16*, 2604. b) Esumi, K.; Torigoe, K. *Progr. Colloid Polym. Sci.*, **2001**, *80*, 117. c) Bao, C.Y.; Jin, M.; Lu, R.; Zhang, T.R.; Zhao, Y.Y. *Mater. Chem. Phys.*, **2003**, *81*, 160. d) Tarazona-Vasquez, F.; Balbuena, P.B. *J. Phys. Chem. B*, **2004**, *108*, 1599. e) Xu, D.-M.; Zhang, K.-D.; Zhu, C.-L. *Journal of Applied Polymer Science*, **2007**, *104*, 422.

CHAPTER 4

Application of Dumbbell Shaped Dendrimers in the Synthesis of Silver Nanoparticles

4. Application of Dumbbell Shaped Dendrimers in the Synthesis of Silver Nanoparticles

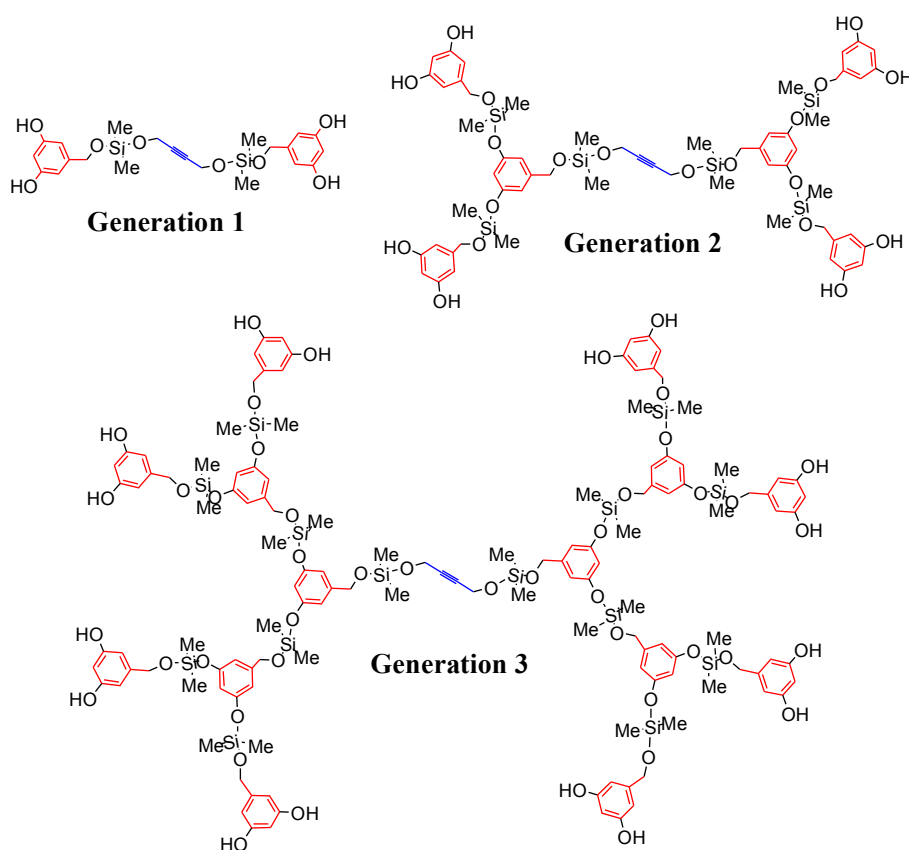
4.1 Introduction

Silver metal nanoparticles continue to arouse intense scientific interest, due to their potential in designing novel materials for applications in a variety of areas, including catalysis, optoelectronics, light amplification etc.¹ As mentioned in Chapter 2, the unique properties of metal particles are associated with their size and shape, and much effort has recently been devoted, in particular, in developing synthetic methodologies that could provide control on shapes of silver metal nanoparticles.² Dendrimers that are hyperbranched and monodisperse in nature,³ are becoming increasingly important in the synthesis of metal nanoparticles.⁴ These globular macromolecules have also been used to construct silver nanoparticles, in a typical procedure that entails addition of a reducing agent to the metal salt in the presence of stabilizing environment of dendrimers.⁵ We report herein a simple methodology in which silver nanoparticles are synthesized in one pot reaction, using a dendrimer structure that combines reactive peripheral hydroxyl groups with a stabilizing acetylenic core/benzene backbone structure. We demonstrate that the shape of the nanoparticles is strongly influenced by the dendrimers, and it evolves from spheres to cubes as the generation number increases.

One of the promising synthetic methodologies to construct silver metal nanoparticles is based on the so called “polyol” synthesis,^{2a} in which an alcohol is reacted with silver salts in the presence of organic stabilizers. The choice of the dendrimer for silver metal particle synthesis was made to include reactive and capping sites in the same ensemble, and in which the internal space around the core changes with the increase in generation number. The dendrimers shown in **Scheme 18**, the structures of which may resemble that of a dumb-bell,⁷ especially so at generations 3 and 4, have both nano-reactor and –stabilizer properties, as they contain phenolic hydroxyl group reactive sites, as well as internal aryl and alkynyl moieties for particle stabilization. As explained in the previous chapter, the dendrimers were constructed from 2-butyne-1,4-diol (BD) core, using simple acid-base hydrolytic chemistry based divergent methodology,⁶ in which 3,5-dihydroxybenzyl alcohol (DHBA) was added in a layer-by-layer fashion around the BD core, linked via Me₂Si groups.⁸

4.2 Results and Discussion

Silver metal nanoparticle synthesis was carried out by adopting a methodology in which silver-acetate is used as the source of metal ions, and the reaction is carried out in water, without any additional reducing agent.⁹ For a typical synthesis of silver metal particles using generation 3 dendrimer, 42 mg (0.015 mmol) of the dendrimer were added to 12.5 mL (0.01 mol/L) of silver acetate solution in water, and the mixture was stirred at room temperature. The original slightly pink color changed to yellow-green. Concentrating the solution on a rotary evaporator at 40°C, led to darkening of the color, and upon complete removal of the solvent, grayish-black solid was obtained. The synthesis was repeated several times for consistency, and the yellow-green solutions as well as the solids were found to be stable for a measured time period of two weeks.



Scheme 18: Structures of generation 1-3 dendrimers.

The characterization of silver particles was carried out using a combination of techniques including transmission electron microscopy (TEM), UV-Vis spectroscopy and X-ray powder diffraction (XRPD). The TEM analysis of the silver particles synthesized using generation 1 dendrimer indicated the presence of generally spherical

shape (**Figure 19**, left), in a variety of sizes with almost 50% of the population in the size range of 5-15 nm.

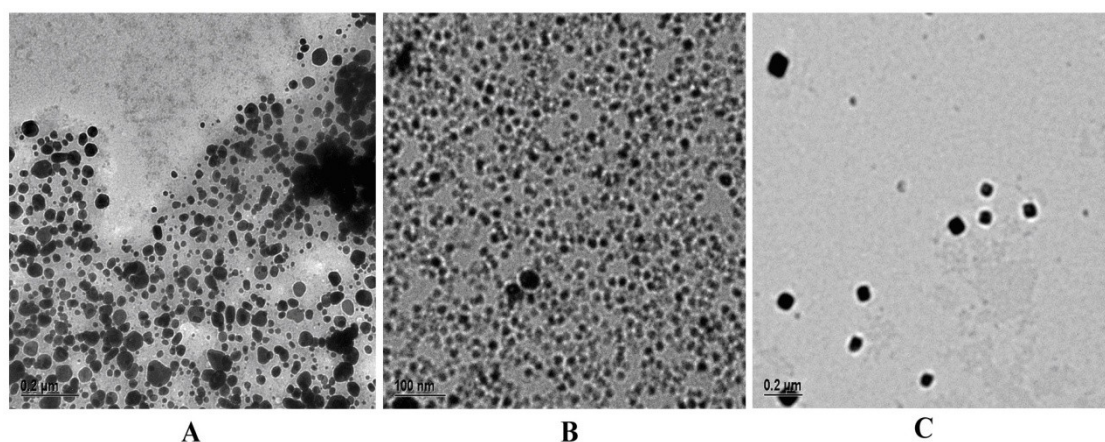


Figure 19: TEM image of silver metal particles synthesized using generation 1(**A**), 2 (**B**) and 3 (**C**) dendrimer templates.

When generation 2 dendrimer is employed, it produces a mixture of spherical and cube shaped particles (**Figure 19**, centre) in a more homogeneous size range with 75% of the particles in 5-15 nm. Using dendrimer generation 3 leads to a dominant cube shaped morphology (**Figure 19** right), and the particle size increases with more particles now in the range of 25-45 nm range.

These changes in silver nanoparticle shape, dependent on the dendrimer generation, were supported by the UV-Vis spectra that showed a broad peak at 415 nm (**Figure 20 A**) for generation 1, peaks at 350 and 440 nm for generation 2 (**Figure 20 B**), a broad peak around 345 nm for the generation 3 and generation 4 dendrimers (**Figures 20 C and 20 D**, respectively) and templated silver particles.

The peaks at 415 and 440 nm are associated with spherical shape, and those at 350 and 345 nm with cube shaped nanoparticles.^{1a,10} These results suggest a change in the shape of silver nanoparticles with the increase in generation number of the silver particles.

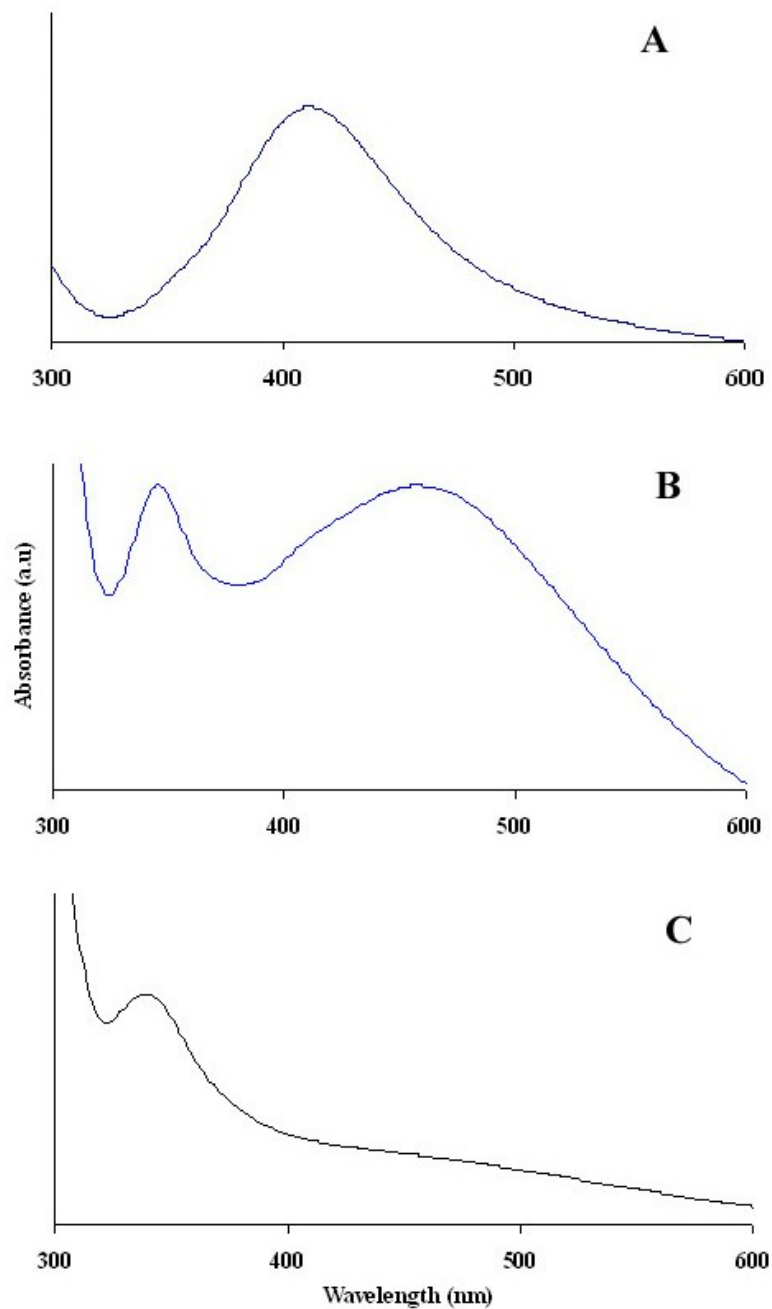


Figure 20: UV-Vis spectra of silver metal particles synthesized using generation 1 (A), 2 (B), and 3 (C) dendrimers as templates.

The XRPD Bragg pattern of these particles showed the presence of reflection peaks typical of a *fcc* structure of silver (**Figure 21**), at 2θ ($^{\circ}$) 38 (111), 44 (200), 65 (220), 77 (311) and 82 (222).

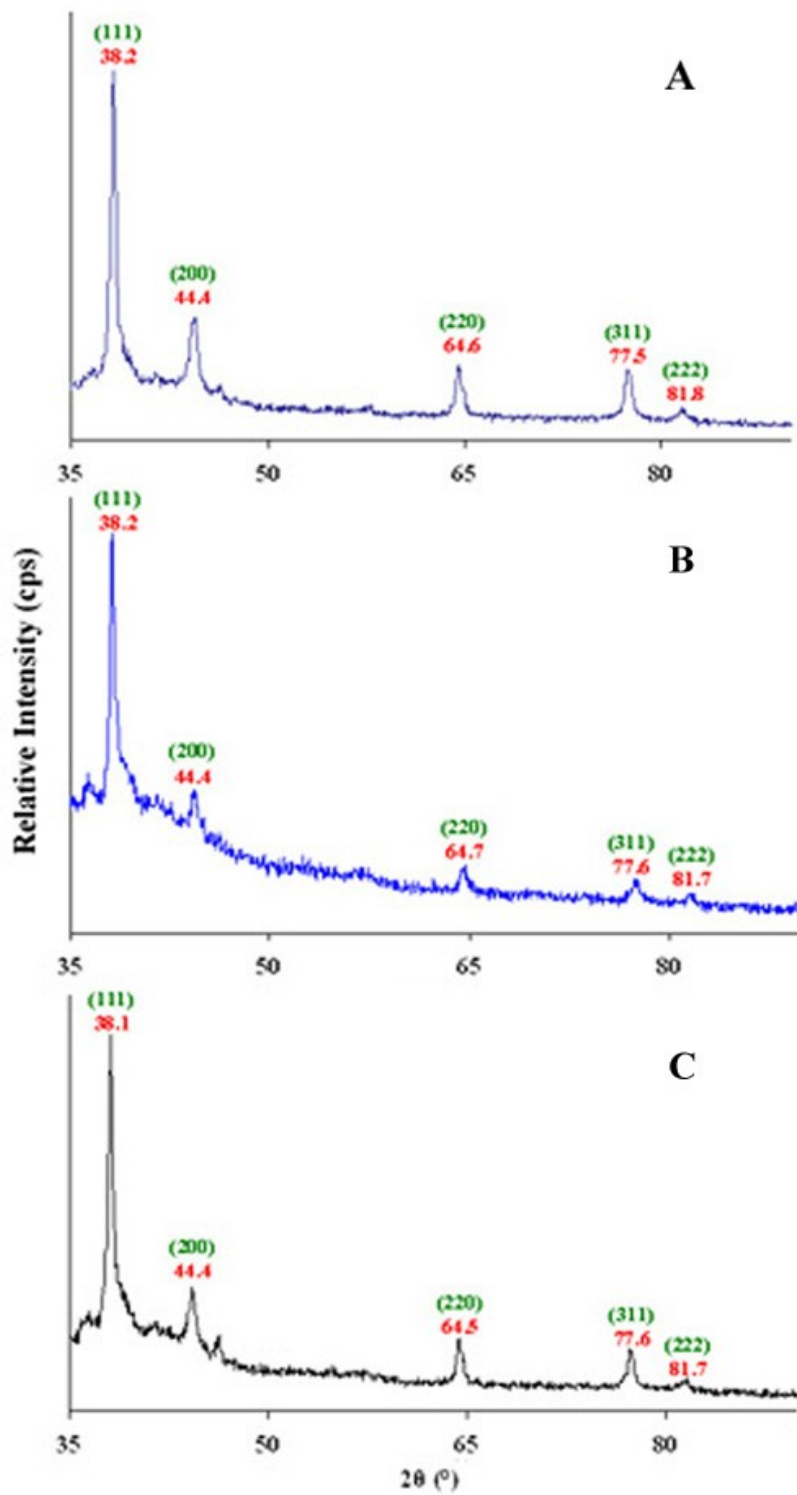


Figure 21: XRPD pattern of silver metal particles synthesized using generation 1(A), 2(B), and 3(C) dendrimers as templates.

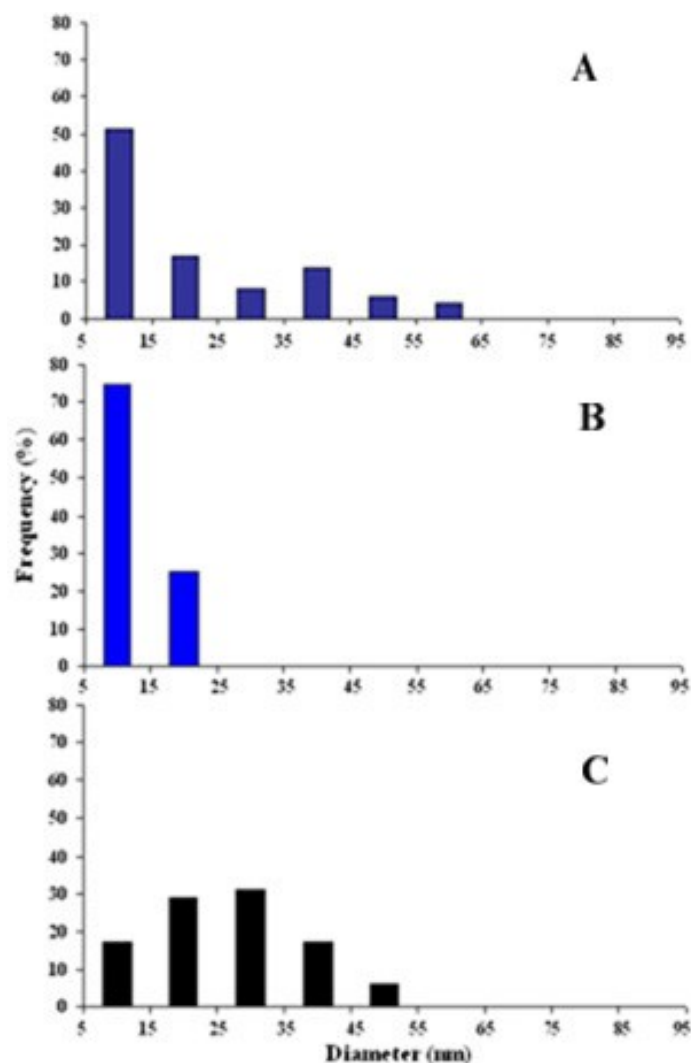
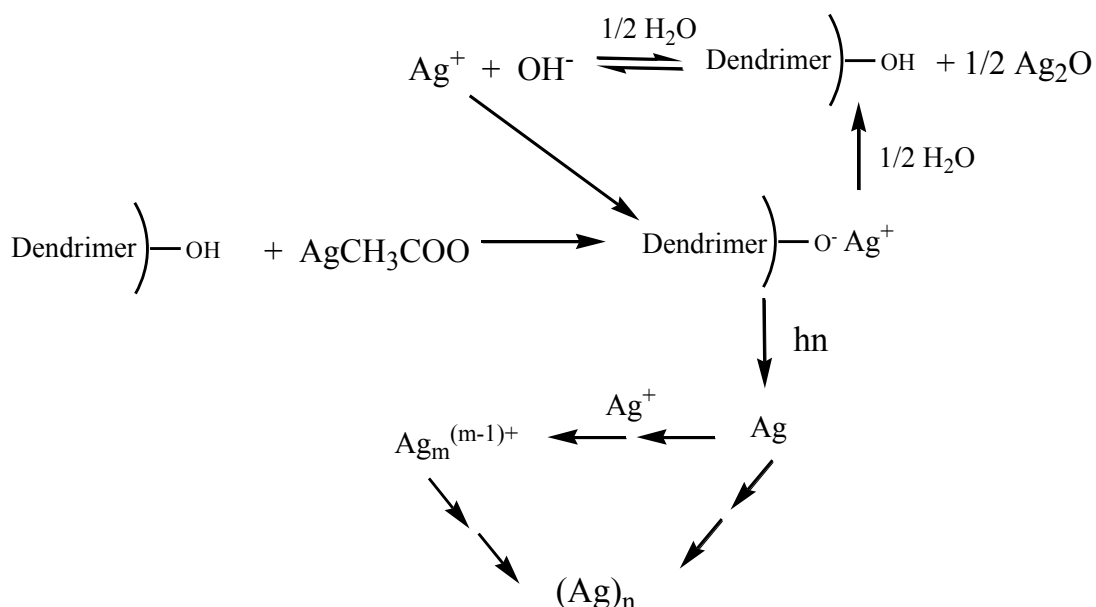


Figure 22: Size distribution graphs for generation 1 (A), 2 (B) and 3 (C) templated silver particles.

Before an explanation of shape change with generation number is sought, it may be useful to consider the formation of silver nanoparticles at ambient temperature without any additional external source of a reducing agent. An understanding of the latter is not obvious, however, some thoughtful insight can be made for this simple process (**Scheme 19**) that lends itself to useful applications, since some dendrimers may not be stable in the presence of reducing agents employed in metal nanoparticle syntheses.^{2,4} It is expected that silver acetate will react with peripheral phenolic hydroxide groups of the dendrimers upon mixing, leading to chemisorption of Ag^+ ions at their surface. The concentration of these ions will depend on the generation number, and although it is expected to increase exponentially (in relation to the OH groups that increase from 4 to 16 in generations 1-3), if all the OH groups react simultaneously, but

it is still expected to be quite low. Since the synthesis of silver nanoparticles is carried out at ambient conditions in water without any exclusion of light, the reduction of these silver ions can get initiated photolytically.¹¹ The extremely low concentration of silver atoms that results in the initial stages, can also accelerate further reduction of Ag^+ ions that will be in relatively much higher concentration, by atom to ion reduction.¹² The corresponding unstable ionic clusters will get reduced in a similar manner much more quickly, leading to further growth of silver particles. The other possible fate of Ag^+ ions post-surface anchoring is the formation of silver oxide in a wet atmosphere. The latter will be in equilibrium with silver hydroxide under these conditions,¹³ and these Ag^+ ions can react with the dendrimer and get recycled into the process. We did not observe any evidence of the precipitated or silver oxide nanoparticles in solution during our characterization of the metal nanoparticles.



Scheme 19: dendrimers templation process of silver nanoparticles

It is clear that the dendrimer generation plays a role in the evolving structure of silver metal nanoparticles. An explanation for this may come from understanding the formation process involved in the build-up to the nanoparticles. It has been postulated that when the metal ions bind at the surface of the template, the particle formation generally takes place at the surface of the dendrimers.¹⁴ It is expected that generations 1 and 2 have a very open structure, while in generation 3 the two arms begin to wrap around the central acetylenic core, and create a defined internal environment (**Scheme 18**). Therefore, generation 1, in particular, will not have any additional internal shape

oriented stabilization architecture that it can provide to the growing silver particles. Considering that the particle formation takes place dominantly in the exterior, near the chemisorbed sites, a spherical shape of particles (stabilized through benzene rings as well as the acetylenic moiety) with minimum surface energy, will evolve. As the structure evolves to generations 2 and 3, the internal environment starts to get defined, more so in generation 3, creating internal cavity around the central acetylenic core. The growing silver particles may obtain more stability by migration into the interior around the central acetylenic moiety. This will help reduce the surface energy that will be higher in the cube than a sphere, by an increased size of the particles, as well as by the pre-organized internal structure of the dendrimers (generation 3). As noted above, size of the silver particles templated using generation 3 is higher than those from 1 and 2.

It is also possible that the particle formation gets initiated inside the dendrimers but at a later stage of the growth they migrate to the exterior of the dendrimers. Further growth of the metal particles while retaining their original shape, might explain the size of the metal nanoparticles which is larger than the dendrimers. We are currently exploring the detailed mechanism of metal particle growth using these dendrimers.

4.3 Conclusions

In conclusion, dendrimers that are built from an acetylenic core and 3,5-dihydroxybenzyl alcohol as the backbone, have been employed in a dual role of nano-reactors and –stabilizers, in the synthesis of silver nanoparticles in a one-step synthesis. The evolving shape of these particles was found to be influenced by the generation number, and cube shaped silver particles are formed when generation 3 dendrimer is used as the template. Such a simple chemical control in the shape of metal nanoparticles is of significance, and may offer potential in tailoring their properties. We are currently elaborating on the scope of this methodology.

Addendum:

This chapter has been submitted to Chemical communication.

4.4 Experimental section

Materials and Measurements

Dendrimers generations 1 to 3 were used as made. All manipulations were performed under air and at room temperature.

Silver acetate (CH_3COOAg , 99%) was purchased from Aldrich and was used as-received without any further purification.

UV-Visible spectra were recorded in water on a Hewlett Packard 8453 with a resolution of 2 nm. Transmission electron microscopy (TEM) measurements were carried out on a JEOL 2000FX microscope operating at an acceleration voltage of 80 kV. X-ray powder diffraction (XRPD) experiments were performed using a Siemens D-5000 diffractometer. It was equipped with a step scanner and a 1.2 kW cobalt tube ($\lambda = 1.78897 \text{ \AA}$) coupled to a silicon detector. The diffraction patterns were acquired in the reflection mode, for 2θ values ranging from 4 to 90 degrees. The X-ray beam was fixed while the sample holder and the detector was moved to scan the solids.

Dendrimer generation 1 templated silver particles

Generation 1 dendrimer ($m = 42 \text{ mg}$, $n = 0.088 \text{ mmol}$) was added to 12.5 mL (0.01 mol/L) of silver acetate solution in water, and the mixture was stirred at room temperature.

The original slightly pink color changed to yellow-green. Concentrating the solution on a rotary evaporator at 40°C , led to darkening of the color, and upon complete removal of the solvent, grayish-black solid was obtained. The synthesis was repeated several times for consistency, and the yellow-green solutions as well as the solids were found to be stable for a measured time period of two weeks.

Dendrimer generation 2 templated silver particles

Generation 2 dendrimer ($m = 42 \text{ mg}$, $n = 0.033 \text{ mmol}$) was added to 12.5 mL (0.01 mol/L) of silver acetate solution in water, and the mixture was stirred at room temperature.

As for generation 1, the original slightly pink color changed to yellow-green. Concentrating the solution on a rotary evaporator at 40°C , led to darkening of the color, and upon complete removal of the solvent, grayish-black solid was obtained. The

synthesis was repeated several times for consistency, and the yellow-green solutions as well as the solids were found to be stable for a measured time period of two weeks.

Dendrimer generation 3 templated silver particles

Generation 3 dendrimer (m= 42 mg, n= 0.015 mmol) was added to 12.5 mL (0.01 mol/L) of silver acetate solution in water, and the mixture was stirred at room temperature.

The original slightly pink color changed to yellow-green. Concentrating the solution on a rotary evaporator at 40°C, led to darkening of the color, and upon complete removal of the solvent, grayish-black solid was obtained. The synthesis was repeated several times for consistency, and the yellow-green solutions as well as the solids were found to be stable for a measured time period of two weeks.

4.5 References

- [1] a) Ledwith, D. M.; Whelan, A. M.; Kelly, J. M. *J. Mater. Chem.*, **2007**, *17*, 2459. b) Daniel, M.-C.; Astruc, D. *Chem. Rev.*, **2004**, *104*, 293. c) Hu, M. S.; Chen, H. L.; Shen, C. H.; Hong, L. S.; Huang, B. R.; Chen, K. H.; Chen, L. C. *Nat. Mater.*, **2006**, *5*, 102. d) Graham, D.; Faulds, K.; Smith, W. E. *Chem. Comm.*, **2006**, 4363.
- [2] a) Wiley, B.; Sun, Y.; Xia, Y. *Acc. Chem. Res.* **2007**, ASAP Article, 10.1021/ar7000974. b) Wei, G.; Zhou, H.; Liu, Z.; Song, Y.; Wang, L.; Sun, L.; Li, Z. *J. Phys. Chem. B*, **2005**, *109*, 8738. c) Sun, Y.; Mayers, B.; Herricks, T.; Xia, Y. *Nano Lett.*, **2003**, *3*, 955. d) Im, S. H.; Lee, Y. T.; Wiley, B.; Xia, Y. *Angew. Chem., Int. Ed.*, **2005**, *44*, 2154. e) Wiley, B.; Sun, Y.; Mayers, B.; Xia, Y. *Chem.–Eur. J.*, **2005**, *11*, 454. f) Sun, Y.; Xia, Y. *Science*, **2002**, *298*, 2176.
- [3] a) Newkome, G.R.; Moorefield, C.N.; Vögtle, F. Dendrimers and Dendrons, Concepts, Syntheses and Applications, Wiley-VCH, 135 Weinheim, **2002**. b) Grayson, S.M.; Fréchet, J.M.J. *Chem. Rev.* **2001**, *101*, 3819. c) Jiang, D.-L.; Aida, T. *Nature (London)*, **1997**, *388*, 454. d) Sayed-Sweet, Y.; Hedstrand, D.M.; Spinder, R.; Tomalia, D.A. *J. Mater. Chem.*, **1997**, *7*(7), 1199.
- [4] a) Wilson, O.M.; Scott, R.W.J.; Garcia-Martinez, J.C.; Crooks, R.M. *J. Am. Chem. Soc.*, **2005**, *127*, 1015. b) Esumi, K.; Akiyama, S.; Yoshimura, T. *Langmuir*, **2003**, *19*, 7679.
- [5] a) Kim, Y.-C.; Oh, S.-K.; Crooks, R.M. *Chem. Mater.*, **2004**, *16*, 167. (b) Esumi, K.; Suzuki, A.; Aihara, N.; Usui, K.; Torigoe, K. *Langmuir*, **1998**, *14*, 3157.
- [6] a) Petrucci, M.G.L.; Guillemette, V.; Dasgupta, M.; Kakkar, A.K. *J. Am. Chem. Soc.*, **1999**, *121*(9), 1968. b) Bourrier, O.; Kakkar, A.K. *J. Mater. Chem.*, **2003**, *13*, 1306. c) Bourrier, O.; Butlin, J.; Hourani, R.; Kakkar, A.K. *Inorganica Chimica Acta*, **2004**, *357*, 3836. d) Hourani, R.; Kakkar, A.K.; Whitehead, M.A. *J. Mater. Chem.*, **2005**, *15*, 2106. e) Czerniewski, A.A.; Liu, X.J.; Rolland, O.; Hourani, R.; Four, M.; Kakkar, A.K. *J. Mater. Chem.*, **2007**, *17*, 2737.
- [7] Some of the examples of dendrimers with dumbbell shape include: a) Ge, Z.; Chen, D.; Zhang, J.; Rao, J.; Yin, J.; Wang, D.; Wan, X.; Shi, W.; Liu, S. *J. Polym. Sci. Part A: Polymer Chemistry*, **2007**, *45*, 1432. b) Huang, B.; Hirst, A.R.; Smith, D.K.; Castelletto, V.; Hamley, I.W. *J. Am. Chem. Soc.*, **2005**, *127*, 7130. c) Tang, X.-D.; Zhang, Q.-Z.; Li, A.-X.; Fan, X.-H.; Chen, X.-F.; Zhou, Q.-F. *Chinese Journal of Chemistry*, **2005**, *23*, 11. d) Lee, M.; Jeong, Y.-S.; Cho, B.-K.; Oh, N.-K.; Zin, W.-

- C. *Chem. Eur. J.*, **2002**, *8*, 876. e) Newkome, G. R.; Lin, X.; Yaxiong, C.; Escamilla, G. H. *J. Org. Chem.*, **1993**, *58*, 3123.
- [8] Manuscript reporting full details of synthesis and characterization of these dendrimers is currently being finalized, and these data are provided as supporting information.
- [9] Armelao, L.; Bottaro, G.; Campostrini, R.; Gialanella, S.; Ischia, M.; Poli, F.; Tondello, E. *Nanotechnology*, **2007**, *18*, 15, 155606.
- [10] Kelly, K. L.; Coronado, E.; Zhao, L. L.; Schatz, G. C. *J. Phys. Chem. B*, **2003**, *107*, 668.
- [11] Shchukin, D.G.; Radtchenko, I.L.; Sukhorukov, G.B. *CHEMPHYSICHEM*, **2003**, *4*, 1101.
- [12] a) Joshi, R.; Mukherjee, T. *Radian Physics and Chemistry*, **2007**, *76*, 811. b) Kaganovski, Y.; Mogiko, E.; Lipovski, A.A.; Rosenbluh, M. *J. Phys: Conference Series*, **2007**, *61*, 508.
- [13] Merga, G.; Wilson, R.; Lynn, G.; Milosavljevic, B.H.; Meisel, D. *J. Phys. Chem. C*, **2007**, *111*, 12220.
- [14] Balogh, L.; Valluzzi, R.; Laverdure, K. S.; Gido, S. P.; Hagnauer, G. L.; Tomalia, D. A. *Journal of Nanoparticle Research*, **1999**, *1*, 353.

CHAPTER 5

Conclusions and Future Outlook

5.1 Conclusions

This thesis reports the elaboration of a divergent synthetic methodology to prepare dumbbell shaped dendrimers that evolve from a linear core with dendritic arms built from 3,5-dihydroxybenzyl alcohol based backbone. The dendrimers build-up follows a simple and highly versatile acid-base hydrolytic methodology under controlled reaction conditions, resulting in the synthesis of generation 1-4 dendrimers in excellent yields. These dendrimers have desired features to self-assemble into aggregates of various sizes *via* hydrogen bonding through peripheral OH groups. During the investigations of their self-assembly, this phenomenon was found to be dependent upon concentration, as well as the generation number.

These dumbbell shaped dendrimers were then successfully employed in the one-step synthesis of silver nanoparticles. Their generation number was found to influence the shape of silver nanoparticles. Generation 3 dendrimer leads to cube shaped silver particles while in generations 1 and 2, spherical silver particles are formed. Controlling the shape of metal nanoparticles using a one-step synthetic process is of significance, and may provide pathways to silver nanoparticles with important and promising properties.

5.1.1 Dumbbell Shaped Dendrimers

The first goal of this thesis was to develop a divergent synthetic methodology to dumbbell shaped dendrimers by constructing dendritic wedges around a linear core, using easily accessible reagents, and under mild reaction conditions. Reaction of 2-butyne-1,4-diol with diaminosilane $\text{Me}_2\text{Si}(\text{NMe}_2)_2$ and subsequently with 3,5-dihydroxybenzyl alcohol *via* the acid base hydrolysis chemistry, led to the synthesis of these dendrimers with the amine as the only by-product. The preparation of dendrimers requires controlled reactions using slow addition of a reagent to the desired core in a layer-by-layer dendritic growth. For example, reaction of two equivalents of $\text{Me}_2\text{Si}(\text{NMe}_2)_2$ to 2-butyne-1,4-diol under controlled reaction conditions resulted in the formation of an aminosilane terminated intermediate. Addition of the latter to two equivalents of 3,5-dihydroxyl benzyl alcohol led to the formation of dendrimer generation 1. Dendrimers up to generation 4 featuring 32 peripheral hydroxyl groups were prepared by iteration of this two step procedure. Continuation of this methodology to construct dumbbell shaped dendrimers of

generations 5 and 6 leads to defects due to incomplete reactions at the surface due to steric constraints.

The presence of hydroxyl groups at the periphery of these dumbbell dendrimers was found to promote their intermolecular association via hydrogen bonding, leading to their self-assembly into aggregates. This behaviour was found to depend on the concentration in a solvent such as THF. The *critical aggregation concentration (cac)*, above which aggregates are formed, was found by analyzing the turbidity of the solution at different concentrations using UV-Vis absorption spectroscopy. It was determined to be 4.9 mg/mL for dendrimer generations 1-3. However fourth generation dendrimer showed a *cac* of 4.1 mg/mL which was quite comparable to the spherical DHBA based dendrimers studied earlier in our group, suggesting clearly that the structure was becoming more globular at the latter generation. The evolution of the size of these aggregates was followed by using transmission electron microscopy.

5.1.2 Applications in Synthesizing Silver Nanoparticles

The potential of dumbbell shaped dendrimers in synthesizing silver metal nanoparticles using a simple one-step methodology was examined. Silver metal particle synthesis was carried out in water due to the solubility of silver acetate reagent and these dendrimers by adopting a methodology in which silver acetate is used as the source of metal ions. The TEM pictures of generation 1 templated silver particles indicated the presence of generally spherical shape in a size range of 5-15 nm. When generation 2 dendrimer is employed, it leads to a mixture of spherical and cube shaped particles of 5-15 nm size range. Using dendrimer generation 3 gives a dominant cube shaped morphology with more particles now in the range of 25-45 nm range. The XRPD Bragg pattern of these particles showed the presence of reflection peaks typical of a *fcc* structure of silver. Therefore, the shape of these particles was found to be dependent on the generation number. Tailoring the shape of silver metal nanoparticles by dendrimers is important, and offers significant potential in developing silver metal nanoparticles with desired properties.

5.2 Future Outlook

- Synthesis of higher generations (5-6) needs to be further explored, as well as the role of steric congestion in controlling the build-up of defect free structure of dendrimers.
- It will be interesting to examine the role of the length of the central core molecule on the evolving and overall morphology of these dendrimers. In this regard, the focal point of the dumbbell shaped dendrimers can be lengthened by using hexa-2,4-diyne-1,6-diol, octa-2,4,6-triyne-1,8-diol,...It will also be of interest to compare their self-assembly with that of dendrimers reported here in this thesis.
- The self-assembly of dumbbell dendrimers on flat surfaces such as silicon wafers is also very important, and it should be explored, and compared with the behavior of globular DHBA based dendrimers.
- Understanding the mechanism of formation and predicting the conditions for obtaining metal nanoparticles of a desired size and shape is highly challenging. The method developed in this thesis is simple and very useful in which dendrimers of generations 1-3 provide the desired stabilizing environment for the growing metal particles. It would be interesting to investigate further their physical properties and also study the evolution of the morphology of the silver nanoparticles by employing higher generations of dendrimers.
- In order to properly account for the effect of light in the production of Ag nanoparticles, control synthesis of Ag nanoparticles in the absence of light, as well as under high radiation conditions should be investigated.
- Finally, this one-step synthesis of silver nanoparticles could be applied to obtain gold or copper nanoparticles by using the appropriate metal salts and the dumbbell shaped dendrimers. The study of their structure-property relationships could then be compared to those of silver nanoparticles.